GL03943
LBL-10562
GREMP-8
UC-66a

Transient Well Testing in Two-Phase Geothermal Reservoirs

S. Robert Aydelotte
INTERCOMP

MARCH 1980

Geothermal Reservoir Engineering Management Program

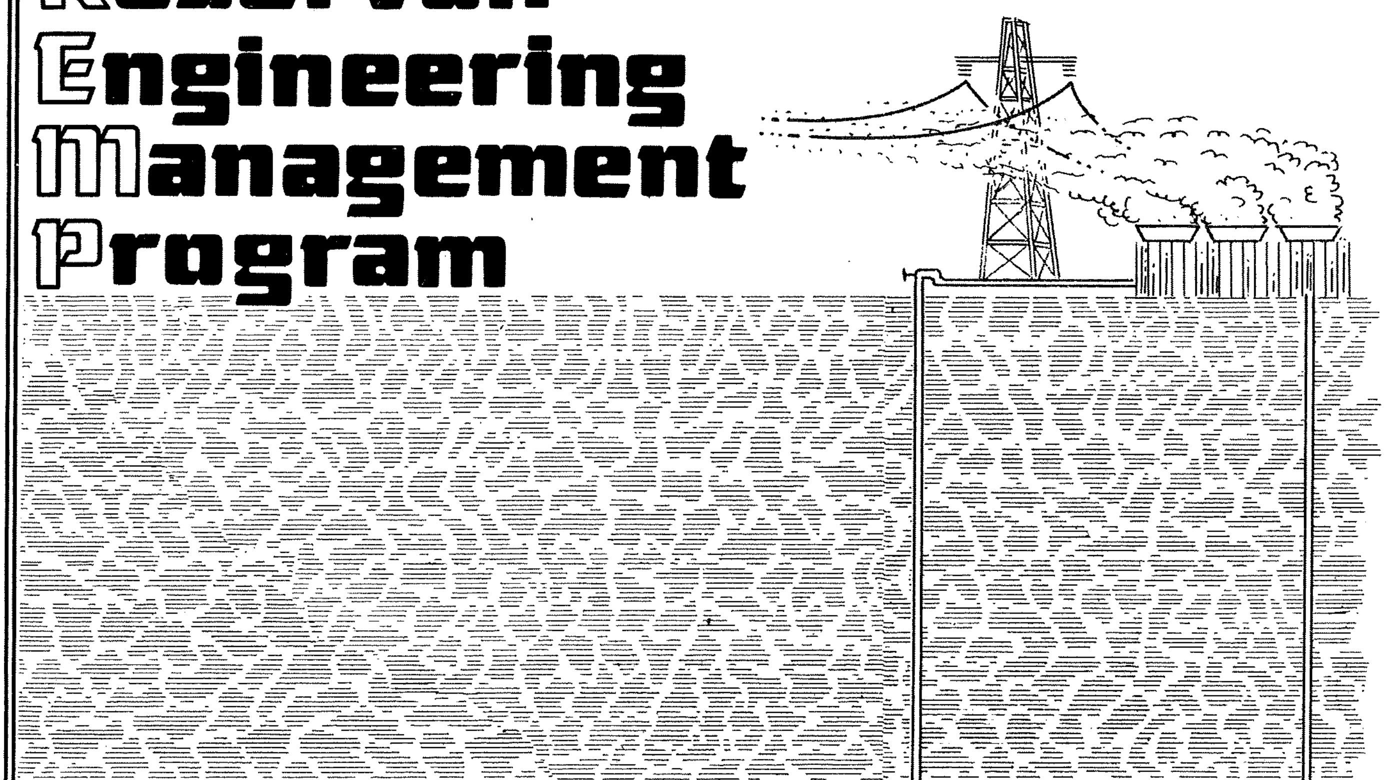

Earth Sciences Division
Lawrence Berkeley Laboratory
University of California, Berkeley

Prepared for U.S. Department of Energy under Contract W-7405-ENG-48

Printed in the United States of America
Available from
National Technical Information Service
U.S. Department of Commerce
5285 Port Royal Road
Springfield, VA 22161
Price Code: A08

LBL-10562

SUBCONTRACT 3976812

TRANSIENT WELL TESTING
IN
TWO-PHASE
GEOTHERMAL RESERVOIRS

Prepared for

UNIVERSITY OF CALIFORNIA
LAWRENCE BERKELEY LABORATORY
BERKELEY, CALIFORNIA 94720

Prepared by

INTERCOMP
Resource Development and Engineering, Inc.

ABSTRACT

A study of well test analysis techniques in two-phase geothermal reservoirs has been conducted using a three-dimensional, two-phase, wellbore and reservoir simulation model. Well tests from Cerro Prieto and the Hawaiian Geothermal Project have been history matched. Using these well tests as a base, the influence of reservoir permeability, porosity, thickness, and heat capacity, along with flow rate and fracturing were studied. Single and two-phase transient well test equations were used to analyze these tests with poor results due to rapidly changing fluid properties and inability to calculate the flowing steam saturation in the reservoir. The injection of cold water into the reservoir does give good data from which formation properties can be calculated.

ACKNOWLEDGEMENTS

This work was performed under purchase order #3976812 for the Lawrence Berkeley Laboratory, University of California, Berkeley, California, as part of the Geothermal Reservoir Engineering Management Program, sponsored by the United States Department of Energy, Division of Geothermal Energy under Contract W-7405-ENG-48.

The guidance and encouragement of John H. Howard, Sirisak Juprasert, Connie Miller and Werner J. Schwarz of the Earth Sciences Division and Paul Marshall, the contract administrator, is gratefully acknowedged.

Table of Contents

LIST OF TABLES

LIST OF FIGURES

LIST OF FIGURES - (CONTINUED)

LIST OF FIGURES - (CONTINUED)

I. INTRODUCTION

The Lawrence Berkeley Laboratory has contracted INTERCOMP Resource Development and Engineering, Inc. to simulate and verify the techniques and procedures of analyzing transient well tests in two-phase geothermal reservoirs. This report presents the results of the study.

The transient pressure response of wells has been extensively investigated in both ground-water hydrology and petroleum literature. Pressure transient analysis has been a very important tool for characterizing reservoir and well parameters in-situ.[1,2] Recently, the experience gained over several decades has been applied to geothermal well testing.[3,4] The most successful applications of existing transient well testing theory have been to the testing of wells producing from essentially single-phase reservoirs.[4,5,6,7] These well testing applications differ from conventional well tests in that generally wellhead data is utilized instead of downhole data due to high downhole temperature, and that the reservoir and fluid are not isothermal.

The application of conventional pressure transient methods to two-phase geothermal reservoirs has not been as successful, however.[7,8] The influence of violent phase changes of boiling or condensation during pressure changes, and the associated thermal gradients created by temperature changes cause the methods developed for single phase flow to be, at least partially, inapplicable. This phase change occurs as the flowing reservoir pressure falls below the saturation pressure at reservoir temperature, and water flashes into steam. Associated with the pressure change of the now saturated water is a change in fluid temperature to the saturation temperature. This change in temperature creates a difference in the rock and fluid temperatures, causing heat to flow from the rock to the flowing fluid.

Several investigators, notably Grant,[9] Garg,[10] and Moench,[11] have attempted to include the effects of boiling in analytical solutions for use in well test interpretation. Each has derived a diffusion type equation which allows for the apparent compressibility of the steam-water mixture, but changes in thermal gradients and saturation dependent effective permeabilities have not been rigorously included.

To evaluate the use of existing transient well testing methods for two-phase reservoir testing, a numerical model capable of simulating two-phase reservoir performance was utilized to generate well test data under a variety of test situations. These data were analyzed to calculate reservoir permeability using one-and two-phase analytical techniques. Some of the reservoir parameters investigated in this study were reservoir porosity, permeability, thickness and heat content. Also the effects of flow rate, skin damage and initial reservoir state were studied.

II. MODEL DESCRIPTION

INTERCOMP's Geothermal Reservoir Simulator was used to simulate the producing characteristics of a single well in a two-phase geothermal reservoir. A second program, INTERCOMP's VSTEAM wellbore model, was coupled to the Geothermal Reservoir model to calculate the changes in producing pressure, temperature and enthalpy as steam-water mixtures flowed up the wellbore. These two models are the basic numerical tools used in this investigation.

The Geothermal Reservoir Simulator consists of two equations expressing the conservation of mass of H_2O and conservation of energy. These equations account for three-dimensional, single or two-phase fluid flow, convective and conductive heat flow in the reservoir and conductive heat transfer between the reservoir and overlying and underlying strata. The phase configuration can vary spatially through the reservoir from single-phase undersaturated water to two-phase steam-water mixture to single-phase superheated steam. The model equations do not account for the presence of inert gases or for varying concentration and precipitation of dissolved salts.

The Geothermal Reservoir Simulator applies to reservoir grids including one-dimensional, two-dimensional r-z, x-z, or x-y, and three-dimensional r-z-θ cylindrical or x-y-z Cartesian coordinates. In radial and cylindrical coordinates, the wellbore of a well at r=0 can be included in the grid. The grid can also include blocks of zero porosity representing hard rock, with no pressures calculated, and blocks of 100% porosity representing fractures or wellbores.

The mass balance on H_2O combines in a single equation the steam-phase and liquid water-phase mass balance equations. The energy balance in the First Law of Thermodynamics applies to each grid block, which is considered as an open system with fixed boundaries. At saturated conditions, all fluid properties are evaluated as single-valued functions of temperature from steam tables, with undersaturated water and superheated steam properties as functions of temperature and pressure. Reservoir thermal conductivities may vary with spatial position, but are treated as independent of pressure, temperature and saturation. Formation rock heat capacity may vary with position but is independent of temperature. Overburden thermal conductivity and heat capacity are constants. A more detailed description of the reservoir model may be found elsewhere.[12]

The two-phase flow of steam and water up the wellbore was simulated by the VSTEAM model also described elsewhere.[13] This wellbore model was linked to the reservoir model at the sandface, and calculated two-phase pressure drop, flow regime changes, phase changes, and heat transfer from the fluid in the wellbore and to the surrounding rock as steam and water traversed from the perforations to the wellhead. These calculations are based upon the empirical results of investigations of two-phase flow in vertical or inclined pipe at essentially isothermal and steady-state conditions. The pressure drop relationships have been coupled with thermodynamic equations governing heat transfer effects to allow the simulation of wellbore problems. This formulation is limited to steady-state wellbore flow calculations, however, and transient wellbore response is not simulated.

III. VERIFICATION OF SIMULATION MODELS

The purpose of this section is to present numerical results which demonstrate that INTERCOMP's Geothermal Reservoir Simulator solves the conservation of mass and energy equations for two phase steam-water flow in the reservoir. Also, since wellhead conditions were desired for possible analytical evaluation, an approach to obtain wellhead flowing conditions in a two-phase wellbore has been verified.

A. RESERVOIR MODEL

This section presents three problems which demonstrate the use of INTERCOMP's Geothermal Reservoir Simulator under a variety of situations. For each problem, the results of the model are compared to published experimental or numerical results.

1. Stanford Bench Model

The first problem presents the use of the reservoir simulator to simulate a one dimensional laboratory bench model[14] during a two phase flow experiment in porous media. The data generated by the bench model consisted of pressure and temperature measurements in a synthetic core during depletion. As the core was initially filled with undersaturated water, the test progressed from one to two phase flow as the core fluid was produced through an outlet valve. A special core holder isolated the core from drastic heat losses and gains, and pressure and temperature sensors measured the fluid condition at various points in the core.

Much of the necessary heat loss and two phase flow characteristics of the core and holder were not reported by the experimenters, and that data reported by Thomas and Pierson[15] were used. The equations for heat flux at the closed end and sides of the core were represented by equations normally used to simulate steady-state heat sources or sinks in geologic time problems. These equations are:

$$q_{side} = 75\ (\text{AREA})\ (T_{source} - T_{core}),\ \text{BTU/DAY} \quad (1)$$

and

$$q_{end} = 2286\ (\text{AREA})\ (T_{source} - T_{core}),\ \text{BTU/DAY} \quad (2)$$

Relative permeabilities for water and steam were calculated from the analytical relationship presented in Reference 15 using the reported endpoints of $Sw_c = 0.30$ and $Sg_c = 0.05$. The calculated relative permeability curves, input in tabular form, are presented in Figure 1. Additional data for the synthetic core are given in Table 1, along with the model grid as described in Reference 15. The reported model grid did not correctly represent the synthetic core as the point of fluid withdrawal was not at the end of the core, so a very small grid block was added to the outlet end of the model. Fluid withdrawals were made from the center of this block at a dimensionless length of 1.0.

The outlet pressure curve given in Figure 2 was input to the model along with the initial pressure and temperature data given in Figures 3 and 4. The model was run for a total time of 300 seconds with this data. The pressure and temperature profiles calculated, shown in Figures 3 and 4, agree very well with the bench model experimental data. The saturations calculated by INTERCOMP's model also agree well with the saturations calculated at 300 seconds by Thomas and Pierson, but the agreement is not as close at 180 seconds. The difference at 180 seconds may be due to the use of tabular relative permeability data, slightly different PVT data, or the use of a simultaneous solution for implicit saturation and pressure at all times with the INTERCOMP model.

2. Two-Phase Drawdown Problem

The second problem simulated was a two-phase drawdown test presented by Garg.[10] The problem consists of producing a homogeneous, isotropic reservoir initially containing undersaturated water at a constant mass rate. As the reservoir is produced, flashing occurs near the wellbore once the pressure drops to the saturation pressure. During the development of this two phase region, calculated wellbore pressures with INTERCOMP's model and Garg's model agree very well, as shown in Figure 6. The data used to generate this drawdown test is listed in Table 2.

In both models, the pressure calculated in the first grid block is corrected to give the pressure in the wellbore. This correction is made assuming that steady state flow exists within the first grid block, and that the pressure drop from the grid block center to the wellbore radius can be calculated from:

$\Delta P = Q/WI$,...................(3)

where:

ΔP = pressure drop from block center to wellbore,

Q = flow rate,

WI = well index related to conditions in the first grid block.

To establish the correct well index, a term KHL is calculated which includes the constant terms and geometric considerations for the well. This term is later multiplied by saturation and pressure dependent terms to obtain the well index variable.

According to Garg, the flowing wellbore pressure is the pressure calculated at 0.56 Δr_1, which is 1.84 feet in this problem. INTERCOMP's grid block logic calculates the first grid block pressure at 2.32 feet. The term KHL corrects for this difference, and is calculated as:

$$KHL = 2 \quad k \quad z / \quad \ln(re/rw) + S \quad \times \frac{.00633}{5.6146}$$

$$= \frac{(2)(3.1416)(10.133)(100)(.00633)}{\ln(2.32/1.84) \quad (5.6146)} = 30.966 \text{...................(4)}$$

This value of KHL produced the match given in Figure 6. The slope of the straight line is about 410 psi/cycle, which is close to the slope of the curve generated by Garg.

3. Two-Phase Reservoir Problem

This reservoir problem involves the production of a vapor-dominated, two-phase, horizontal geothermal reservoir and a comparison of the calculated saturations. This problem was first presented by Toronyi,[16] and was later described and duplicated by Thomas and Pierson.[15] The reservoir consists of a single well located in a 6000 by 600 foot reservoir initially at an 80% steam saturation. The well is produced at a constant rate for 78.3 days, which represents a cumulative production of 19 percent of the mass in place. The reported relative permeability values were adjusted slightly to account for a minor difference in water viscosity values input, and the porosity of the rock was modified so that exactly 19% of the reported mass in place was produced at 78.3 days. These and other data are listed in Table 3.

A comparison of the steam saturations at 78.3 days as calculated by Toronyi and INTERCOMP's model is presented in Figure 7. The agreement between the two models is good, but the values calculated by Thomas and Pierson agree much better with Toronyi's work.

B. WELLBORE MODEL

The purpose of this portion of Task I was to demonstrate the ability of the vertical two-phase wellbore model to represent the conditions and results of actual field tests. The data used for this demonstration was from the Broadlands area in New Zealand, and is presented in part in Reference 13.

The data matched consists of two of a series of flowing temperature and pressure profiles measured in Broadlands No. 13 during 1969. A description of this well is given in Table 4. The tests were conducted by flowing a well at a given rate, and running pressure and temperature bombs into the wellbore during flow. Unfortunately, a rate history was not provided with the data and no reserovir characteristics can be calculated from these tests. The data was provided by the Ministry of Works, New Zealand by private communication, and consists of:

a) a description of Broadlands 11 and 13 geothermal wells;
b) total mass rate and total enthalpy for several flow tests;
c) pressure gradients and wellhead pressures for several flow tests;
d) temperature gradients for several flow and shut-in tests.

Test number 9 in Broadlands 13 was chosen to be matched because flowing bottomhole temperatures were measured in that test. Test number 11 was also simulated because it corresponded to a different test in the same well, and offered the largest rate difference with test 9.

To match these two tests, only a very short drawdown test was simulated. The purpose of this test was to draw the reservoir down to the correct bottomhole conditions as measured in the wellbore, and to provide the wellbore with the proper fluid input. Reservoir permeability was adjusted to vary the reservoir drawdown at the specified rates. The reservoir and wellbore characteristics given in Tables 4 and 5 were used to match the test data given in Tables 6 and 7.

An excellent match of the two tests was achieved during the short drawdown tests, as in Figures 8 and 9. The wellhead conditions of well 13 during test 9 were calculated at 426°F and 317 psig, with a total enthalpy of 532 BTU/lb. The pressure drop calculated by the model was 0.101 psi/ft, which matched the 0.101 psi/ft gradient actually measured. The wellhead conditions of test 11 were calculated as 446°F and 481 psig, with a total enthalpy of 516 BTU/lb. The calculated and measured overall pressure gradients were 0.169 psi/ft and 0.168 psi/ft, respectively.

The only error in the two simulation runs is that the calculated enthalpy does not match the measured wellhead enthalpy. This discrepancy is probably due to either using a different standard condition, or from errors in the reservoir description used in the match. One assumption, the reservoir temperature of 535°F, agrees with the shut-in temperatures reported in Figure 9, but can greatly effect enthalpy and steam quality at the wellhead and may be the source of error.

The computer runs made for all the above verification simulations are given in a separate binder entitled Appendix A.

IV. GEOTHERMAL WELL TEST DATA

As a resource base, data from well tests at Cerro Prieto, Mexico, the Hawaiian Geothermal Project, Wairakei and Broadlands in New Zealand, and several geothermal fields in California, and Italy were collected. Many of the published well test data found in industry or in the literature consist of tests of single-phase flow or tests in which flashing occurs in the wellbore. At the time of this study, only one test from Cerro Prieto and several tests from the Hawaiian Geothermal Project (HGP) described two-phase flow data in sufficient detail for use in this study. Other test data may be available, but little has been published to date. This study, therefore, uses only these two reservoirs as data bases.

A. CERRO PRIETO DATA

The actual well test data utilized was presented as a multi-rate test of a producing well by Rivera-R. and Ramey.[17] The test was patterned after a two-rate testing procedure described by Selim,[18] and consisted of measuring bottomhole and wellhead pressures after a rate change in the flowing well. The well was produced at a stabilized rate prior to the test, and standard bourdon tube pressure gauges were used downhole.

The Cerro Prieto geothermal field is located at the southern end of the Salton Trough, a geologic feature crossing the California-Mexico border and containing other geothermal fields such as Heber and East Mesa. The Cerro Prieto field is a liquid dominated system consisting of alternating sandstone and shale layers resting on a highly fractured granitic basement. Fluid is produced as a steam-water mixture with bottomhole temperature in excess of 300°C and producing rates greater than 24,000 B/D.

The nature of the Cerro Prieto reservoir has not been well defined in the literature. The reservoir has been described as "a very complex, probably highly fractured structure" in one area by some investigators,[19] and in another area as an unfractured porous-permeable medium.[20] Results from interference testing indicate that formation permeability thickness products (kh) on the order of 46,206 md-ft are present,[19] while transient, single well tests have yielded results of about 6,385 md-ft.[17] Well tests conducted in the single phase East Mesa field suggest that the first estimate of reservoir kh is more correct for structures in the Salton Trough.

The well test was conducted on well M-21A. This well is completed with a slotted liner open to 508.6 feet of pay, and is produced through 7 5/8" casing. The actual date of the test was not reported, but is estimated as early 1977. At this time the reservoir contained 316°C (601°F) fluid with an enthalpy of 343 kcal/kg (618 BTU/lb). These flowing conditions are a decrease from the 363°C (685°F) and 513 kcal/kg (924 BTU/lb) initial flow conditions reported in September of 1974. Prior to the well test, the well is estimated to have been producing 179.5 tons/hr (396 th.lb/hr). The well rate was stabilized at 111.0 tons/hr (244.7 th.lb/hr) for two days immediately before the test.

The test was initiated with the lowering of a standard bourdon-type pressure gauge and recording the stabilized bottomhole flowing pressure for 15 minutes. The well rate was then reduced to about 66.1 tons/hr. (145.7 th.lb/hr) for 24 minutes, and then returned to the stabilized rate for 21 minutes. Wellhead pressures and mass flow rates were continually measured during the test, which yielded the data presented in Figures 10 through 13. A slight discrepancy appears in the data occuring at the times when the rate changes, but the data was used as presented.

The reservoir description of the Cerro Prieto reservoir was obtained as a synthesis of data from several sources. The reservoir thickness was defined as the net interval open to production through the slotted liner. Formation heat capacity and conductivity, and the heat conductivity and capacity of the overburden and underburden were taken from data on the East Mesa field. The initial reservoir description determined from transient testing[17] is a reservoir permeability of 12.6 md and a porosity of 20 percent. The reservoir temperature and pressure at the time of the test were estimated to be 544°F and 997 psia, and a steam saturation near the wellbore of 30 percent. A complete description of the reservoir and wellbore is given in Table 8.

The quality of the test data is fair, but additional data must be obtained during transient testing of two-phase wells. Obtaining wellhead steam quality or total fluid enthalpy by some means is very important. Also, rates should be accurately measured and corrected so that the rate and pressure data agree as to the time of significant events. These items may have been recorded, but they were not reported with the other data. Another more serious problem concerns the lack of adequate relative permeability data for steam-water flow. The data used for the Cerro Prieto well test is based on an analytical relationship for two-phase flow in clean sandstone, and is presented in Figure 14. These curves are probably incorrect, and present a severe handicap as they influence calculated steam quality, reservoir pressure and reservoir temperature changes during flowing tests.

B. HAWAIIAN GEOTHERMAL PROJECT DATA

Data from the Hawaiian Geothermal Project (HGP) has been obtained from several reports[20] furnished by HGP and the University of Hawaii, and some production data furnished directly by HGP. The well tests have been conducted on an exploratory well drilled in the Kapoho Geothermal Reservoir. This is a liquid-dominated reservoir on the island of Hawaii near the Kilauea volcano. The reservoir is believed to be composed of volcanic basalt that contains open fracture zones separated by unfractured, impermeable zones.

The HGP-A well was completed in April, 1976, with a 7 5/8" slotted liner from 2216 ft to 6435 ft. It was flow tested several times between July, 1976 and May, 1977. The original reservoir pressure at 6250 ft was estimated as about 2300 psia, and the bottomhole temperature at the same datum was about 640°F (338°C). During production, fluid entered the wellbore from zones at 4300 feet and 6200 feet, with the top zone probably producing high quality steam and the lower layers producing undersaturated water. Several temperature profiles are given in Figure 14 along with a partial description of reservoir layering and fluid distribution.

The major tests conducted on HGP-A were:

1. July, 1976 - 4 hour flow test and buildup;
2. November, 1976 - 2 week flow test and buildup;
3. December, 1976 - 6 1/2 day variable discharge test and buildup;
4. January, 1977 - 2 week throttled flow test and buildup;
5. March, 1977 - 42 day flow test and buildup.

During most of these tests, the following information was recorded or calculated:

1. Wellhead pressure and temperature;
2. Total mass rate, steam rate and quality;
3. Fluid enthalpy and thermal power;
4. Temperature and pressure profiles;
5. Fluid level during buildup.

A Kuster pressure and temperature bomb was lowered in the well to obtain profiles at various times, but no continuous bottomhole readings were obtained. Of this data, the July, 1976 data was too short and the December, 1976 test was not completed. The other three drawdown and multi-rate tests are presented in Figures 15 through 20.

Buildup data for this well was obtained from water level and wellhead pressure measurements after each flow test. These buildup tests indicated that the reservoir had a permeability-thickness of about 1000 md-ft and probably was severely damaged. The temperature recovery as measured in the wellbore was the same for each test, however condensation and cooling did cause temperature variations in the wellbore after shut-in.

A complete description of the reservoir and wellbore of the HGP-A well is given in Table 9. As shown in Figure 14, the reservoir is divided into three zones. The top and bottom zones are considered to be fractured and productive, separated by a massive, unfractured center zone. The top zone also produces saturated steam as indicated on temperature surveys, and is hotter than the central zone. There is some evidence that the top zone acts as a steam cap and expands downwards during very high flow rates, but this was not considered in this study. The lower zones contain undersaturated water which may flash to steam near the wellbore. The Kapoho reservoir is suspected as being very large, and subject to recharge.

The reservoir is characterized as being low porosity, about 3 percent, and low permeability, an average of 0.4 md over the 2435 foot interval. This permeability is probably too low for the more productive top and bottom zones. The wellbore has been characterized as being severly damaged, but the pressure drop across the damaged zone seems to be decreasing with each successive flow test. The heat capacity and heat conductivity data for the reservoir and overburden were assumed to be 40 BTU/FT^3-^{o}F and 35 BTU/FT-DAY-^{o}F, respectively, which are slightly higher than for the Cerro Prieto field.

The quality of the data seems to be exceptionally good except for the lack of continuous flowing bottomhole pressures. Again, there exists the problem of no relative permeability data. For this test, a different set of relative permeability data was used, as shown in Figure 22. This data is based upon the calculated steam-water relative permeability ratios presented by Ehlig-Economides,[22] (see Figure 23), and some observations on steam-water relative permeabilities in cyclic steam injection wells.[23] These curves do not resemble conventional relative permeability curves and are probably not accurate. They do fit the observed behavior of one field in New Zealand, but they may not apply to the Kapoho reservoir.

V. SIMULATION OF GEOTHERMAL WELL TESTS

The Cerro Prieto and HGP well tests were simulated using the geothermal reservoir and wellbore model described earlier. The history matches obtained are reasonable, but not unique. The parameters used to obtain the history match were reservoir permeability and steam saturation, with minor adjustments to reservoir temperature and pressure. Also, for the Cerro Prieto M-21A well test match, the length of the wellbore was altered to produce a more correct pressure drop to the surface.

The Cerro Prieto M-21A well test data was matched using the rates given in Figure 24. A good match was obtained with a reservoir permeability of 75 md over the 508.6 foot pay, a 20 percent porosity, and a skin factor of -2.29. This corresponds to a formation permeability-thickness of 38,147 md-ft. The match is presented in Figures 25 through 27. The uniqueness of the reservoir permeability is shown in Figure 28, which shows other trial matches at lower permeabilities. The pressure drop through the tubing is calculated as steady state flow, but this assumption is not too bad. The length of the flowing wellbore was shortened to 3608 feet for this match, and the correlation of Hagedorn and Brown with slippage was used. The history match was repeated with several other empirical correlations for two-phase flow using a 3990 foot flow length, producing the results given in Figure 29. The greatly different pressure drops calculated by the different correlations does little to increase the confidence of the wellhead history match, or the accuracy of the pressure drop calculations.

The overall history match is reasonably good. This history match was used as the basis for many other simulated well tests. These tests were simulated to illustrate the influences of flow rate, permeability, porosity, thickness, skin damage, and formation temperature upon a tested well. These simulations of the history match and simulated well tests are included as Appendix B, and summaries of these well tests are presented in Appendix D. These well tests will be analyzed in the next section.

The HGP-A well tests were simulated using the three layer model described earlier. To match the wellhead pressures of the multi-rate test, the permeability-thickness of the reserovir was increased from 1000 md-ft to 5900 md-ft, with an average skin factor of about +15. This reservoir description did not match the initial flow data very well in the multi-rate test, shown in Figures 30 and 31. The same description did not match either of the other two tests as well, again particularly the early flowing data, as in Figures 32 and 33. These matches were particularly difficult because of the lack of bottomhole data. This made it impossible to separate wellbore effects from transient reservoir response.

The HGP-A reservoir and wellbore description was used to investigate the effects of a fracture system in the reservoir. These simulations are included in Appendix C, with summaries in Appendix D.

VI. WELL TEST ANALYSIS

The analysis of the transient wellhead and bottomhole pressure data has been done using several different techniques. These techniques differ in assumptions made about fluid properties, description of fluid phases, and the handling of relative permeabilities. Using existing one-phase test analysis techniques the results from both wellhead and sandface pressure analysis are unreliable for geothermal wells producing both steam and water at the sandface. The analysis of test data from wells producing only a single phase isothermally is much more reliable.

A. SINGLE PHASE APPROXIMATIONS

The basic analysis simplification of single phase approximations is that the steam-water mixture can be accurately represented as a single phase having average fluid properties, and test data can be accurately analyzed using a correctly specified "total" density and viscosity. Implicit to this approximation is the assumption that the saturations of steam and water are constant near the wellbore, and that no phase change occurs between the sandface and the measurement point. To use this type of analysis, it is necessary to measure the volumes or masses of the respective phases.

A subset of this approximation is to assume that only one phase is flowing, and the response of the other phase is negligible. This situation exists often in single-phase reservoirs where condensation or vaporization occurs only in the wellbore or in the reservoir to a very limited extent. The assumptions used in single phase analysis can be violated without creating large inaccuracies in many tests involving the evolution of a gaseous phase during liquid phase production as long as the liquid phase remains volumetrically greater than the evolved gas phase. This routinely occurs in the production testing of oil wells. Problems have been noted during the testing of volatile reservoirs, however, and definitely are present in two-phase geothermal wells.

The most practical single-phase testing procedure for testing two-phase geothermal reservoirs is the injection and falloff test. This test involves injecting cool water into the reservoir for a period of time while measuring the increase in sandface pressure with conventional equipment. The reservoir near the wellbore should begin to approximate single-phase behavior, from which reservoir permeability can be calculated. Once the injection is stopped, the pressure and temperature recovery at the sandface can be measured to re-calculate reservoir permeability and possibly indicate heat conductivity and capacity of the rock near the wellbore. The advantages of this procedure are that existing technology and techniques can be utilized, and the effects of two-phase flow can be greatly reduced.

The basic equation for single-phase pressure test interpretations is the logarithmic approximation of the line source solution of the diffusivity equation resulting from the combination of Darcy's Law and the continuity equation. The use of the diffusivity equation assumes isothermal flow of fluids of small and constant compressibility, constant permeability, porosity and viscosity, and that pressure gradients are small. The final approximate solution also includes the assumptions of radial flow throughout entire formation thickness, a homogeneous and isotropic porous medium of uniform thickness, and negligible gravitational forces.[1]

The basic equation described above in standard oil field units is:

$$P_{wf} = P_i - \frac{162.6\, q\mu\beta}{kh}\left[\log\left(\frac{kt}{\emptyset\mu c_t r_w^2}\right) - 3.23 + 0.87S\right] \qquad (5)$$

where the terms are:

P_{wf} - flowing wellbore pressure (at sandface), psi
P_i - initial reservoir pressure, psi
q - volumetric flow rate at standard conditions, STB/day
μ - average fluid viscosity at reservoir conditions, cp
β - average fluid volume factor to convert from standard to reservoir volumetric condition, RB/STB
k - formation permeability, md
h - formation thickness, ft
t - flowing time, hrs
$\emptyset$ - formation porosity, fraction
c_t - total compressibility (includes rock and fluid compressibilities), psi^{-1}
r_w - wellbore radius, ft
S - Wellbore skin factor, dimensionless.

The measurement of volumetric flow rates is not common practice in geothermal fields, so other forms of this equation present rates as mass flow rates and steam quality fractions, defined as the mass fractions of steam. The mass flow rate can then be multiplied by specific volumes, v, to yield the volumetric flow rates. This equation has been presented in geothermal units as:[17]

$$P_{wf} = P_i - 527.4 \frac{w v_{sc} \mu \beta}{kh} \left[\log \left(\frac{kt}{\phi \mu c_t r_w^2} \right) + 0.891 + 0.87S \right] \quad \text{..................(6)}$$

where the altered units are:

P	-	kg/cm^2
w	-	ton/hr
v_{sc}	-	cm^3/gr
h	-	m
c_t	-	$(kg/cm^2)^{-1}$
r_w	-	cm.

In this study, the standard oil field units were used except for flow rate units. Flow rates were used as mass flow rates, and specific volumes were defined at reservoir conditions to eliminate the volume factor. These changes produced the following equation:

$$P_{wf} = P_i - 695.05 \frac{w v \mu}{kh} \left[\log \left(\frac{kt}{\phi \mu c_t r_w^2} \right) - 1.847 + 0.87S \right] \quad \text{..................(7)}$$

The units of this equation are:

P	-	psi
w	-	lb/hr
v	-	ft^3/lb (at reservoir conditions)
μ	-	cp
h	-	ft
t	-	days
ϕ	-	fraction

c_t - psi^{-1}
r_w - ft
S - dimensionless.

These units were chosen as consistent with the units used in INTERCOMP's Geothermal Reservoir Simulatior. The use of these equations generally involves plotting sandface pressure, P_{wf}, against the logarithm of time. During radial flow conditions, this plot should produce a straight line with a slope defined as:

$$m = 695.05 \frac{wv\mu}{kh} \qquad (8)$$

This equation can be solved for kh or k if the other parameters are known or can be estimated, but the permeability calculated is the effective permeability which includes relative permeability effects. The average specific volume and viscosity should be calculated as a mass average product based upon the reservoir flowing steam quality.

A second parameter which could be derived from the well test is the wellbore skin damage factor, S. This can be calculated by re-arranging the flow equation above, and substituting the measured slope for the multiplier outside the parenthesis. The skin factor can then be calculated based upon known formation properties and the pressure drop between the initial pressure and the ideal pressure at one hour. This ideal pressure is defined as the pressure located upon the straight line of slope m at a time of one hour, and may not correspond to the measured pressure at one hour. This equation for skin from the drawdown test is:

$$S = 1.151 \left[\frac{P_i - P_{1hr}}{m} - \log \left(\frac{k}{\phi \mu c_t r_w^2} \right) + 3.227 \right] \qquad (9)$$

The last term, +3.227, may be changed to +1.847 if the ideal pressure at one day is used.

To evaluate the skin factor, k should be evaluated from the slope, m, and ϕ and P_i should be known. The fluid viscosity should be an average value based upon saturations in the reservoir. The total compressibility, however, must account for the phase change of the fluids, and cannot simply be represented as the sum of steam, water and rock compressibilities.[9] One method of estimating the total compressibility of the system is to assume that phase change is the dominant effect, and estimate "apparent" compressibility with the following relationship:[24]

$$c_t = \frac{1}{\phi}\left[(1-\phi)\,\rho_f C_f + \phi\, S_w\, \rho_w C_w\right](7.749 \times P^{-1.66}) \qquad (10)$$

where:

c_t - "apparent" compressibility caused by phase change, psi^{-1}
ϕ - formation porosity, fraction
$\rho_f C_f$ - formation heat capacity, BTU/ft^3 - ^oF
S_w - water saturation, fraction
ρ_w - water density, lb/ft^3
C_w - water heat capacity, BTU/lb - ^oF
P - pressure, psia

Using this equation, the "apparent" compressibility for a range of pressures, formation heat capacities, and porosities has been calculated and are given in Figure 34.

The calculation of the wellbore skin factor involves many assumptions which are often violated, and the value of skin is influenced to some degree by all of the errors present in calculating average fluid properties, determining correct straight lines, and estimating true system compressibility. The calculation of skin becomes much more difficult when the phase changes near the wellbore become very large.

In spite of all the previously mentioned problems encountered in attempting to analyze two-phase data by single phase techniques, possibly the most serious drawback is the assumption of isothermal flow. The change in temperature with pressure during two-phase flow causes heat to flow between the fluid and the formation. The net gain or loss of heat tends to offset the change of phase of the flowing fluid, and influences the pressure measured at the wellbore.

An additional complication of using single phase theory involves the choosing of average conditions. To correctly evaluate a test, the fluid and formation properties must be true averages in both time and space. Just as fluid properties can vary with pressure in time and space, formation properties such as thickness, permeability and porosity can be considered functions of temperature and/or pressure, or can vary spatially due to heterogeneous deposition or history. Usually, variations in formation parameters are ignored, and the pressure dependent properties are calculated at an average pressure. In this study, the average pressure during a test is chosen at the temporal mid-point of the test. The average steam quality is also defined at that time.

B. Two-Phase Approximations

Two-phase equations describe the flow of a steam-water mixture in the reservoir as fluids of different mobilities. Each fluid is represented with a correct specific volume, viscosity, and relative permeability factor, but each of these terms must be evaluated as an average in time and space. Therefore, a better representative of the flowing fluid is obtained, while some limitations remain.

The basic equation proposed to handle two-phase flow can be constructed by the replacement of total kinematic viscosity, v_T, for average fluid properties in Equation 7. Total kinematic viscosity combines relative permeability terms along with densities and viscosities as:

$$v_T = \left[\frac{k_{rs} \; \rho_s}{\mu_s} + \frac{k_{rw} \; \rho_w}{\mu_w} \right]^{-1} \quad \text{..............................(11)}$$

This was used by Garg[10] to represent two-phase flow by defining total kinematic mobility as:

$$(k/v)_T = \left[\frac{k \; k_{rs} \; \rho_s}{\mu_s} + \frac{k \; k_{rw} \; \rho_w}{\mu_w} \right] \quad \text{..............................(12)}$$

Utilizing these equations, the two flowing phases in the reservoir are more properly represented, but the application of these relationships to transient well test analysis is limited. The total kinematic mobility can be calculated from the straight line on a semi-log plot of pressure against time. Formation permeability cannot be calculated from total kinematic mobility unless the relative permeabilities found in total kinematic viscosity are estimated. The total kinematic mobility is not constant [10, 11] during flow tests however, and only an average value can be calculated. The influence of heat transfer is assumed negligable by this analysis technique.

Using a relationship presented by Grant and Sorrey[24], a relative permeability ratio between water and steam can be estimated from production data during a well test. The equation presented is:

$$\frac{k_{rw}}{k_{rs}} = \frac{v_w}{v_s} \frac{(H_s - H_T)}{(H_T - H_w)} \quad \text{.........................(13a)}$$

Utilizing the definition of steam quality, X, this equation can be represented as:

$$\frac{k_{rw}}{k_{rs}} = \frac{\mu_w}{\mu_s} \frac{\rho_s}{\rho_w} \frac{X}{(1-X)} \quad \text{................................(13b)}$$

If relative permeabilities for steam and water are known, this relationship provides the additional data required to specify each phase relative permeability. The task remaining is to correctly estimate flowing steam quality in the reservoir from wellhead measurements. Changes in steam quality at the sand face due to skin effects further complicate this problem.

Changes from one to two-phase flow and vice-versa during testing require that two-phase mobilities and compressibilities be used in the test analysis. As mentioned before, total kinematic mobility can change during a test, with the greatest changes occuring during the transition between one and two-phase flow. At this time, the change in apparent compressibility can be several orders of magnitude[9], which will also alter the pressure behavior of the well.

C. Wellbore Effects

During flow testing, wellhead measurements of pressure and temperature are generally obtained in addition to bottomhole data. The wellhead data is used to calculate mass flow rate and surface steam quality. One assumption which can be made during test analysis is that wellbore heat losses are negligable, and that bottomhole enthalpy equals wellhead enthalpy. Then, if bottomhole pressure is known, the sandface steam quality can be calculated. For many problems, the wellbore heat losses can be significant. To correct for heat loss effects, a simple calculation such as the one described by Satter[25] can be used to estimate bottomhole conditions.

The effects of wellbore storage in geothermal wells has been shown to be quite different than the effects routinely noted in oil and gas wells.[26] Because geothermal reservoirs have greater fluid producing capacities than hydrocarbon reservoirs, the early time transient behavior of geothermal wellbores do not follow the classical solutions outlined for oil and gas wells. Particularly, the early time unit slope due to wellbore storage is altered, and may not be present. Also, the early time bottomhole response can be influenced by condensation or evaporation in the wellbore during the test. These phase changes can cause the sandface flow rate to change even after other wellbore storage effects have died out.

The length of time that wellbore storage effects are significant is determined by the wellbore conditions at the time of the test, and the type of test. For one two-phase well, wellbore storage effects during drawdown tests lasted ten times longer than did wellbore storage effects during buildup tests.[27] Also, erratic pressure changes at both the wellhead and sandface have been predicted.[26]

In order to use wellhead data to calculate reservoir parameters from transient well tests data, all wellbore storage effects and heat loss effects must be negligible. The test must be designed to produce a constant pressure drop through the wellbore so that wellhead pressure changes mirror sandface pressure changes. These conditions are not likely to occur during very short transient tests, particularly if a well is shut-in before or during the test.

D. Multiple Rate Analyses

Almost all transient well tests are conducted in such a manner as to involve more than a single producing rate. To analyse such tests, the principle of superposition is used to combine the pressure effects of multiple rates. The analysis of multi-rate tests is slightly more complicated than for single rate tests since a plotting function, such as the Horner time ratio, must be calculated. To analyse two-rate tests, the modified equation representing the approximate analytical solution is:

$$P_{wf} = P_i - 695.05\,\frac{w_2 v_2 \mu_2}{kh}\left[\log\left(\frac{k}{\phi \mu c_T r_w^2}\right) - 1.847 + 0.87S\right]$$
$$-695.05\,\frac{w_1 v_1 \mu_1}{kh}\left[\log\left(\frac{t+\Delta t}{\Delta t}\right) + \frac{w_2 v_2 \mu_2}{w_1 v_1 \;\; 1}\log(\Delta t)\right] \quad \text{........(14)}$$

To utilize this equation, measured sandface pressure, P_{wf}, is plotted against the plotting function, defined as:

$$PF = \log \frac{t+\Delta t}{\Delta t} + \frac{w_2 v_2 \mu_2}{w_1 v_1 \mu_1} \log (\Delta t) \quad \ldots\ldots (15)$$

From this plot on cartesian paper, a straight line should result which represents the reservoir permeability as follows:

$$k = 695.05 \frac{w_1 v_1 \mu_1}{mh} \quad \ldots\ldots (16)$$

This analysis technique is less certain than single rate analyses because average fluid conditions must be defined for multiple rates, reservoir heat transfer effects are more complicated, and saturation dependent relative permeabilities may change from one rate to another.

E. Effects of Well Flow Rate

Using the reservoir and wellbore description used in history matching the Cerro Prieto M-21A well test, a series of two-rate flow tests were made to investigate the influence of producing rate upon the analysis of well test. Five tests were simulated with the following flow times and rates:

Test 1-400,000 lb/hr for 7 days, 100,000 lb/hr for 7 days;
Test 2-100,000 lb/hr for 7 days, 350,000 lb/hr for 7 days;
Test 3-300,000 lb/hr for 7 days, 200,000 lb/hr for 7 days;
Test 4-300,000 lb/hr for 21 days, 200,000 lb/hr for 7 days;
Test 5-200,000 lb/hr for 7 days, 300,000 lb/hr for 7 days.

Tabulations and graphs of these tests are presented in Appendix D. The single rate drawdown tests were first analysed using the single-phase equations presented earlier for both sandface and wellhead data for permeability and skin. The tests were re-analysed for permeability using two-phase equations and the relative permeability data of Figures 14 and 35. The results of these calculations are presented in Table 10, which includes the analysis of the second flow rates for permeability using two-rate, single phase equations.

These results show that one-phase calculations based upon wellhead pressure and quality data are the least inaccurate technique for calculating reservoir permeability. Wellhead data almost always resulted in higher calculated permeabilities than sandface data, and two-phase equation results were consistantly greater than single-phase equation results. The single and two-rate sandface data results were more consistant than the wellhead data results, and were incorrect because of saturation dependent relative permeabilities. The accuracy of the single phase equations with wellhead data is probably more coincidental than rigorously justified because more assumptions and approximations were made than with other methods. These results are shown in Figure 36.

The multi-rate calculations produced better results than did single rate calculations for many of the tests. The use of multi-rate test schedules does not overcome many of the problems associated with these tests, and they are more difficult to conduct. However, multi-rate tests are quite useful for testing already producing wells, and can be used to confirm the results of other tests.

Skin factors calculated from single phase equations show a decrease with increasing rate, and are not very accurate. These skin factors were calculated using the "apparent" compressibility due to vaporization or condensation of steam-water mixtures.

Three simulations were made on the Hawaiian Geothermal Project well to duplicate the results of the Cerro Prieto well tests. These tests were run at rates of 86,000 lb/hr., 75,000 lb/hr., and 65,000 lb/hr. The analysis of these tests produced the results given in Table 10. The same trends were noticed in these test results: higher permeabilities calculated at higher flow rates and the wellhead data calculated permeabilities larger than the sandface data. The calculated permeabilities were very close to the actual overall permeability of 2.4 md. This may be due to multi-phase flow only occurring in the bottom layer of the reservoir model, with the top layer producing only steam and the middle layer producing only water. Even though both steam and water entered the wellbore, the test behaved more like a single phase test since relative permeability effects were negligible.

F. Injection Testing

Well test 6 was simulated with the injection of water at 100^{o}F into the two-phase reservoir described earlier. The reservoir grid system was reduced to a 200 foot radial system for this simulation to increase numerical accuracy. The test data was generated by 350,000 lb/hr. of water into the reservoir for two hours, and then doubling the rate for another two hours. The results of this test procedure are calculated permeabilities of 63.2 md. and 77.1 md. for each of the two tests, and a calculated skin factor of -1.55. At the end of the test, only water existed for a radius of 13 feet around the wellbore, and temperature and pressure increases were calculated out to over 30 feet.

G. Effects of Wellbore Skin Damage

Two additional well tests were simulated with increased wellbore stimulation to study the effects of the skin zone around the wellbore. Skin is represented analytically as an additional pressure drop occurring as fluid enters the wellbore and is idealized as having no thickness. Mathematically, in the reservoir model, skin is represented as a region of increased or decreased permeability surrounding the wellbore. Skin is altered in the model by increasing or decreasing the permeability of this region.

During the history matching of the M-21A well test data, it was observed that the results of the test were very sensitive to permeability changes near the wellbore where fluid velocities and pressure gradients are the greatest. Small changes in skin factors created large pressure changes at the wellhead and the sandface.

As presented in Appendix D, increasing the skin factor from -2.29 to -2.31 and -2.33 altered the pressure response level of the well. The slope of the straight lines on the semi-log graphs were not greatly influenced, and permeabilities of 31.7 and 25.1 were calculated for skin factors of -2.31 and -2.33 respectively. Skin factors calculated from these tests were -0.59 and -1.14.

H. Effects of Reservoir Temperature

Since two-phase reservoir temperature and pressure are linked by the physical properties of steam and water, any changes in temperature must be accompanied by changes in pressure. The enthalpy of the reservoir fluid can be altered by changing the fluid saturations at a given temperature and pressure. For well test 9, the initial steam saturation in the reservoir was reduced to zero while the reservoir was maintained at a saturated condition. The reservoir temperature was then decreased by 10°F to produce an undersaturated reservoir at the same pressure in well test 10.

Both tests produced two-phase steam and water during the well test when produced at a high rate, but at a low rate the initially undersaturated reservoir produced only water. Steam qualities during both tests were lower than earlier simulations, reflecting the lower fluid enthalpies. Reservoir permeabilities calculated from these simulated well tests were 32.09 and 30.32 md. from single phase equations using sandface data. Values for skin factor were +0.04 and -0.09.

I. Effects of Reservoir Permeability

Using reservoir permeabilities of 35 md., 50 md., 75 md., and 100 md., two-rate well tests were simulated at 300,000 lb/hr. The simulated well test at 35 md. was unable to sustain the required rate for longer than two days, and less data was used to interpret the test. The sandface pressure response during three of these tests are given in Figure 37. The analysis of these tests give the following results from single phase equations:

Test	Actual Permeability, md.	Calculated Permeability, md.	Calculated / Actual	Skin
11	35.0	18.09	0.52	+2.67
12	50.0	23.11	0.46	+0.62
13	75.0	31.33	0.42	+1.30
14	100.0	41.23	0.41	+1.27

The calculated permeabilities do increase with true formation permeability, but the calculated results are more inaccurate with increasing permeability. Calculated skin factors are erratic and not very accurate.

J. Effects of Formation Thickness

According to analytical equations, changes in formation thickness should behave the same as changes in formation permeability, and the same pressure response should be calculated whenever the formation permeability-thickness product is the same. Several simulations with a formation permeability of 75 md. and thicknesses of 169.54 feet, 339.08 feet, and 678.16 feet were made to investigate the influence of formation thickness on calculated permeability.

In Figures 38 and 39, a comparison of two simulations with the same formation permeability-thicknesses shows that identical slopes are not present. The model predicts that the influence of formation height is not the same as that of formation permeability. This indicates that the analytical equations used in both one and two-phase well test analysis are incorrect.

K. Effects of Formation Porosity

The predicted response of changing porosity is an upward or downward shift of the drawdown curve from the analytical equations, and no change in slope should be observed. Simulated well tests with 20, 10 and 5 percent formation porosities, as in Figure 40, do show change in slope along with the expected vertical movement. These simulations indicate that decreasing formation porosity has the same effect as decreasing formation permeability or thickness.

L. Influence of Heat Transfer

One assumption made during the derivation of the single and two-phase flow equations was negligible heat transfer between the fluid and rock. This assumption was tested by making a simulation in which the rock contained no heat. This simulation resulted in almost the same performance as when heat transfer is considered except that an upward shift in pressure resulted (See Figure 41). The calculated steam saturations around the wellbore, shown in Figure 42, were changed considerably, as was the produced steam quality. The assumption of no heat transfer between rock and flowing fluid is not the only source of error in the analysis of these tests, as for this one example, the formation permeability calculated was unchanged.

M. Effect of Fractures

The simulation of two-phase flow in fractured geothermal reservoirs is much more difficult than flow in unfractured reservoirs. To represent a fractured reservoir, the HGP-A reservoir was redefined as a six layer system containing two horizontal fractures. The fractures were located between previously defined layers 1 and 2 and between 2 and 3. Also, layer 2 was separated into two equal layers.

The fractures in these simulations were about one-eigth of an inch wide, and were assigned a permeability of approximately 110 D. This gave the two fractures a conductivity of 1.2 D-ft. each. The matrix permeabilities were reduced to 0.46 md., 0.04 md., and 0.55 md. for the three layers. The total reservoir permeability-thickness was 2,749 md-ft., which is about one-half of the previous formation permeability-thickness.

Several attempts were made to simulate these fractures in the HGP-A well, but oscillations in the predicted pressure response could not be eliminated without re-defining the reservoir characteristics completely. A second set of simulations was attempted using an r-z-θ mode and representing a single vertical fracture through each of the three layers, but this produced no better results. One effect noted from these simulations was that calculated pressure drops decreased even though the formation permeability-thickness decreased. A second observation noted from these simulations was that lower quality steam was produced from the wellbore, while the flash front moved deeper into the unsaturated reservoir. These changes in overall flow characteristics indicate that the presence of fractures may be detectable from well tests.

V. CONCLUSIONS

The simulation of geothermal well tests in two-phase geothermal reservoirs has shown that conventional one-phase analytical solutions are not completely satisfactory techniques. Some allowances of two-phase flow conditions must be made in order to correctly characterize the reservoir. Two-phase methods of analysis require additional data concerning fluid relative permeabilities and phase saturations in the reservoir, and potentially can produce better results.

Conventional flow equations and well test interpretation technique do not correctly represent the flow of steam and water in geothermal reservoirs. Unlike tests in hydrocarbon reservoirs, formation permeability and thickness do not "trade-off" and produce identical test results for identical permeability-thickness products. Also, formation porosity influences the slope of the pressure response instead of just altering the level of response, and the production rate does not have a linear influence on the pressure response.

Two of the analytical problems with the flow of steam and water are the effects of heat transfer between flowing fluid and the rock, and the large apparent compressibility due to the phase behavior of the fluids. The influence of heat transfer was found to be small for one simulation. This simulated well test showed that heat transfer between fluid and rock during a drawdown test acted like an additional skin zone around the wellbore and shifted the pressure response downwards. The flash front was better defined due to heat transfer, and higher steam saturations were present behind the flash front.

Apparent compressibility can be predicted as a function of pressure and rock properties to allow for phase changes during well testing, but the changes of compressibility with time during the test have not been considered. As shown in calculated data presented earlier, the apparent compressibility can change by two orders of magnitude during drawdown testing. This change appears as a change in the logarithmic term of the analytical equations, and can influence the slope of the semi-log pressure response. Changes in pressure also alter the vicosities and specific volumes of both steam and water, but the proper use of average properties can overcome this problem.

Another problem encountered in the analysis of test data is the estimation of flowing reservoir conditions from wellhead measurements. Since fluid enthalpy cannot yet be measured downhole and saturations estimation techniques are unproven, allowing for phase changes down the tubing and at the sandface make the calculation of fluid mobilities in the reservoir uncertain. This problem is reduced somewhat when steam and water are flowing in a segregated manner as in the HGP-A well tests.

This study has also shown that an analysis based upon wellhead measurements may not be reliable, and may produce answers either higher or lower than the actual reservoir value. Single phase analyses of sandface data result in low values of permeability because relative permeability effects are ignored. Two-phase data must use the correct relative permeability data corrected for phase changes at the sandface for accurate formation permeability estimates.

Further work should be conducted to investigate the influence of fractures on the pressure response of two-phase geothermal well tests. Also, it is necessary to further refine all the analytical solutions for use in two-phase wells as no techniques in use in industry are completely adequate.

For transient well testing in two-phase geothermal reservoirs, the most reliable test results can be obtained from injection and falloff testing by the injection of cold water into the reservoir. These tests can utilize existing technology and hardware to produce valid test data after a one-phase region has been established near the wellbore. Injection testing into production wells may completely eliminate production testing in many reservoirs. Also, injection testing can be used with multi-rate testing to measure relative permeability effects during drawdowns, and possibly could be used to calculate reservoir saturations.

REFERENCES

1. Matthews, C.S., and Russell, D.G.: "Pressure Build-Up and Flow Tests in Wells", Monograph series, Society of Petroleum Engineers of AIME, Dallas, (1967), Volume 1.

2. Earlougher, R.C.: "Advances in Well Test Analysis", Monograph series, Society of Petroleum Engineers of AIME, Dallas, (1977), Volume 5.

3. Chen, B.H.: "Geothermal Reservoir and Well Test Analysis: A Literature Survey", Technical Memorandum No. 2, Hawaii Geothermal Project, National Technical Information Service, U.S. Dept. of Commerce, Springfield, VA. (Sept., 1974).

4. Ramey, H.J., Jr.: "Pressure Transient Analysis for Geothermal Wells", Proceedings of Second United Nations Symposium on the Development and Use of Geothermal Resources, San Francisco, CA., (May, 1975), Volume 3, p. 1749-1757.

5. Barelli, A., Manetti, G., Celati, R., and Neri, G.: "Build-Up and Back-Pressure Tests on Italian Geothermal Wells," Proceedings of Second United Nations Symposium on the Development and Use of Geothermal Resources, San Francisco, CA., (May, 1975), Volume 3, p. 1537-1546.

6. Witherspoon, P.A., Narasimhan, T.N., and McEdwards, D.G.: "Results of Interference Tests from Two Geothermal Reservoirs", SPE 6056, 51st Annual Fall Technical Meeting of SPE-AIME at New Orleans, Oct. 3-6, 1976.

7. Rice, L.F.: "Pressure Drawdown and Buildup Analysis in Geothermal Reservoirs", Proceedings of 11th IECE Conference of AICE (1976), Volume I, p. 798-801.

8. Gulati, M.S.: "Pressure and Temperature Buildup in Geothermal Wells", Proceedings of First Stanford Geothermal Workshop, Stanford University, Palo Alto, CA., Dec. 15-17, 1975.

9. Grant, M.A.: "Two-Phase Linear Geothermal Pressure Transients: A Comparison with Single-Phase Transients", New Zealand Journal of Science, (1978), Volume 21, p. 355-364.

10. Garg, S.K.: "Pressure Transient Analysis for Two-Phase (Liquid Water/Steam) Geothermal Reservoirs", SPE 7479 presented at 53rd Annual Fall Technical Meeting of SPE-AIME at Houston, Texas, Oct. 1-3, 1978.

11. Moench, G.F.: "Radial Steam Flow in Two-Phase Geothermal Reservoirs-Comparison of Analytical and Finite-Difference Solutions for Transient Pressure Drawdown", SPE 7959 presented at the 1979 California Regional Meeting of SPE-AIME at Ventura, CA., April 18-20, 1979.

12. Coats, K.H.: "Geothermal Reservoir Modeling", SPE 6892 presented at 52nd Annual Fall Technical Meeting of SPE-AIME, Denver, Colorado, Oct. 9-12, 1977.

13. Gould, T.L.: "Vertical Two-Phase Steam-Water Flow in Geothermal Wells", Journal of Petroleum Technology, (August, 1974), p. 833-842.

14. Kruger, P., and Ramey, H.J., Jr.: "Stimulation and Reservoir Engineering of Geothermal Resources", Stanford Geothermal Program Report No. SGP-TR-1, June, 1974.

15. Thomas, K.L., and Pierson, R.: "Three Dimensional Geothermal Reservoir Simulation", SPE 6104 presented at 51st Annual Fall Technical Meeting of SPE-AIME in New Orleans, Oct. 3-6, 1976.

16. Toronyi, R.M.: "Two-Phase, Two-Dimensional Simulation of a Geothermal Reservoir and the Wellbore System", PhD Thesis, Penn. State University, University Park, PA., (1974).

17. Rivera-R.,J., and Ramey, H.J., Jr.: "Application of Two-Rate Flow Tests to the Determination of Geothermal Reservoir Parameters", SPE 6887 presented at the 52nd Annual Fall Technical Meeting at Denver, Colorado, Oct. 9-12, 1977.

18. Salim, M.A.: "A Modification of the Two-Rate Flow Method for Determination of Reservoir Parameters", J. Institute of Petroleum, Volume 53, No. 527, November 1967, P. 343-352.

19. Rivera-R.,J., Samaniego-V., and Schroader, R.C.: "Pressure Transient Testing at

Cerro Prieto Geothermal Field", unpublished technical paper, Lawerence Berkeley Laboratory, Berkeley, CA.

20. James, R.: "Drawdown Test Results Differentiate Between Crack Flow and Porous Bed Permeability", Proceedings of the Second United Nations Symposium on the Development and Use of Geothermal Resources, San Francisco, CA., (May, 1975), Volume 3, p. 1693-1696.

21. Yuen, P.C., Chen, B.H., Kikara, D.H., Seki, A.S., and Takahasi, P.K.: "HGP-A Reservoir Engineering", Technical Report from the Hawaii Geothermal Project, University of Hawaii, Honolulu, Hawaii, September 1978. (Other reports listed in reference).

22. Ehlig-Economides, C.: "Recent Developments in Well Test Analysis", presented at 4th Stanford Geothermal Workshop held at Stanford University, Palo Alto, CA., December, 1978.

23. Dietrich, J.D.: "Relative Permeability During Cyclic Steam Stimulation of Heavy Oil Reservoirs", SPE 7968 presented at 1979 California Regional Meeting of SPE-AIME in Ventura, CA., April 18-20, 1979.

24. Grant, M.A., and Sorrey, M.L.: "The Compressibility and Hydraulic Diffusivity of a Water-Steam Flow", to appear in Water Resources Research, (in press).

25. Satter, A.: "Heat Losses During Flow of Steam Down a Wellbore", Journal of Petroleum Technology, (July, 1965), p. 845-851.

26. Miller, C.W.: "Wellbore Storage Effects in Geothermal Wells", SPE 8203, presented at 54th Annual Fall Technical Meeting of SPE-AIME in Las Vegas, Nevada, Sept. 23-26, 1979.

27. Gringarten, A.C.: "Well Testing In Two-Phase Geothermal Wells", SPE 7480 presented at 53rd Annual Fall Technical Meeting of SPE-AIME in Houston, Texas, Oct. 1-3, 1978.

TABLES

TABLE 1
DESCRIPTION OF SYNTHETIC CORE
STANFORD BENCH MODEL

Initial Pressure	267 psia
Permeability	98.5 md
Porosity	.36
Initial Temperature	377.8 ^{o}F to 361.4 ^{o}F
Initial Water Saturation	1.0
Rock Compressibility	3×10^{-6} psi^{-1}
Formation Specific Heat	40 BTU/ft^{3}-^{o}F
Thermal Conductivity	29 BTU/^{o}F-ft-day
Length of Core	23.5 inches
Diameter of Core	2 inches
ΔX	.0979166, .195833, .195833, . . ., .0969166, .001 ft.

TABLE 2
DRAWDOWN TEST DATA
FOR GARG'S TWO-PHASE PROBLEM

Initial Pressure	1305.2 psia
Initial Temperature	572 ^{o}F
Permeability	10.133 md
Porosity	0.2
Initial Water Saturation	1.0
Rock Compressibility	0.0 psi^{-1}
Formation Specific Heat	39.53 BTU/ft^{3}-^{o}F
Thermal Conductivity	72.72 BTU/ft-day-^{o}F
Thickness	100 ft
R_w =	1.84 ft
R_e =	24,128 ft.
Radial Grid Increments	$\Delta r_1 = \Delta r_2 = ... = \Delta r_{11} = 3.281$ ft, $\Delta r_{n+1} = (\Delta r_n)\ (1.2)$
Mass Flow Rate =	33,840 lb$_m$/hr

TABLE 3
RESERVOIR DATA
FOR TORONYI'S TWO-PHASE PROBLEM

Initial Temperature	494.9 °F
Initial Pressure	652.0 psia
Permeability	1000 md
Porosity	0.501
Initial Water Saturation	0.20
Formation Compressibility	5.0×10^{-6} psi^{-1}
Formation Specific Heat	38.62 BTU/ft^3-°F
Thermal Conductivity	23.98 BTU/ft-day-°F
Length of Reservoir	6000 ft
Width of Reservoir	600 ft
Thickness of Reservoir	1000 ft
ΔX =	1000 ft
ΔY =	100 ft
Mass Flow Rate	200,000 lb_m/hr

Relative Permeability Data:

Sw	krw	krg
0.05	0.0	1.0000
0.10	0.000001	0.8895
0.15	0.000115	0.7814
0.20	0.000580	0.6771

TABLE 4
DESCRIPTION OF WELLBORE, BROADLANDS 13

1. 8-5/8 J55 36 lb casing from surface to 1459'
2. 7-5/8 J55 26.4 lb casing from 1459' to 2602'
3. 6-5/8 J65 24 lb slotted liner from 2602' to 3534'

TABLE 5
RESERVOIR PROPERTIES
FOR BROADLANDS 13 PROBLEM

Permeability	2 md
Formation Thickness	1000 ft
Porosity	0.20
Rock Compressibility	4×10^{-6} psi^{-1}
Rock Heat Capacity	30.0 BTU/lb ^{o}F
Rock Thermal Diffusivity (Wellbore)	1.5 ft^2/hr
Rock Thermal Conductivity	30.0 BTU/ft-hr-^{o}F
Overburden Thermal Conductivity	30.0 BTU/ft-hr-^{o}F
Overburden Specific Heat	20.0 BTU/ft^3-^{o}F
No Underburden Heat Loss	
Specific Gravity of Water	1.0
Surface Tension of Water	72 dynes/cm
Surface Temperature	100^{o}F
Reservoir Depth	3483 ft.
Initial Reservoir Pressure	1324 psig
Initial Reservoir Temperature	535^{o}F

TABLE 6

FLOW TEST 9 IN BROADLANDS 13

6-26-69 @ 230,000 lb/hr and 575 BTU/lb

TIME	WHP, psig	DEPTH, ft.	TEMP, °C	PRESSURE, psig
14:45	310	3400	-	654
14:55	310	3200	-	593
15:02	310	3000	251	565
15:10	310	2800	248	540
15:17	310	2600	244	512

TABLE 7

FLOW TEST 11 IN BROADLANDS 13

7-10-69 @ 136,000 lb/hr and 605 BTU/lb

TIME	WHP, psig	DEPTH, ft.	TEMP, °C	PRESSURE, psig
15:30	465	3400	-	1040
15:36	465	3200	-	963
15:41	465	3000	-	897
15:47	465	2800	-	842
15:53	465	2600	-	799

TABLE 8
DESCRIPTION OF RESERVOIR AND WELLBORE
CERRO PRIETO M-21A

A. RESERVOIR PROPERTIES

Depth	3739 ft.
Permeability (From History Match)	75 md.
Porosity	0.20
Thickness	508.62 ft.
Rock Compressibility	4×10^{-6} psi^{-1}
Rock Heat Capacity	39.53 BTU/FT^3-^{o}F
Rock Thermal Conductivity	35.0 BTU/FT-DAY-^{o}F
Over/Underburden Heat Capacity	35.0 BTU/FT-^{o}F
Over/Underburden Thermal Capacity	31.0 BTU/FT-^{o}F
Radial Extent	24,128 ft.

B. WELLBORE PROPERTIES

Length	3608 ft.
Radius (0'-3607')	6,969 in.
(3607'-3608')	5.921 in.
Roughness (0'-3607')	0.0006 in.
(3607'-3608')	0.0018 in.
Heat Transfer Coefficient	1.25 BTU/FT^2-HR-^{o}F
Surface Temperature	90.0^{o}F
Bottomhole Temperature	543^{o}F

Steady State Heat Loss

Linear Temperature Gradient to Surface

Hagedorn-Brown Two Phase Correlation with Slippage

C. INITIAL CONDITIONS

Pressure	996.5 psia
Temperature	543.8 ^{o}F
Steam Saturation (0'-3000')	0.30
(3000'-24128')	0.00

TABLE 9

DESCRIPTION OF RESERVOIR AND WELLBORE

HGP-A

A. RESERVOIR PROPERTIES

Depth	4000 ft.
Permeability (From History Match) -	
Layer 1	7.85 md
Layer 2	0.71 md
Layer 3	8.95 md
Porosity (All Layers)	0.03
Thickness - Layer 1	300 ft
Layer 2	1900 ft
Layer 3	235 ft
Rock Compressibility (All Layers)	5×10^{-6} psi^{-1}
Rock Heat Capacity (All Layers)	40 BTU/FT^3-$^\circ$F
Rock Thermal Conductivity (All Layers)	35 BTU/FT-DAY-$^\circ$F
Over/Underburden Heat Capacity	40 BTU/FT^3-$^\circ$F
Over/Underburden Thermal Capacity	35 BTU/FT-DAY-$^\circ$F
Radial Extent (All Layers)	25,000 ft

B. WELLBORE PROPERTIES

Length	4000 ft
Radius (0'-2000')	8.755 in.
(2000'-4000')	6.969 in.
Roughness (0'-2000')	0.0018 in.
(2000'-4000')	0.0054 in.
Heat Transfer Coefficient	1.25 BTU/FT^2-HR-$^\circ$F
Surface Temperature	90°F
Bottomhole Temperature	567.1 $^\circ$F

Transient Heat Loss

Geothermal Gradient: Depth, ft.	Temperature, °F
0-500	106.23
500-1108	123.22
1108-1662	130.22
1662-2216	274.31
2216-2662	433.20
2662-3108	545.6
3108-3554	545.6

Hagedorn-Brown Two-Phase Correlation with Slippage

C. INITIAL CONDITIONS

Pressure -	Layer 1	1624.2 psia
	Layer 2	1988.2 psia
	Layer 3	2331.4 psia
Temperature -	Layer 1	565.3 °F
	Layer 2	561.0 °F
	Layer 3	619.2 °F
Steam Saturation -	Layer 1	1.0
	Layer 2	0.0
	Layer 3	0.0

TABLE 10. THE INFLUENCE OF

FLOW RATE ON THE RESULTS OF TEST ANALYSIS

SINGLE RATE DRAWDOWNS OF SEVEN DAYS EACH - CERRO PRIETO

Test	Rate, lb/hr	Calculated Permeability, md Wellhead 1 PH.	Calculated Permeability, md Wellhead 2 PH.	Calculated Permeability, md Sandface 1 PH.	Calculated Permeability, md Sandface 2 PH.	1PH. Sandface Calculated Skin
1	400,000	88.40	242.62	32.60	116.21	+0.72
2	100,000	94.77	176.56	30.44	128.54	+1.88
3	300,000	65.28	217.80	31.10	121.17	+1.30
5	200,000	70.96	263.92	31.92	128.78	+1.60

MULTI-RATE DRAWDOWNS OF SEVEN DAYS PER RATE - CERRO PRIETO

Test	1st Rate, lb/hr	2nd Rate, lb/hr	Calculated Permeability, md Single Phase Equations Wellhead	Calculated Permeability, md Single Phase Equations Sandface
1	400,000	100,000	55.90	67.66
2	100,000	350,000	28.42	41.56
3	300,000	200,000	61.22	43.23
4	300,000 *	200,000	63.33	41.96
5	200,000	300,000	70.26	35.71

* 21 DAY DRAWDOWN

SINGLE RATE DRAWDOWN OF FOURTY-ONE DAYS - HGP-A

Test	Rate, lb/hr	Calculated Permeability, md Single Phase Equations Wellhead	Calculated Permeability, md Single Phase Equations Sandface
1	86,000	2.97	2.58
2	75,000	2.53	1.65
3	65,000	2.21	1.51

FIGURES

ANALYTICAL RELATIVE PERMEABILITY
CURVES FOR $Sw_c = 0.3$ & $Sg_c = 0.05$

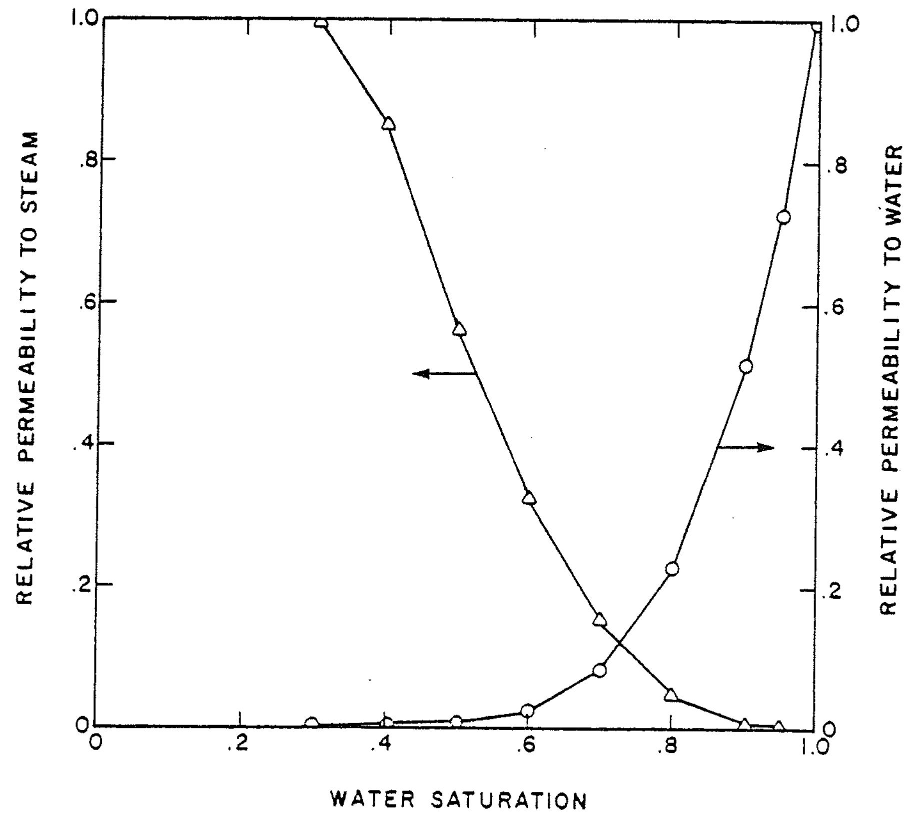

FIGURE 1

OUTLET PRESSURE DATA FOR BENCH MODEL
(FROM STANFORD REPORT, SGP-TR-1)

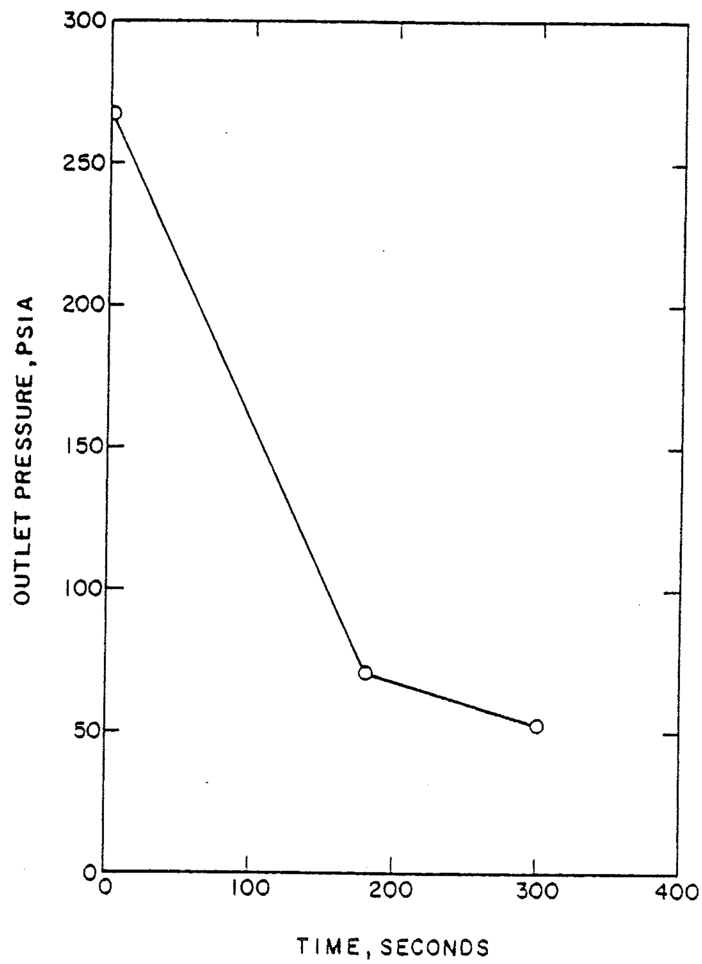

FIGURE 2

COMPARISON OF MEASURED AND CALCULATED PRESSURES AT 300 SECONDS FOR BENCH MODEL

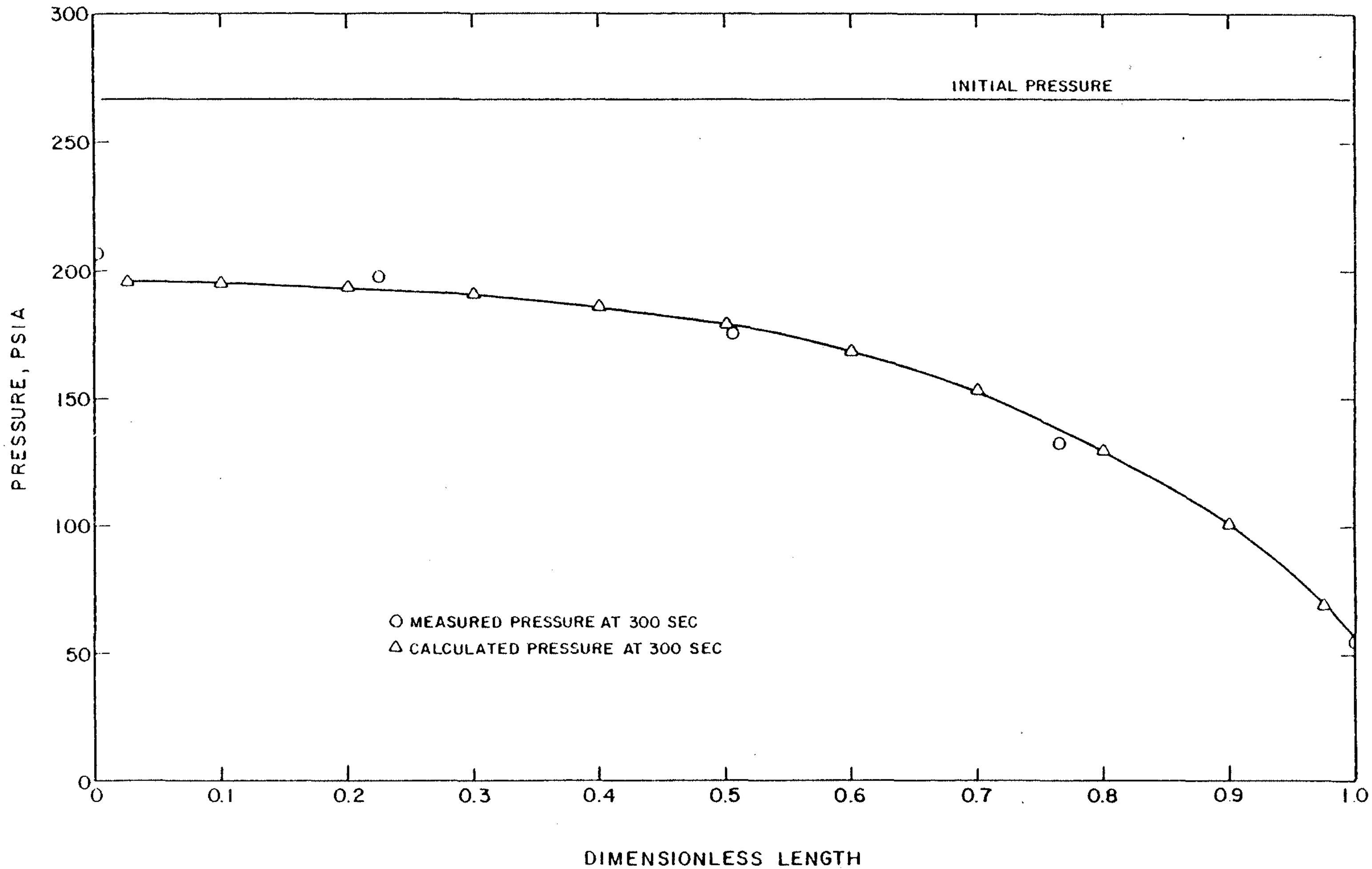

FIGURE 3

COMPARISON OF MEASURED AND CALCULATED TEMPERATURES AT 300 SECONDS FOR BENCH MODEL

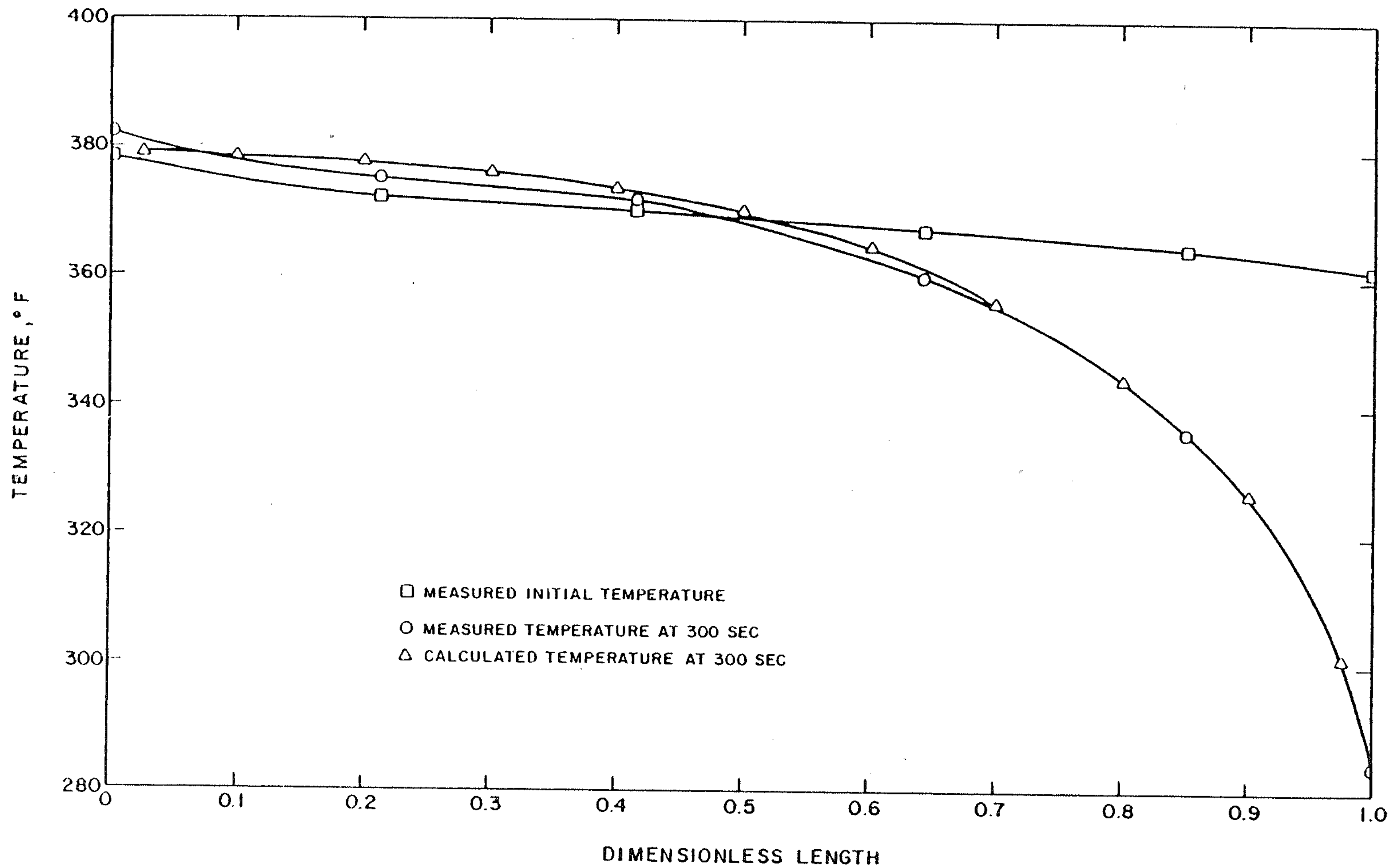

FIGURE 4

COMPARISON OF CALCULATED SATURATIONS
AT 180 AND 300 SECONDS FOR BENCH MODEL

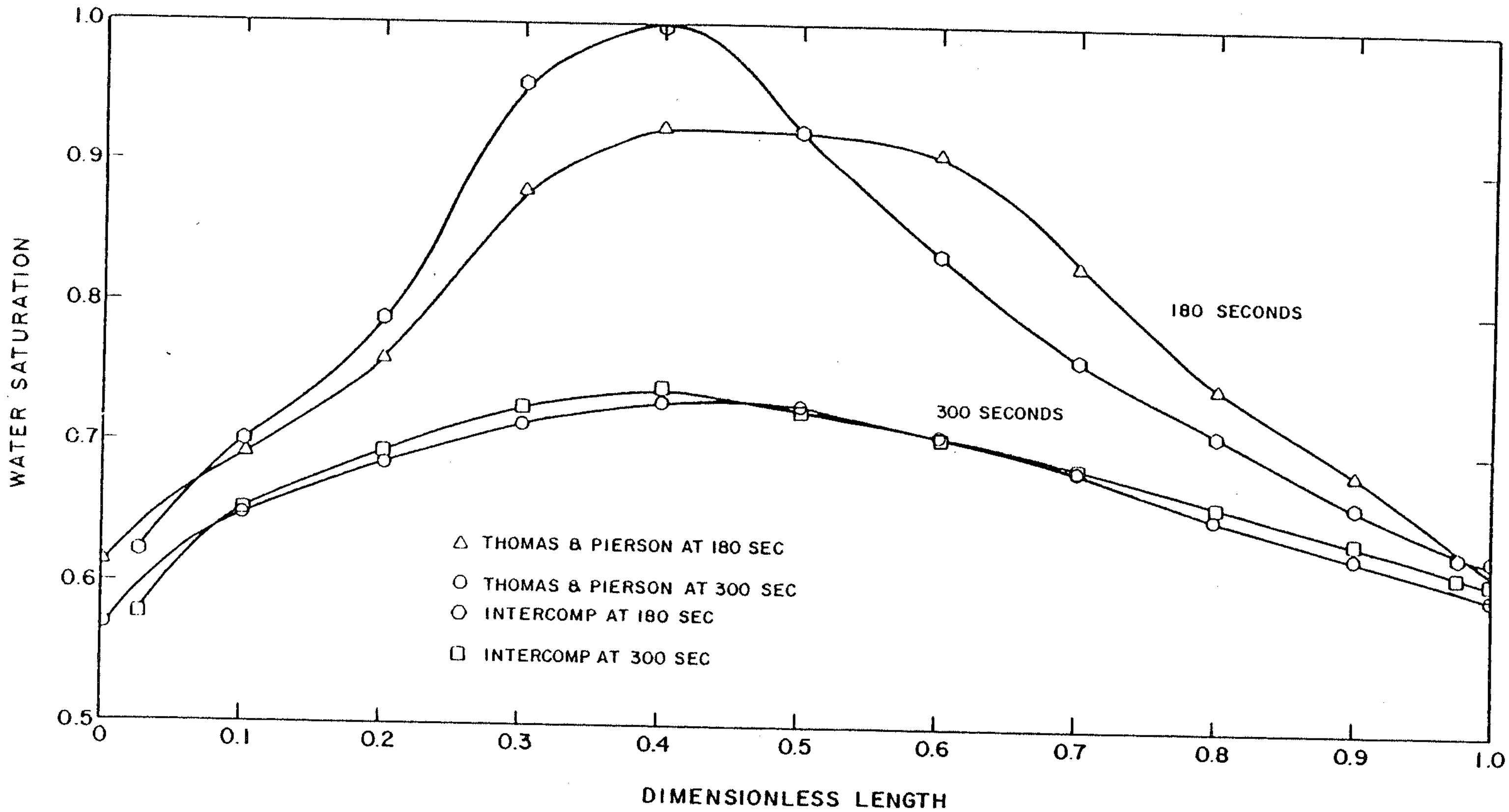

FIGURE 5

TWO – PHASE DRAWDOWN
COMPAIRING INTERCOMP'S AND GARG'S NUMERICAL RESULTS

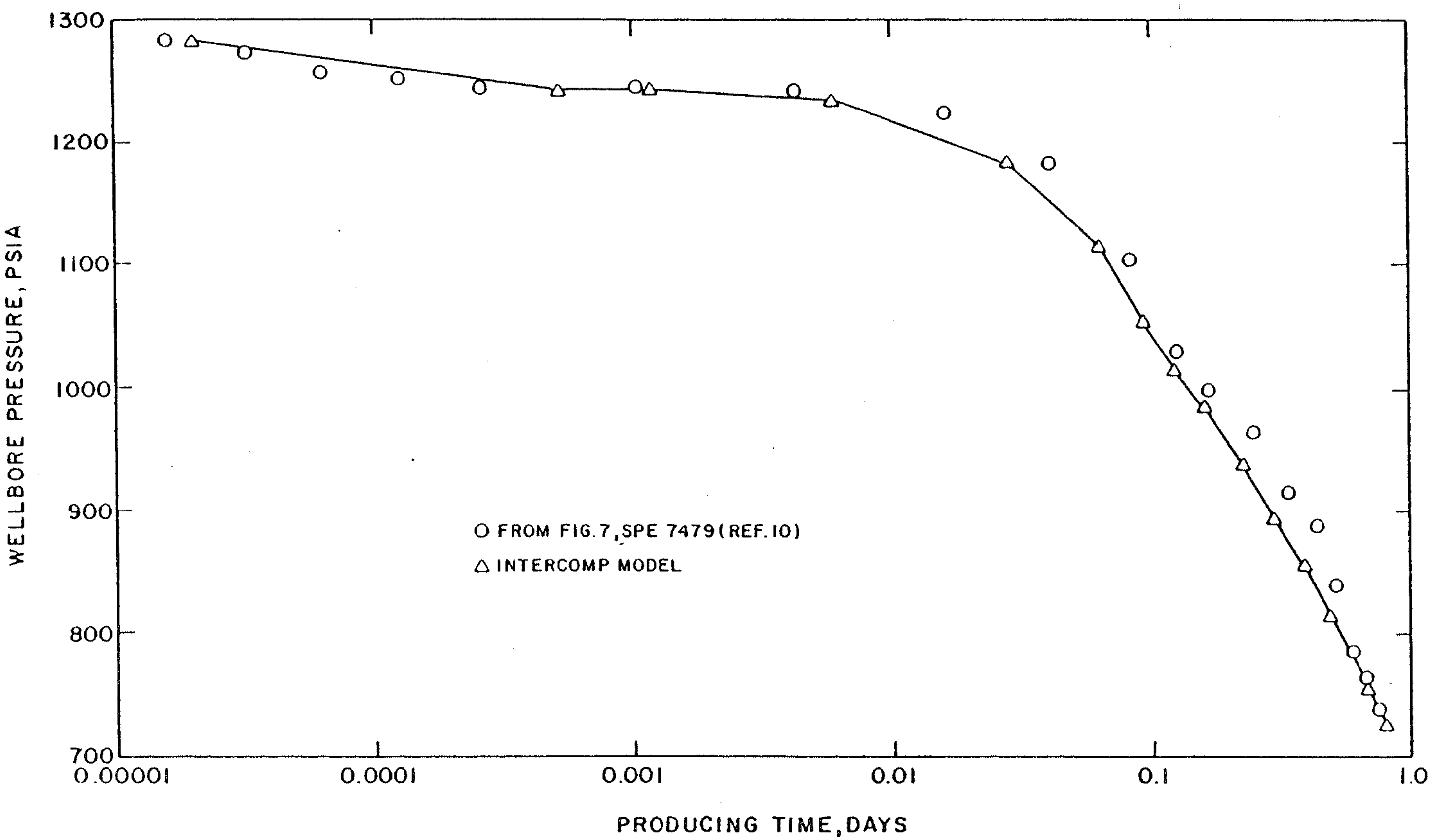

FIGURE 6

COMPARISON OF CALCULATED SATURATIONS
FOR THE TWO-PHASE RESERVOIR
PROBLEM OF TORONYI

.817	.827	.847	.882	.851	.836
.817	.827	.847	.883	.851	.836
.817	.827	.847	.882	.851	.836
.817	.827	.847	.882	.851	.836
.817	.827	.847	.880	.851	.836
.817	.827	.847	.880	.851	.836

A. STEAM SATURATIONS CALCULATED BY TORONYI

.819	.828	.848	.879	.851	.838
.819	.828	.848	.880	.851	.838
.819	.828	.848	.874	.851	.838
.819	.828	.848	.879	.851	.838
.819	.828	.848	.877	.851	.838
.819	.828	.848	.877	.851	.838

B. STEAM SATURATIONS CALCULATED BY INTERCOMP

FIGURE 7

PRESSURE MATCH OF BROADLAND WELLBORE DATA

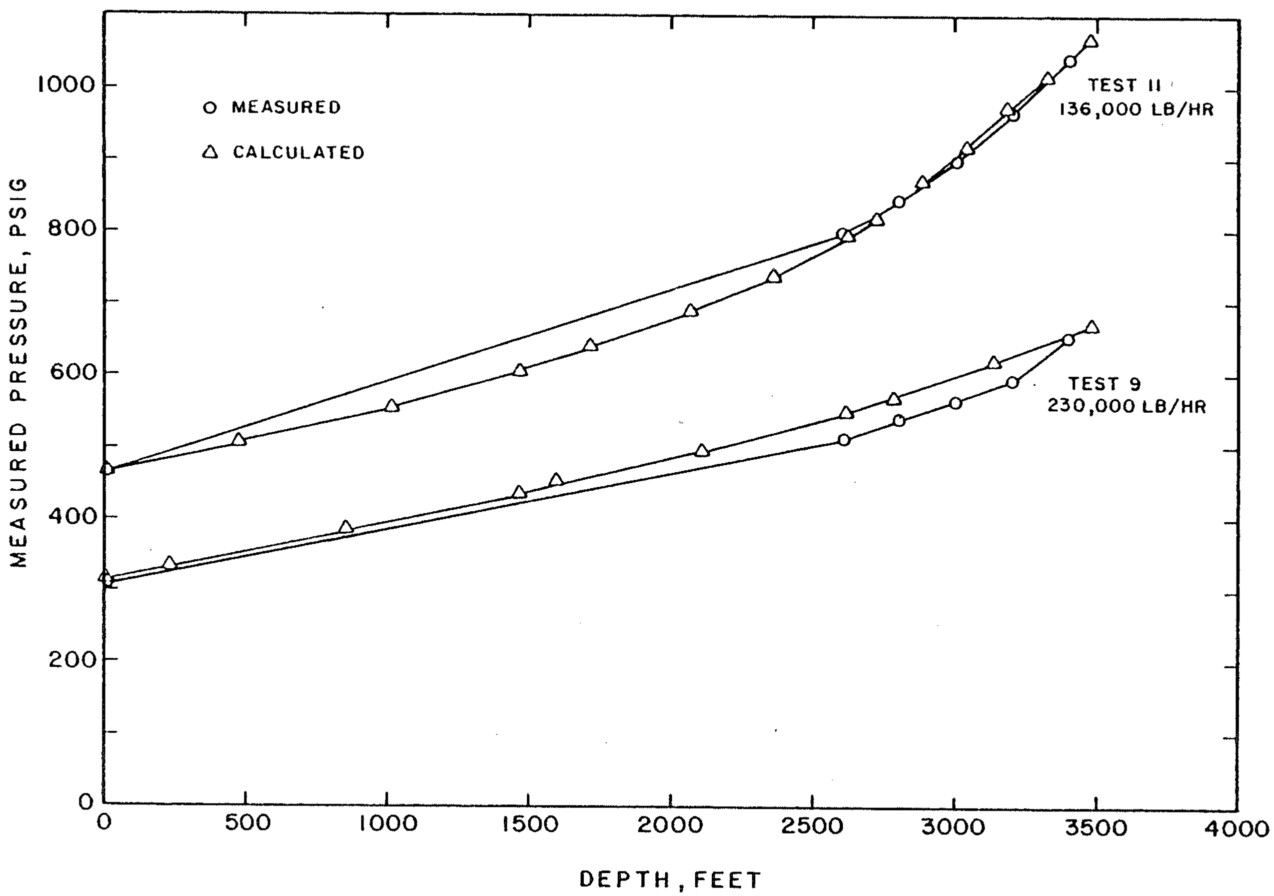

FIGURE 8

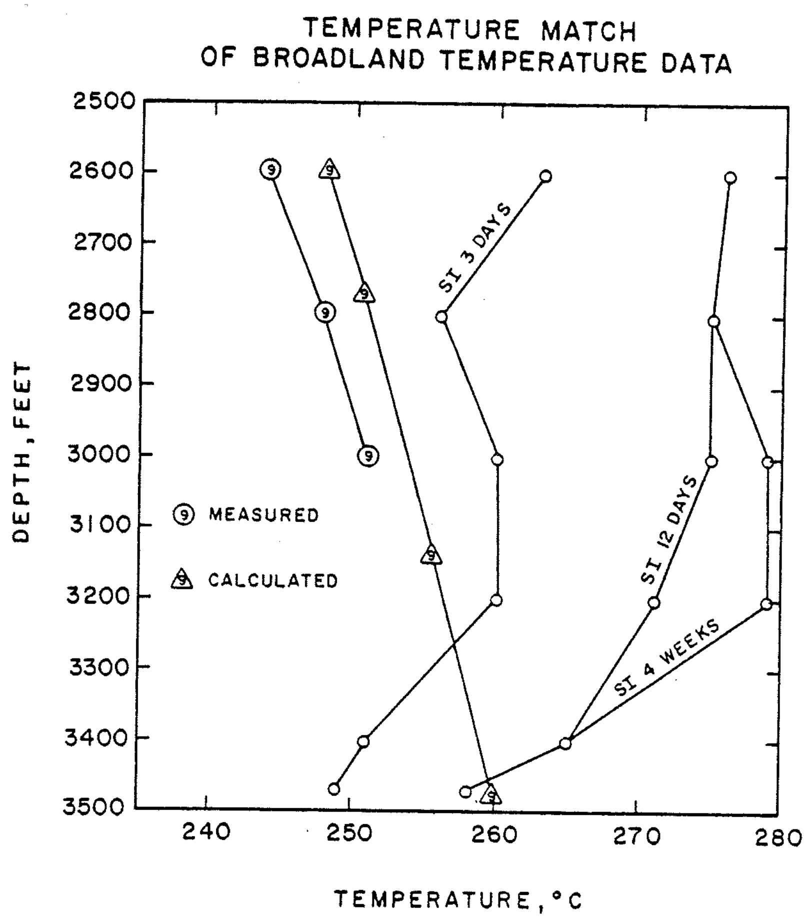
TEMPERATURE MATCH
OF BROADLAND TEMPERATURE DATA
2500
2600
2700
2800
2900
3000
3100
3200
3300
3400
3500
DEPTH, FEET
240
250
260
270
280
TEMPERATURE, °C
SI 3 DAYS
SI 12 DAYS
SI 4 WEEKS
MEASURED
CALCULATED

FIGURE 9

MEASURED MASS FLOW RATE FOR CERRO PRIETO WELL TEST

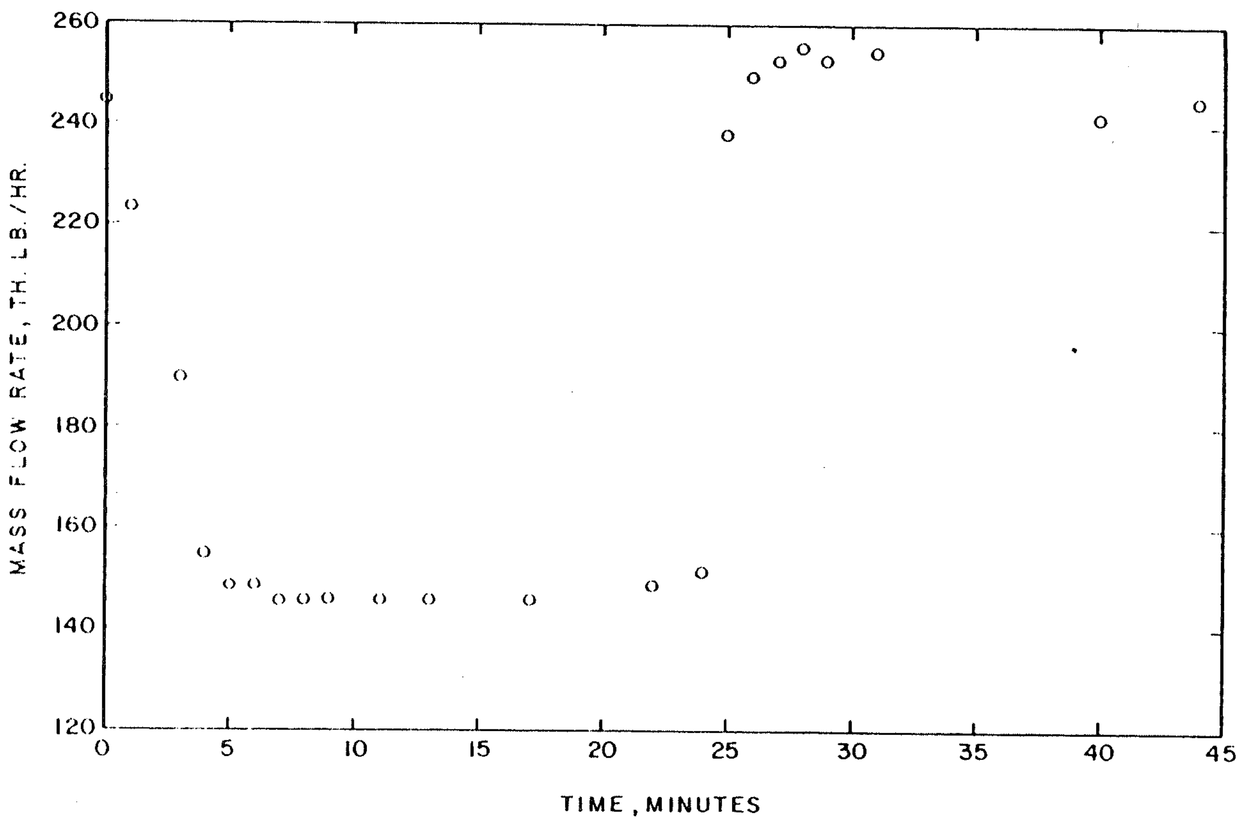

FIGURE 10

MEASURED WELLHEAD PRESSURE
FOR CERRO PRIETO WELL TEST

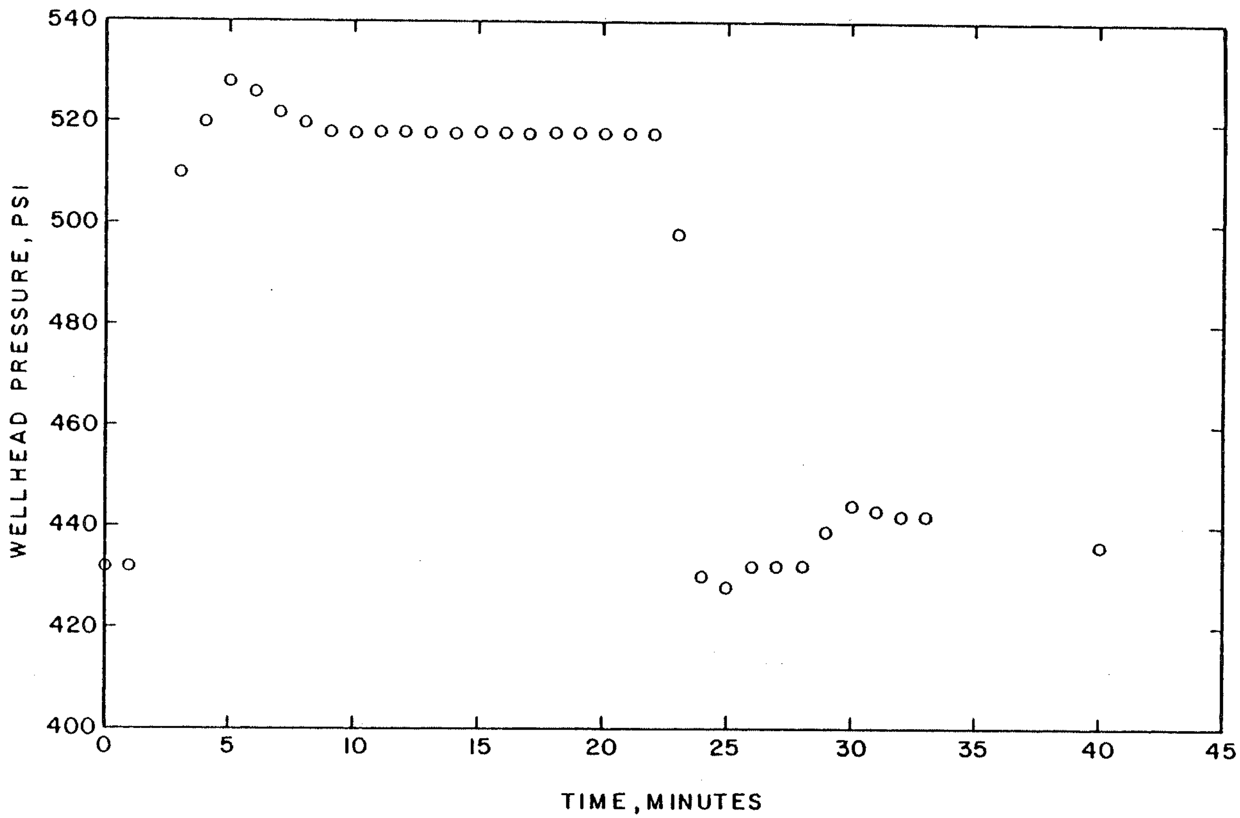

FIGURE 11

MEASURED BOTTOM-HOLE PRESSURES
FOR CERRO PRIETO WELL TEST

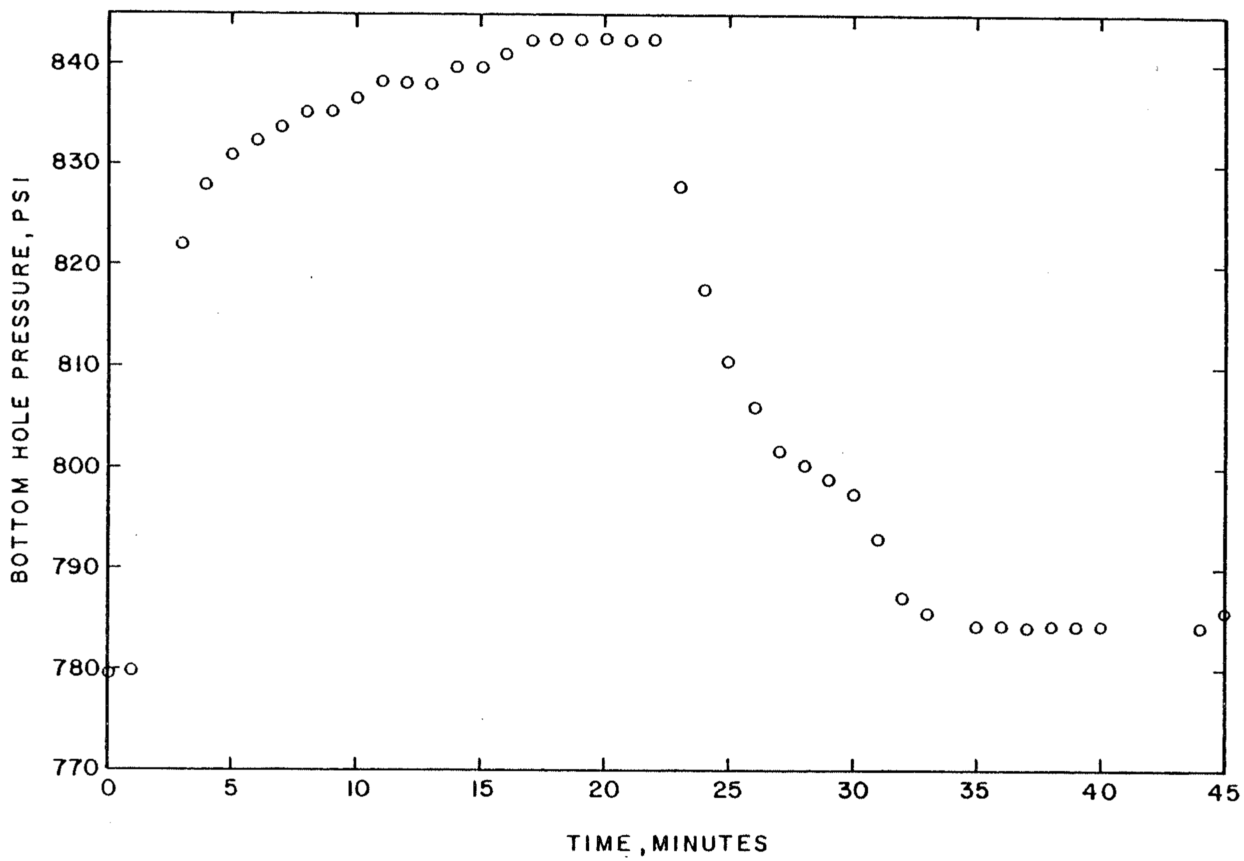

FIGURE 12

MEASURED PRESSURE DROP IN TUBING
FOR CERRO PRIETO WELL TEST

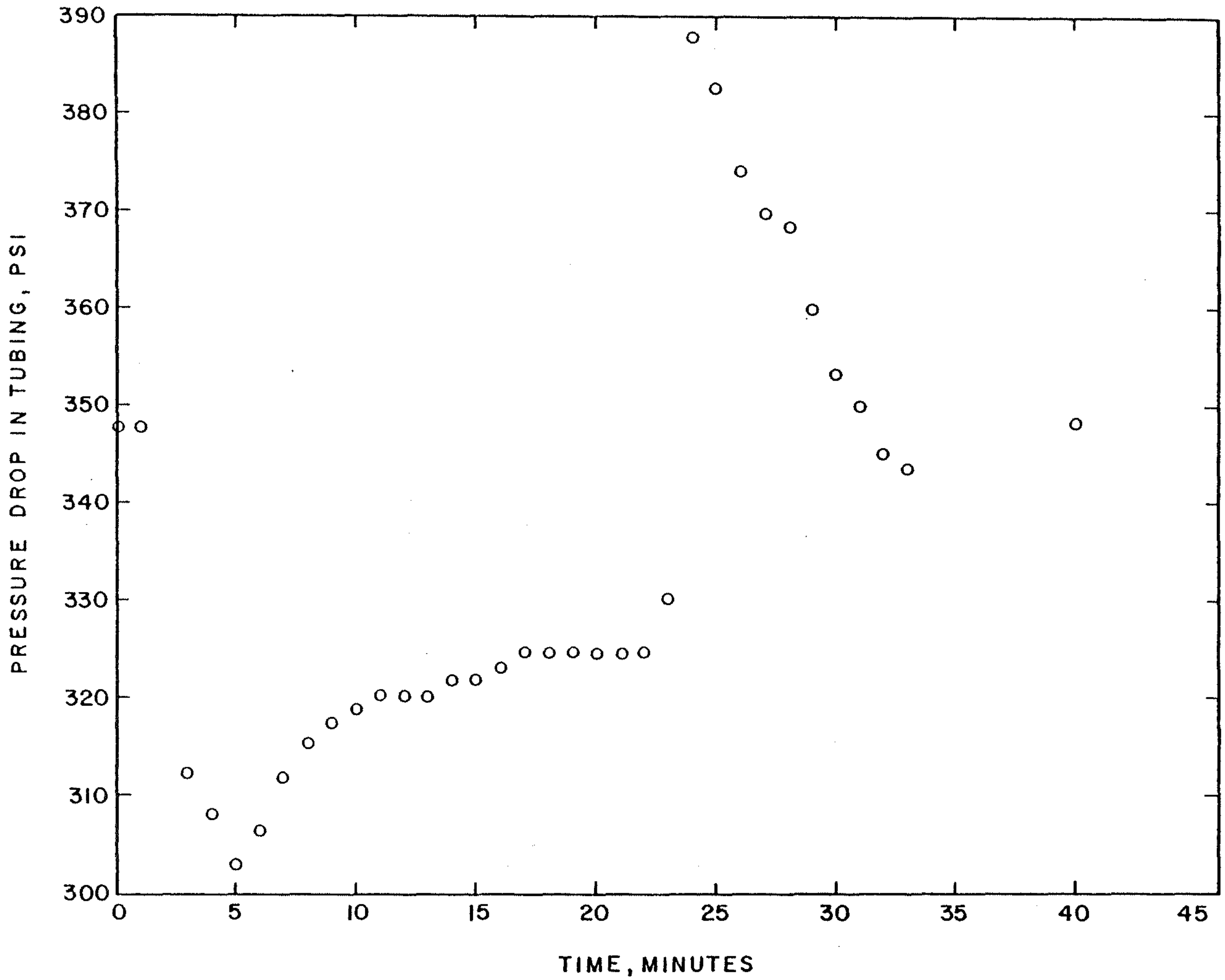

FIGURE 13

CERRO PRIETO RELATIVE PERMEABILITY CURVES

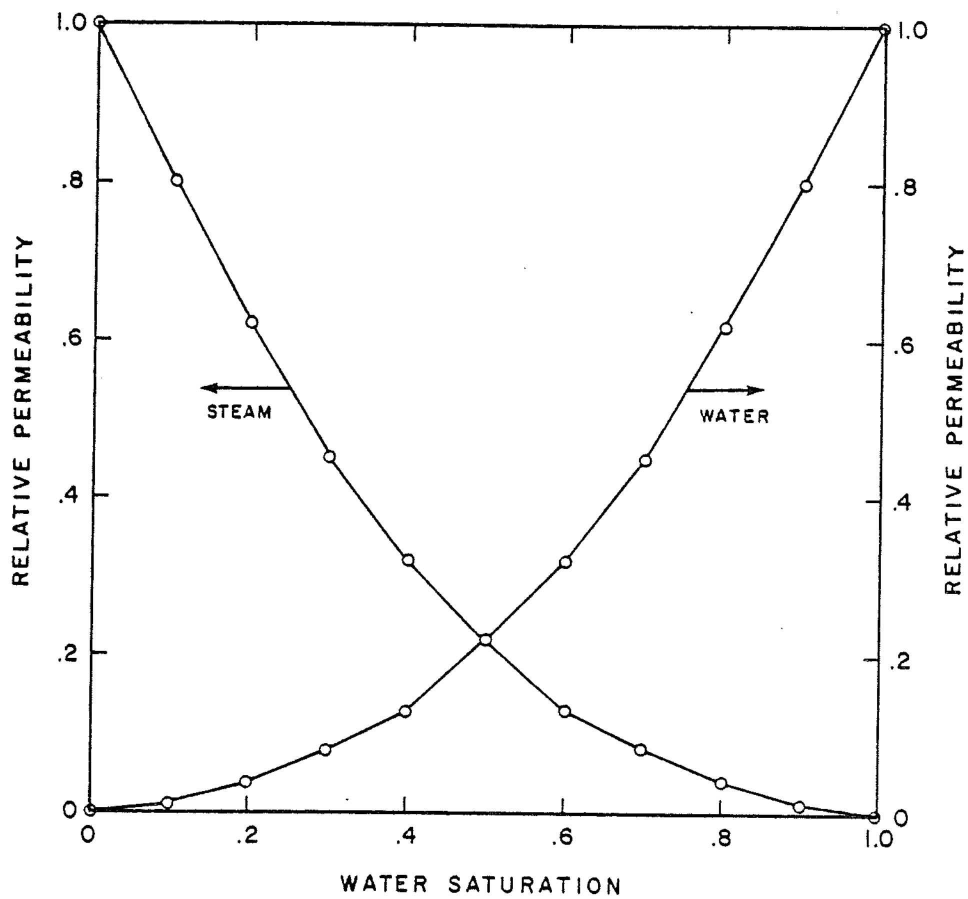

FIGURE 14

TEMPERATURE–DEPTH PLOT
FOR HGP-A (FROM REF. 21)

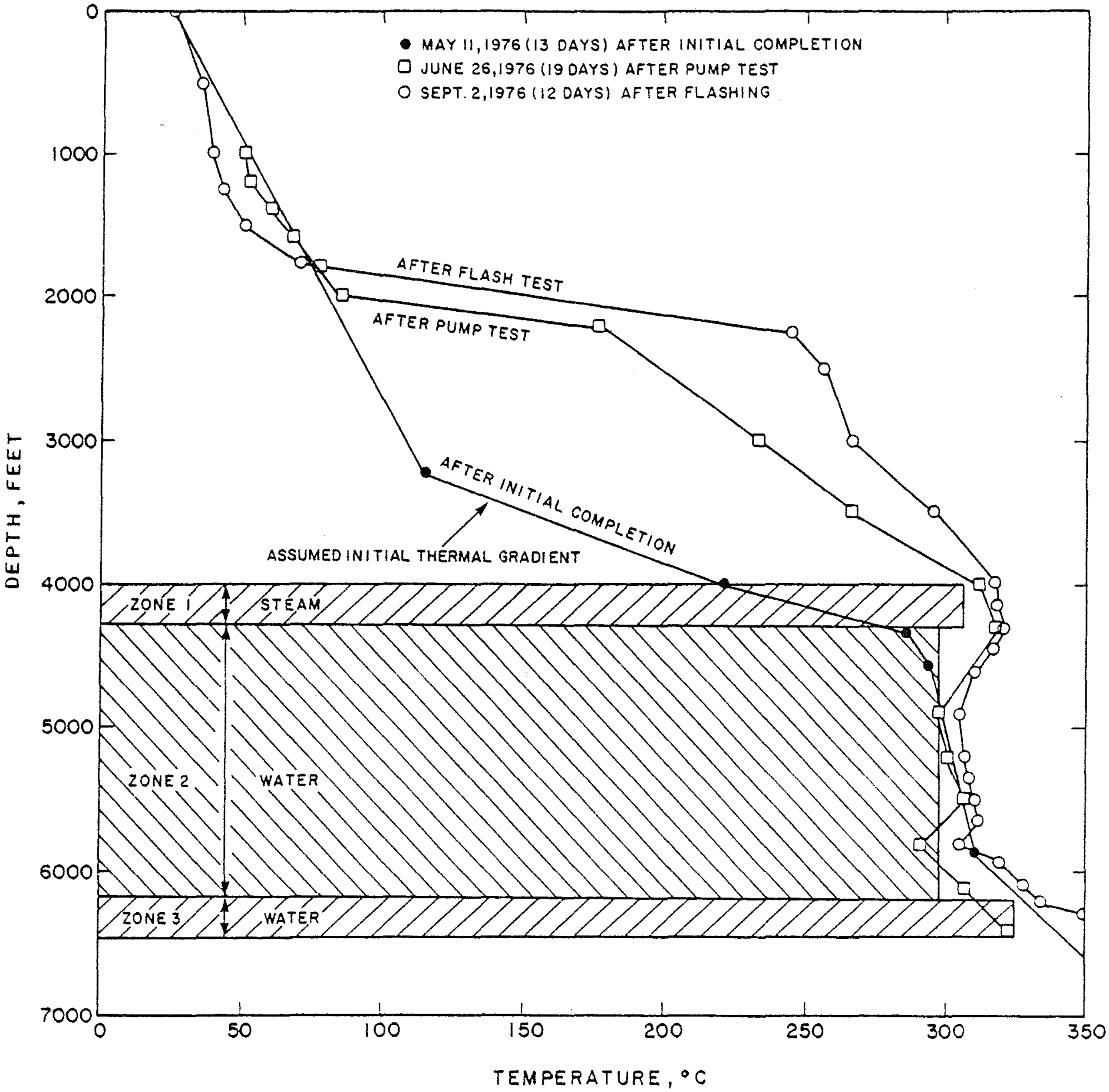

FIGURE 15

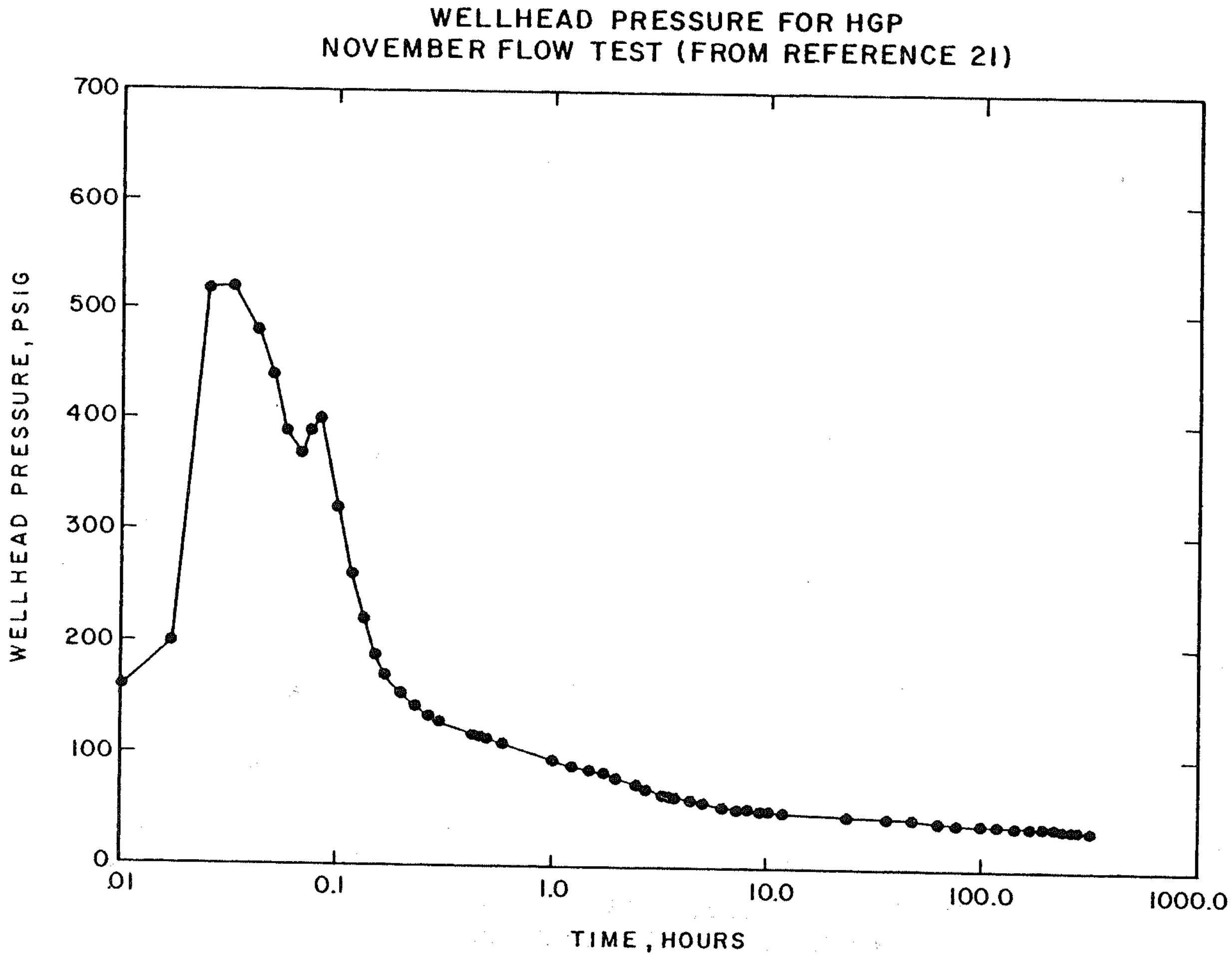
WELLHEAD PRESSURE FOR HGP
NOVEMBER FLOW TEST (FROM REFERENCE 21)
WELLHEAD PRESSURE, PSIG
700
600
500
400
300
200
100
0
.01
0.1
1.0
10.0
100.0
1000.0
TIME, HOURS

FIGURE 16

TOTAL MASS FLOW RATE FOR HGP
NOVEMBER FLOW TEST (FROM REFERENCE 21)

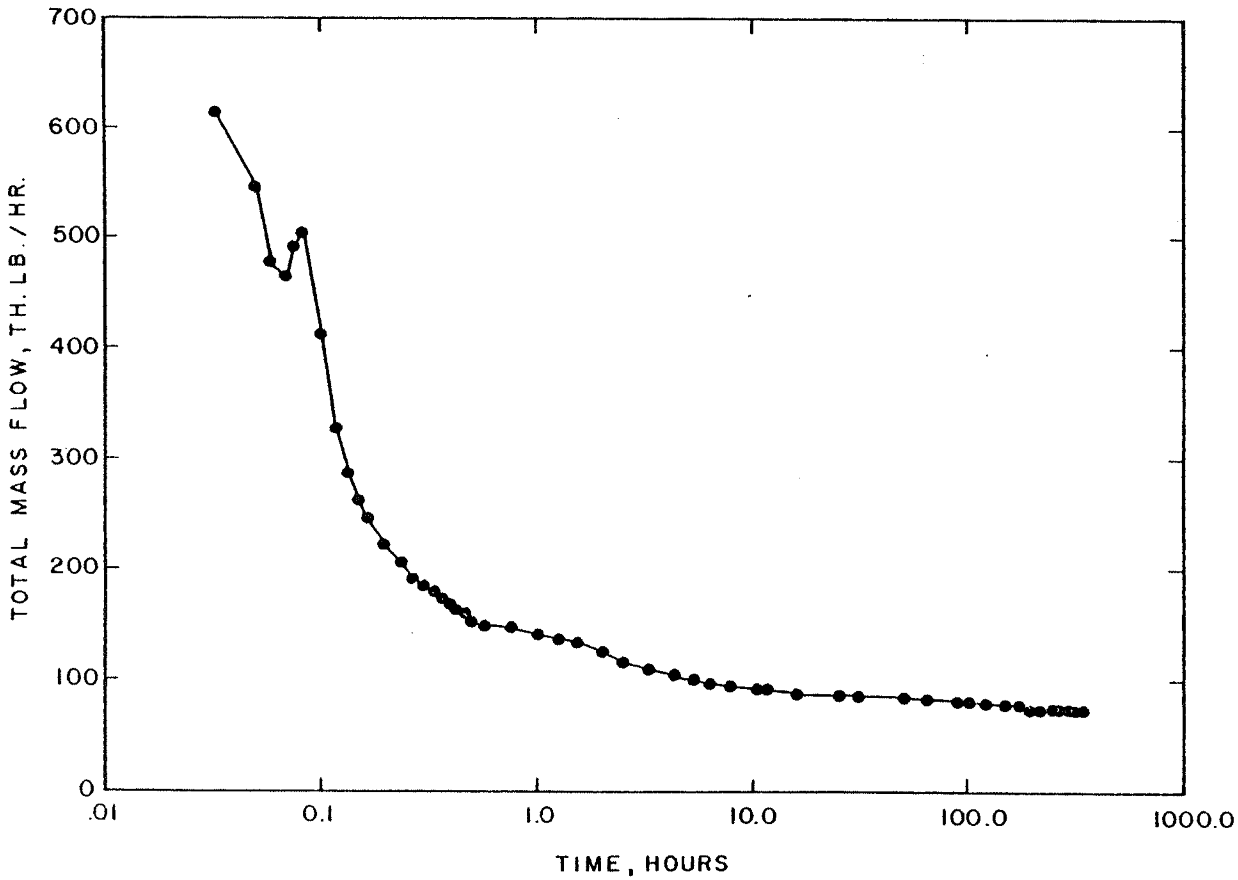

FIGURE 17

WELLHEAD PRESSURE DURING HGP MULTI-RATE TEST

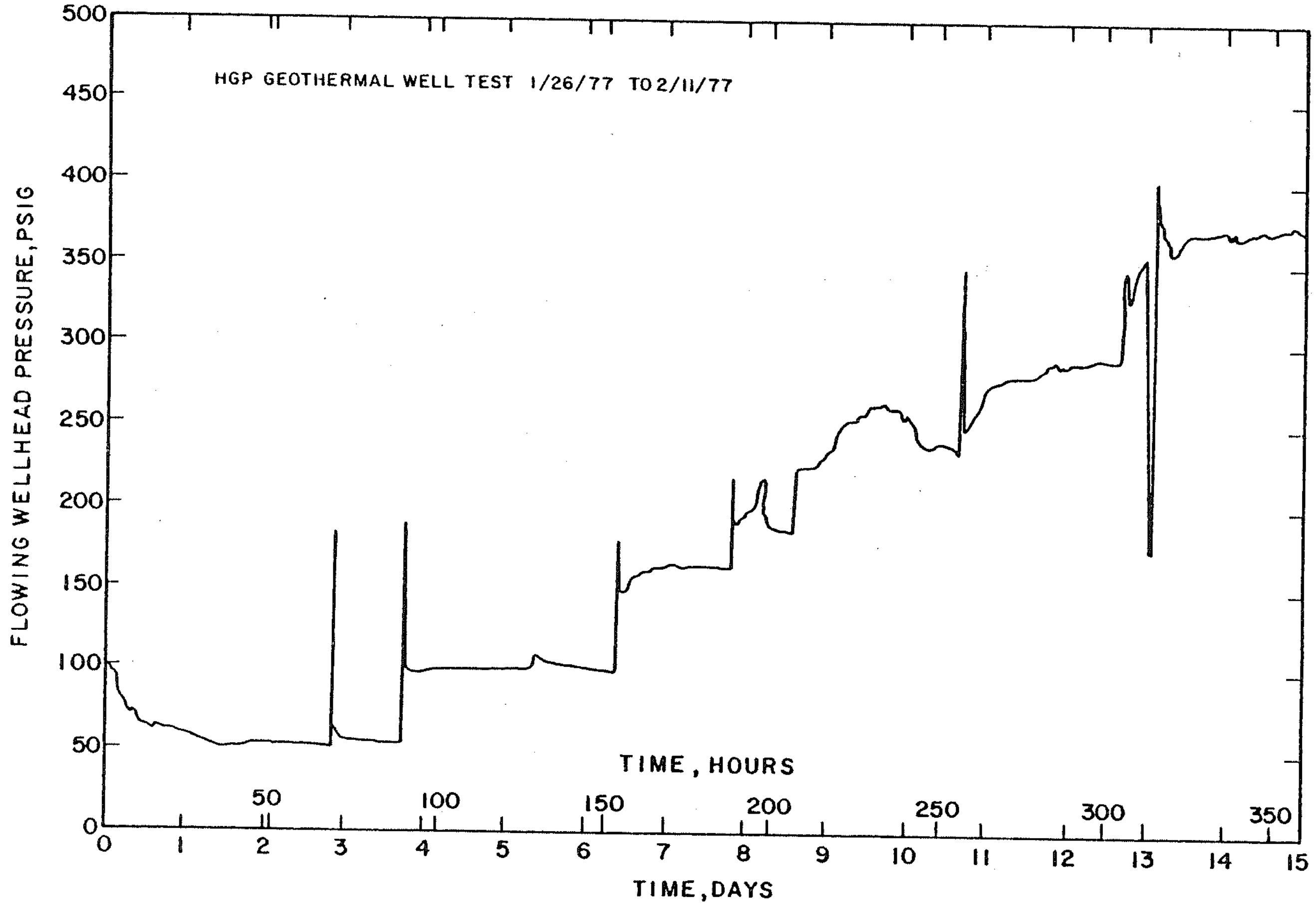

FIGURE 18

TOTAL MASS FLOW RATE
DURING HGP MULTI-RATE TEST

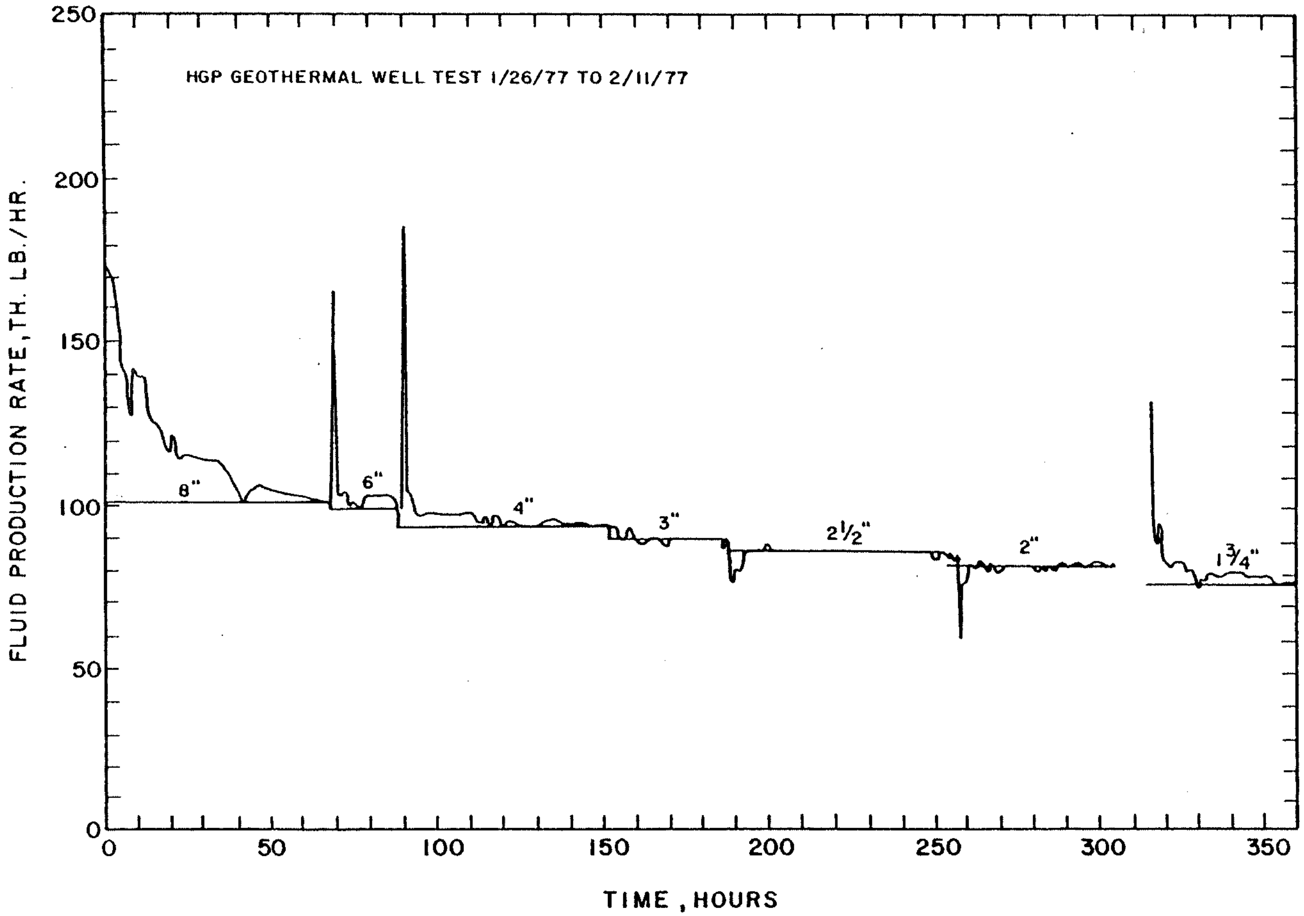

FIGURE 19

WELLHEAD PRESSURE FOR HGP MARCH – MAY FLOW TEST

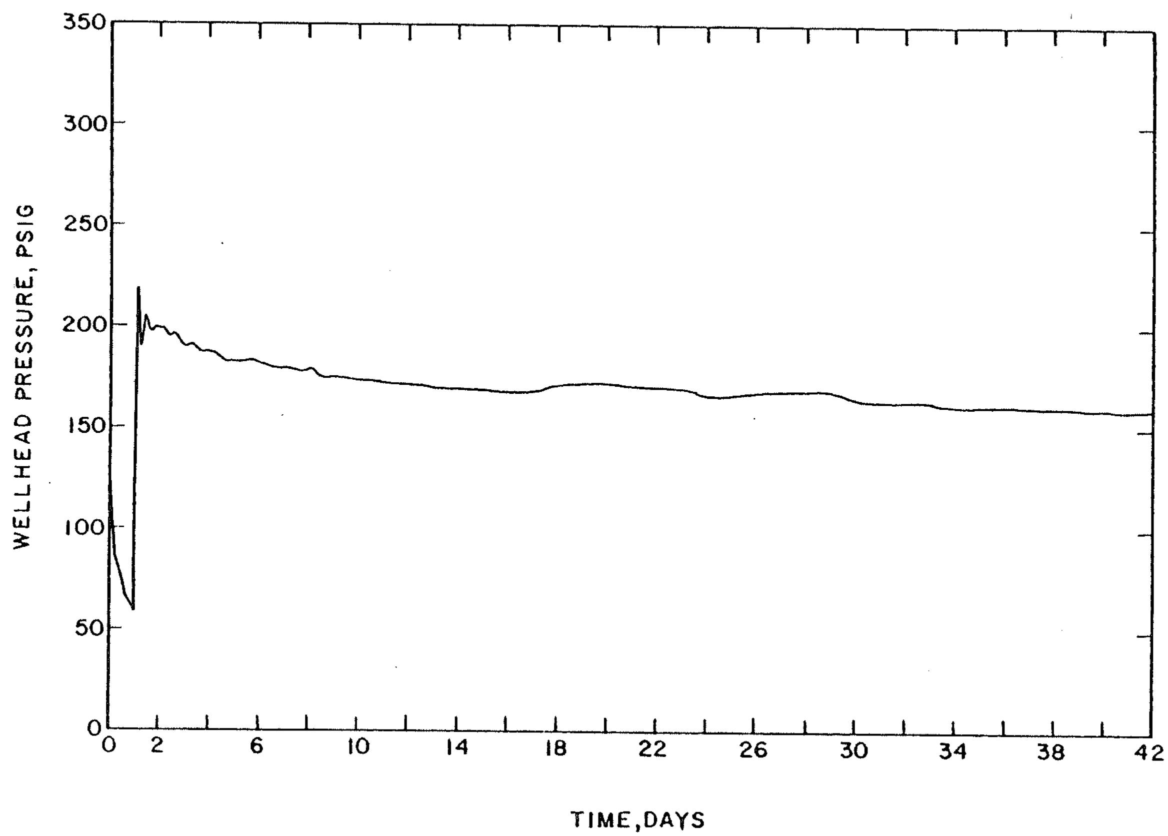

FIGURE 20

TOTAL MASS FLOW RATE FOR HGP MARCH-MAY FLOW TEST

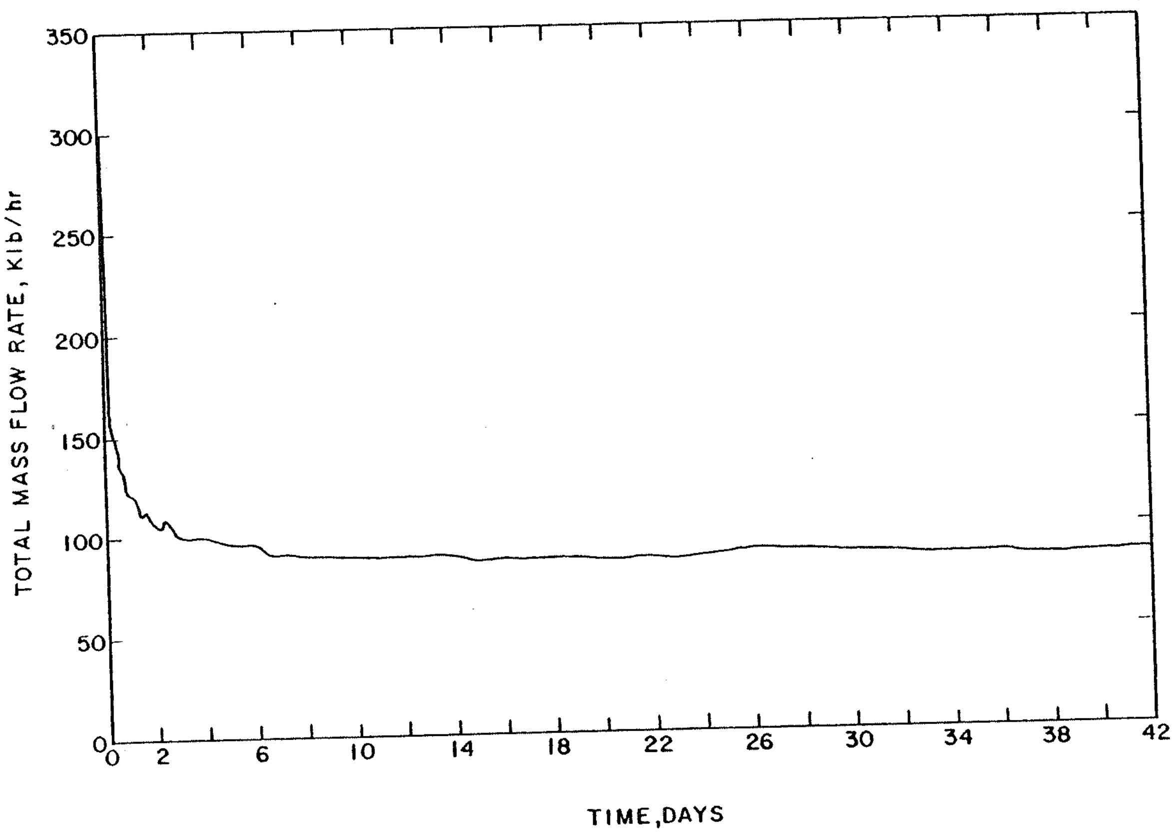

FIGURE 21

RELATIVE PERMEABILITY DATA
USED FOR HGP-A WELL TESTS

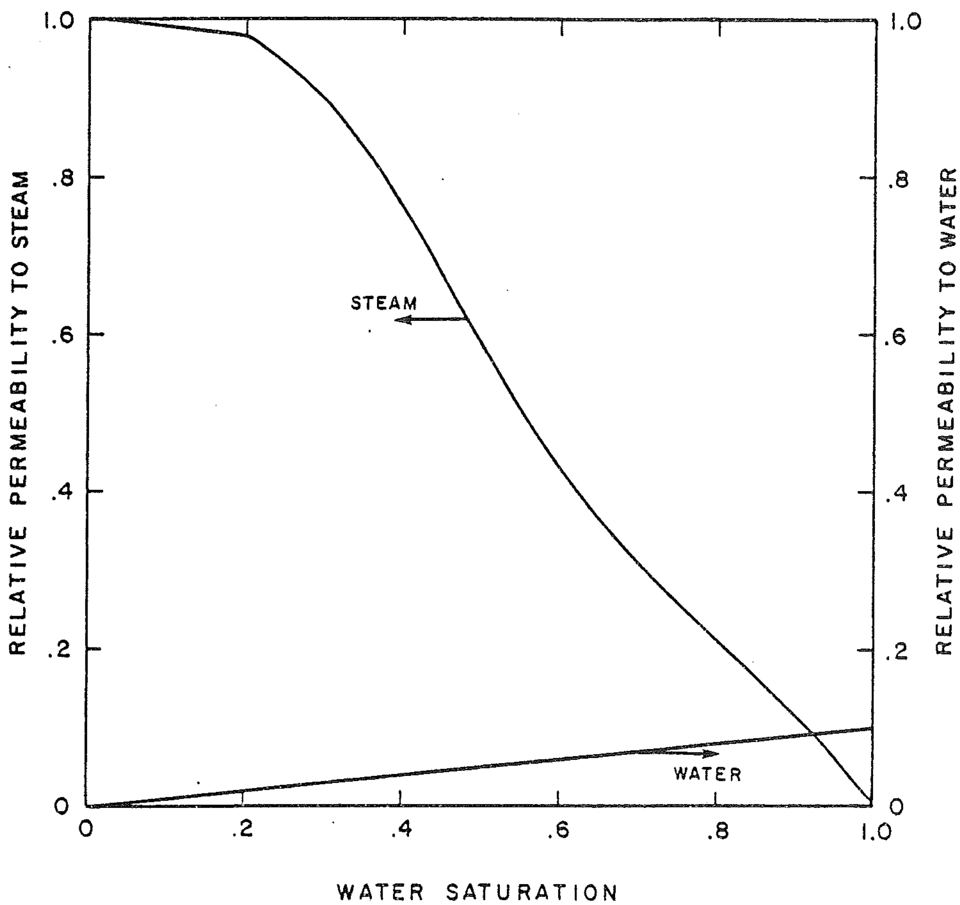

FIGURE 22

WAIRAILEI WELL TEST DERIVED
RELATIVE PERMEABILITIES (FROM REF. 22)

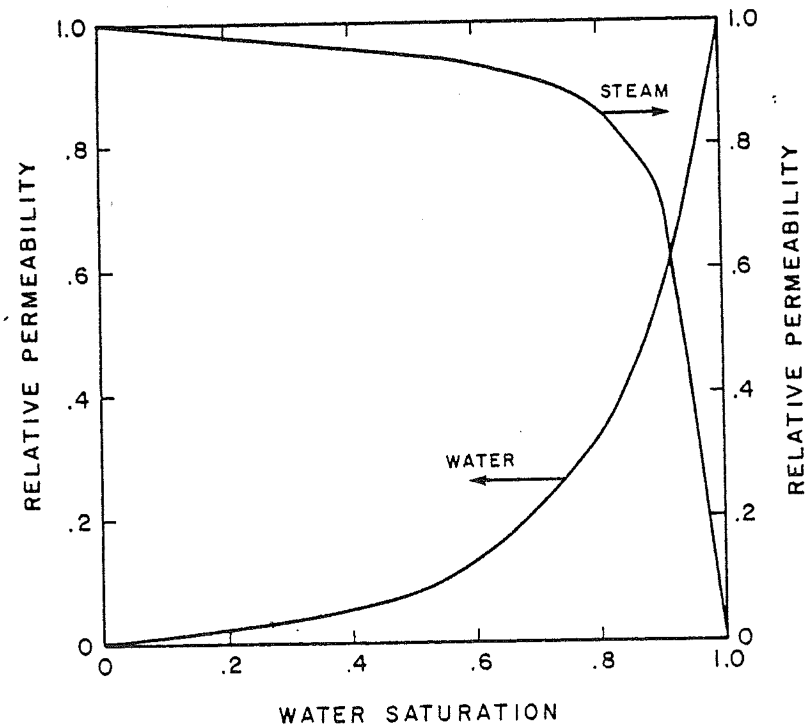

FIGURE 23

INPUT RATES FOR CERRO PRIETO WELL TEST

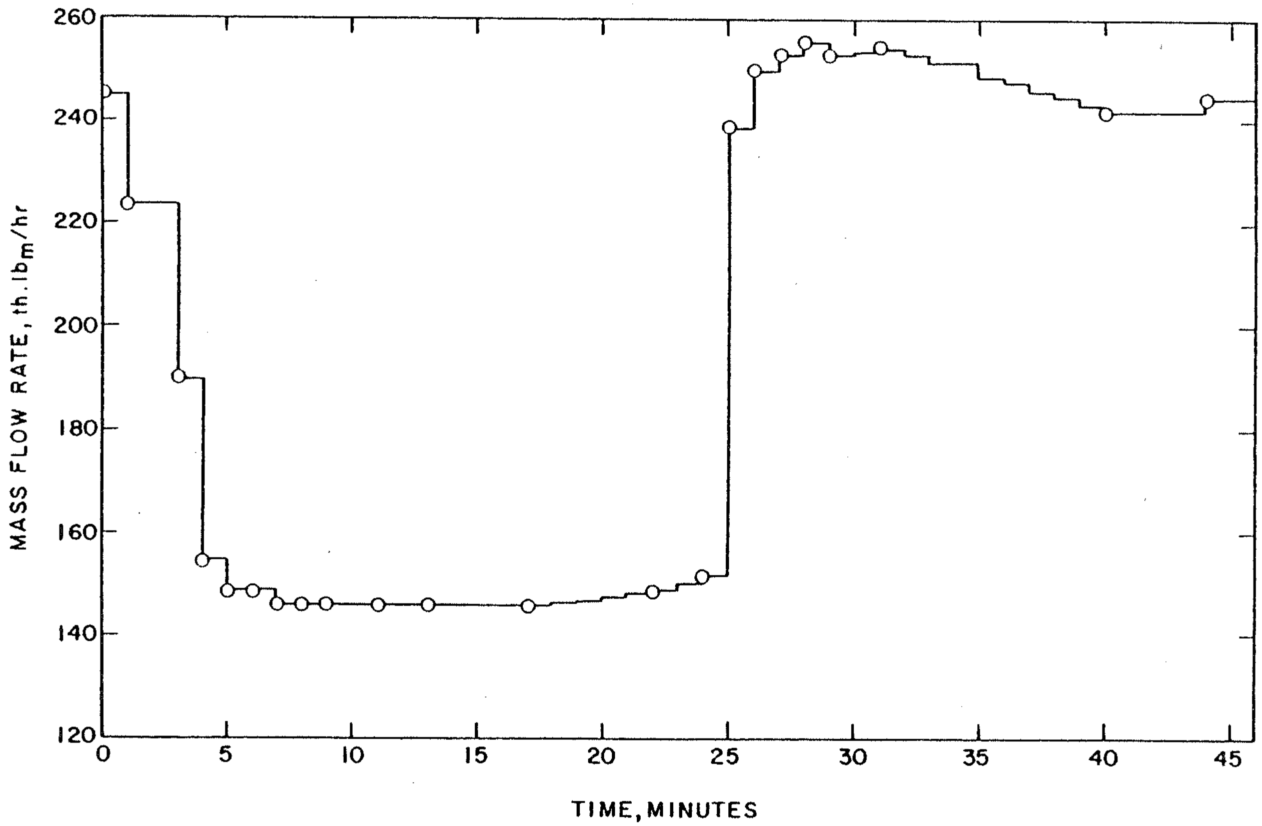

FIGURE 24

HISTORY MATCH OF WELLHEAD PRESSURES
FOR CERRO PRIETO M-21A TEST

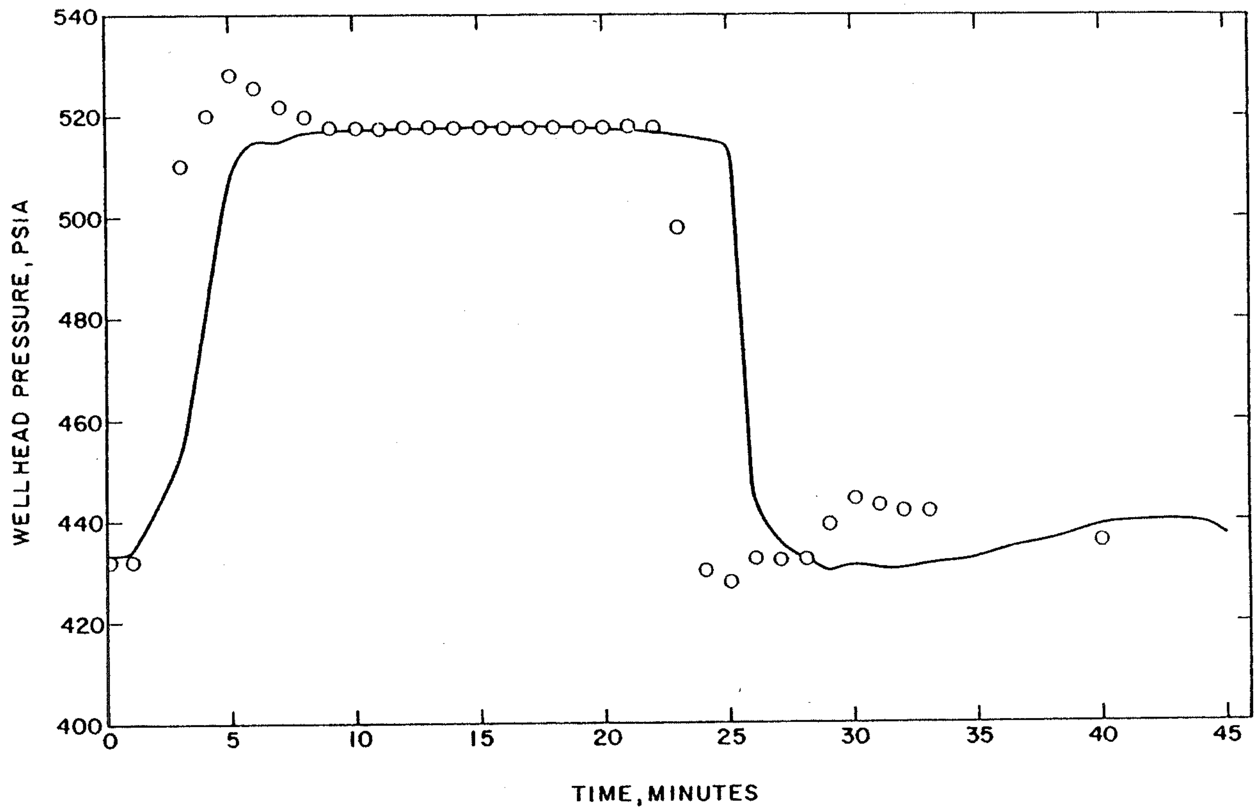

FIGURE 25

HISTORY MATCH OF BOTTOM HOLE PRESSURES
FOR CERRO PRIETO M-21A TEST

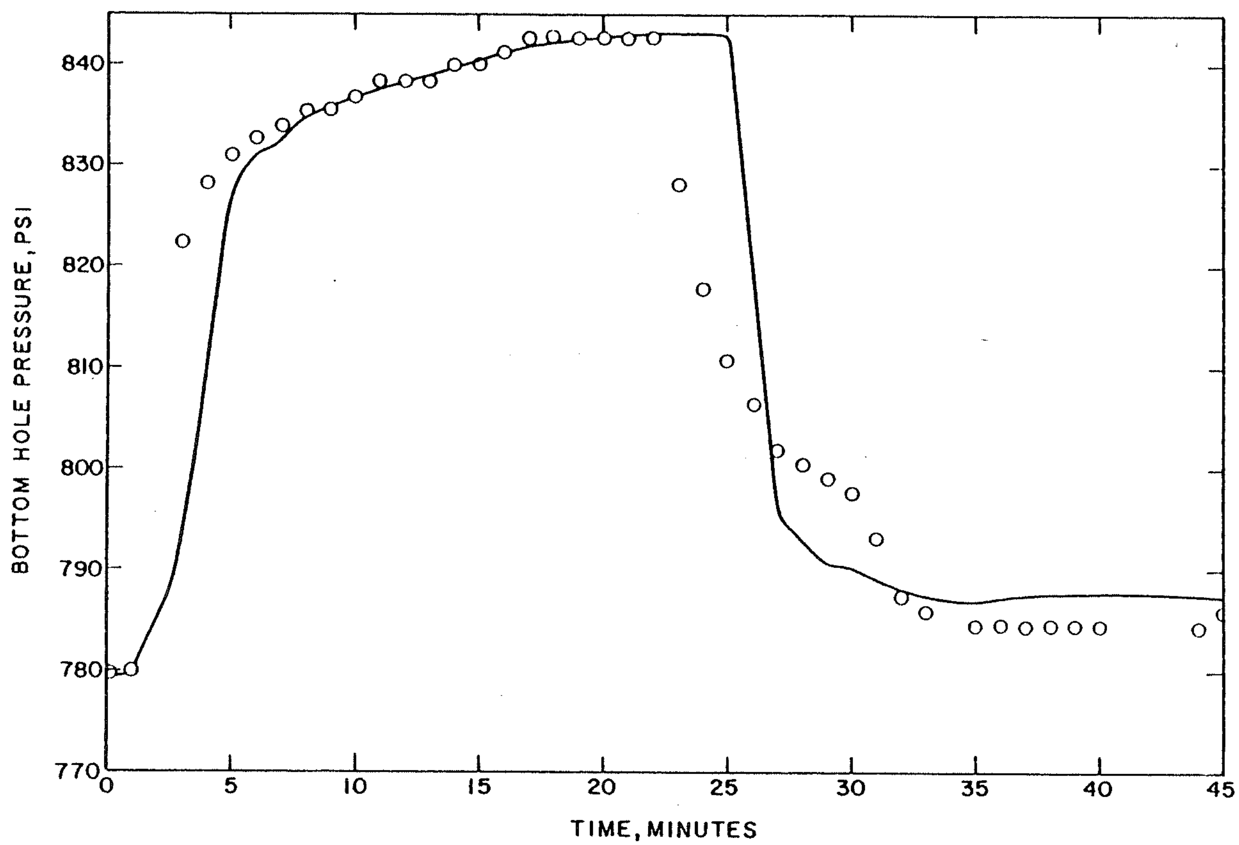

FIGURE 26

HISTORY MATCH OF PRESSURE DROP IN TUBING
FOR CERRO PRIETO M-21A TEST

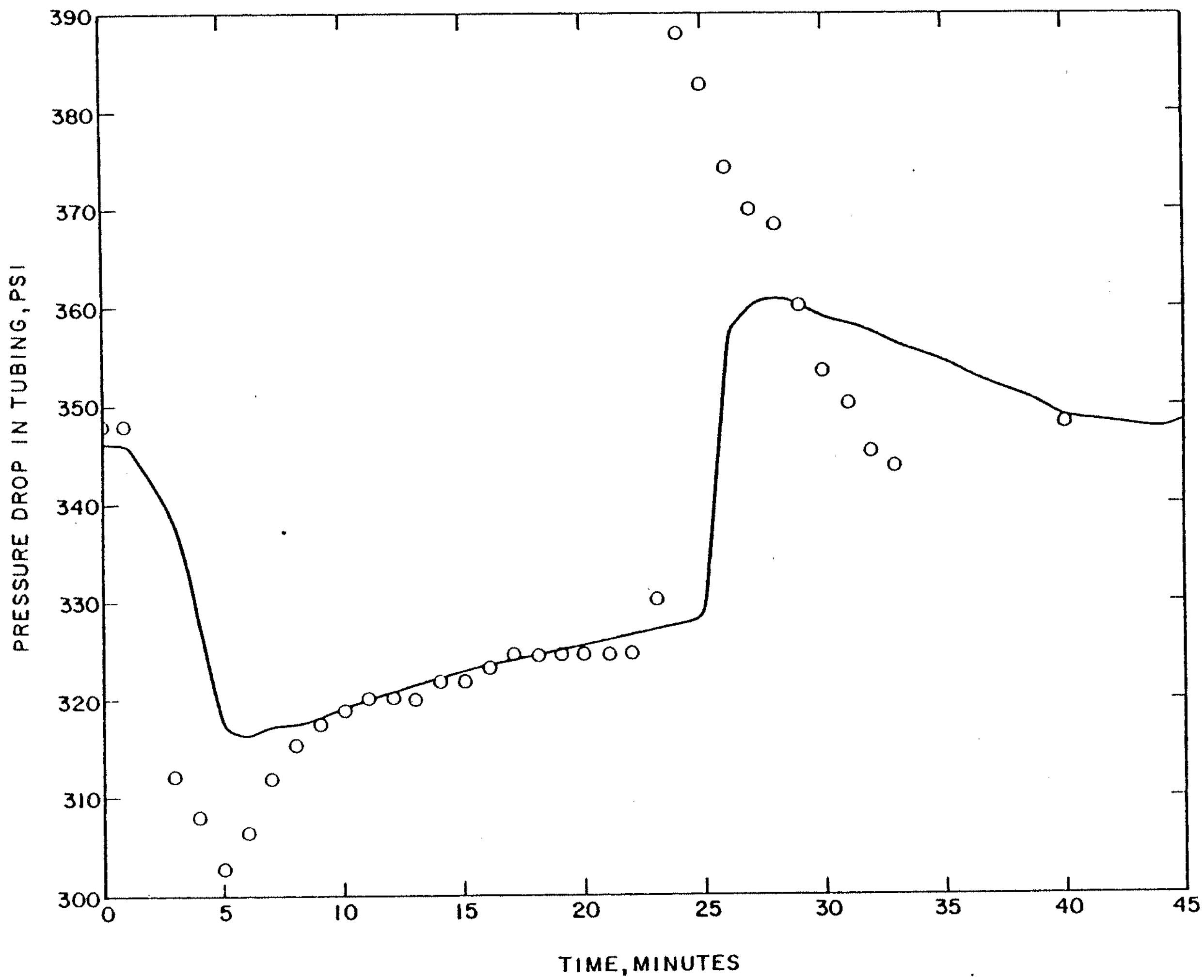

FIGURE 27

EFFECT OF PERMEABILITY ON MATCH
OF CERRO PRIETO M-21A TEST MATCH

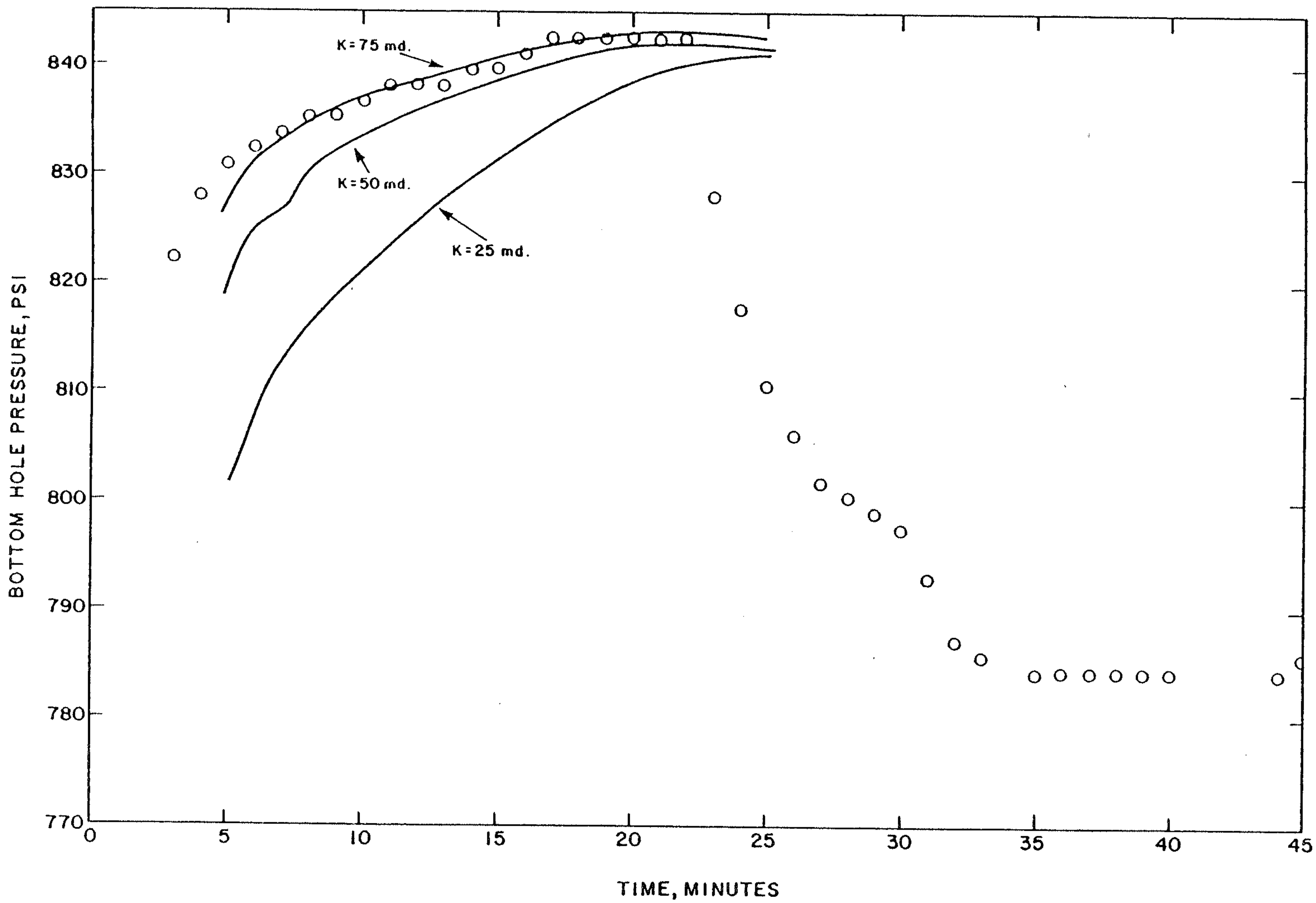

FIGURE 28

INFLUENCE OF TWO-PHASE CORRELATIONS
ON PRESSURE DROP IN TUBING

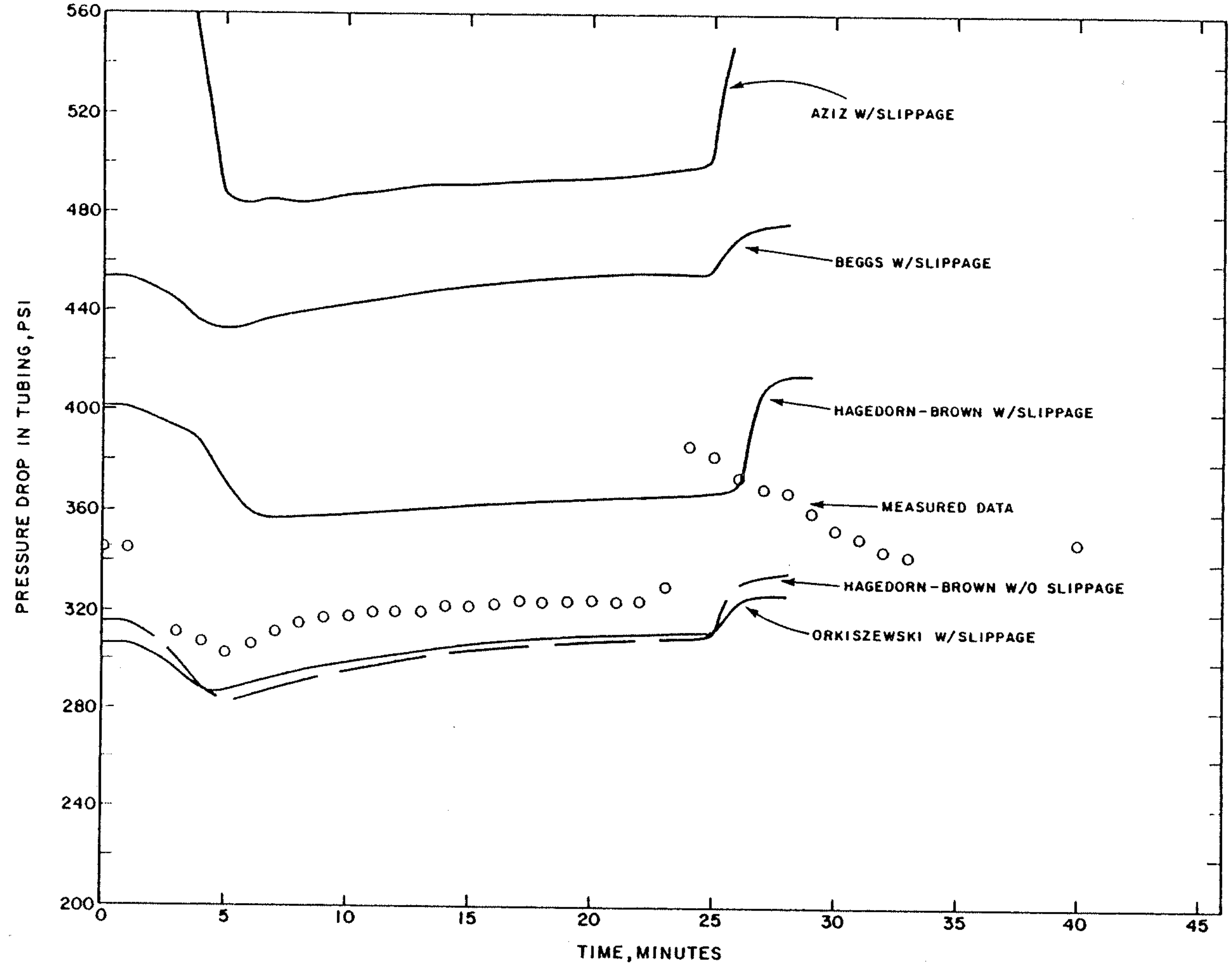

FIGURE 29

MATCH OF FLOW RATE FOR JANUARY MULTI-RATE TEST, HGP-A

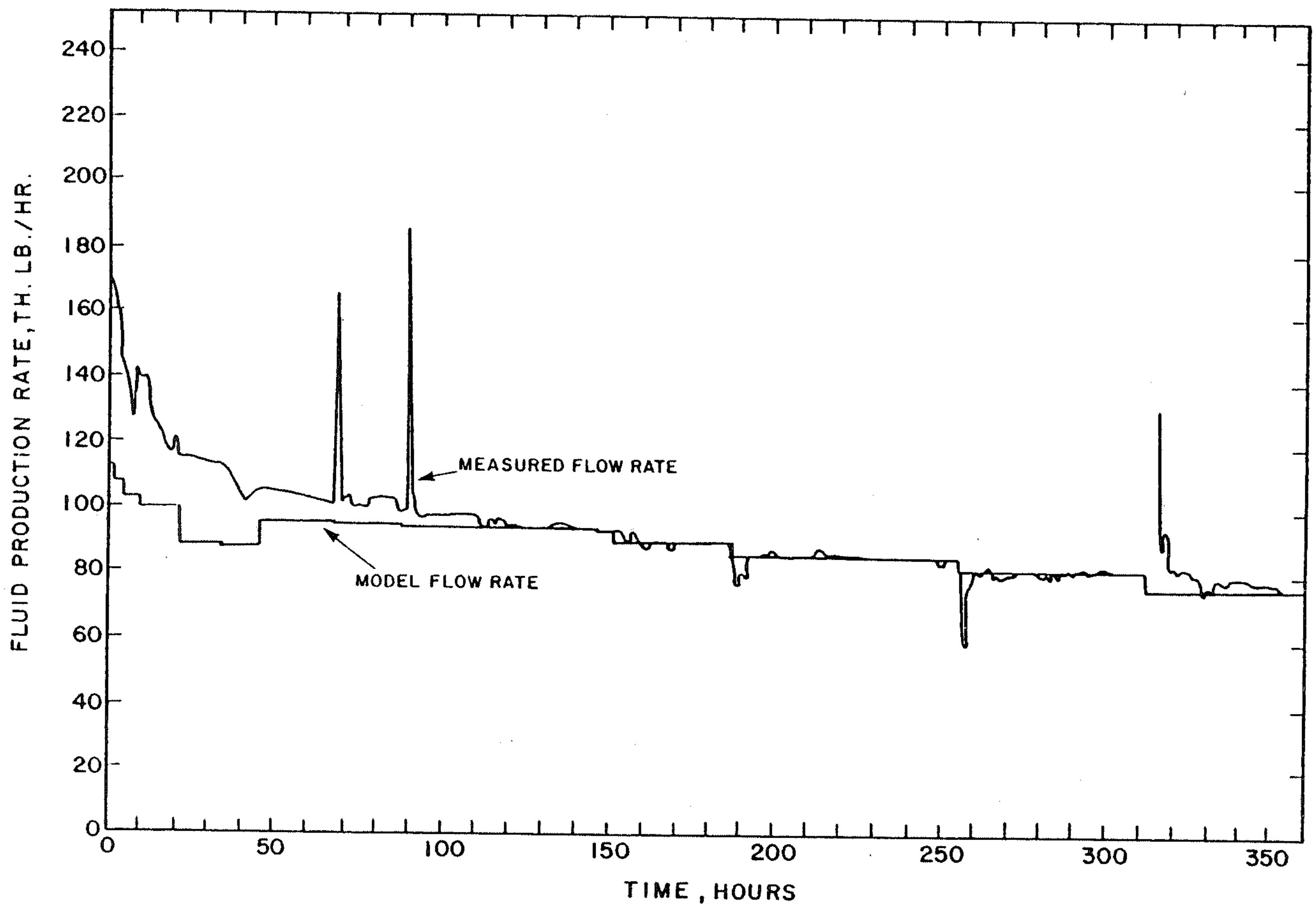

FIGURE 30

MATCH OF WELLHEAD PRESSURES
FOR JANUARY MULTI-RATE TEST, HGP-A

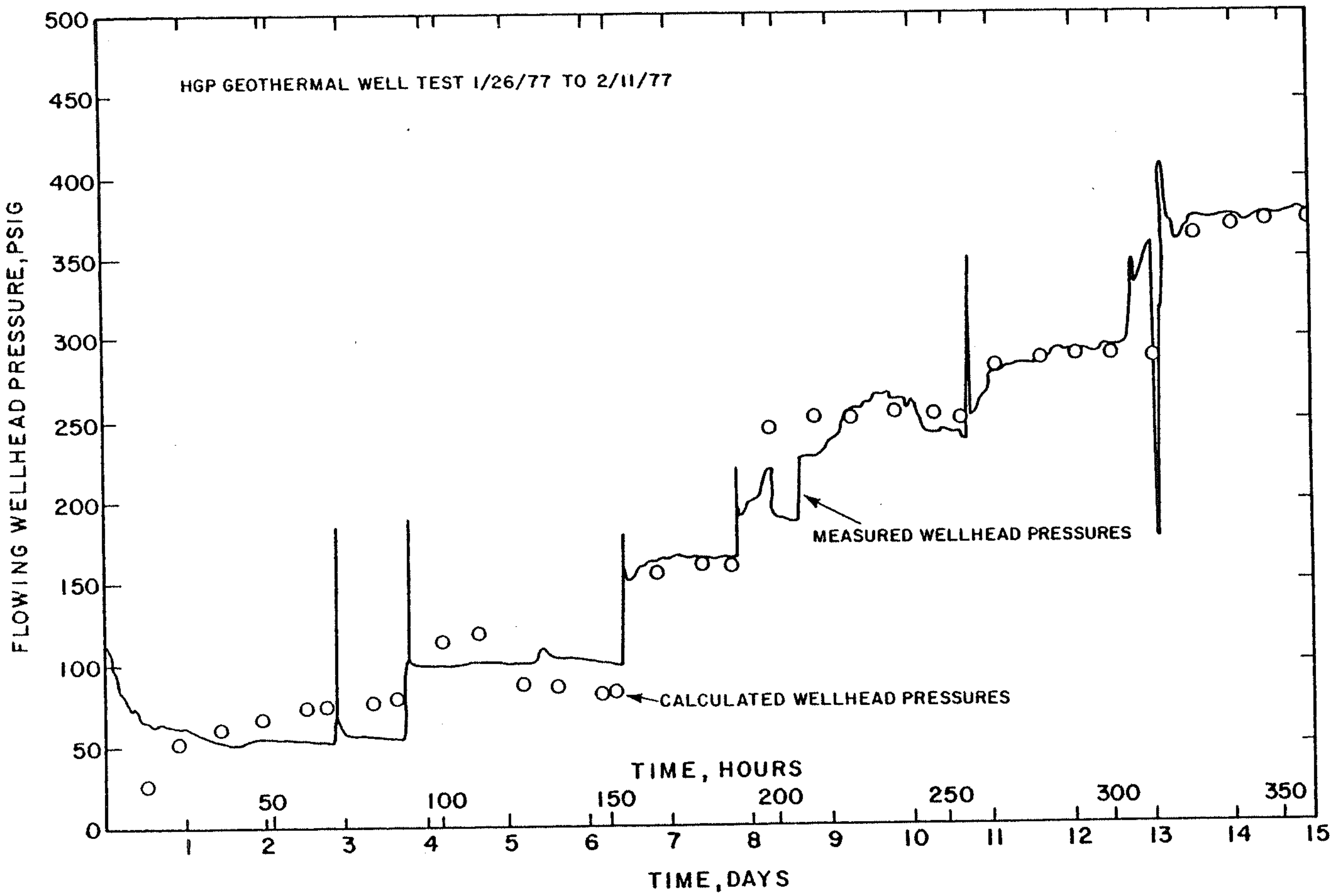

FIGURE 31

MATCH OF TOTAL MASS FLOW RATE DURING MARCH-MAY FLOW TESTS, HGP-A

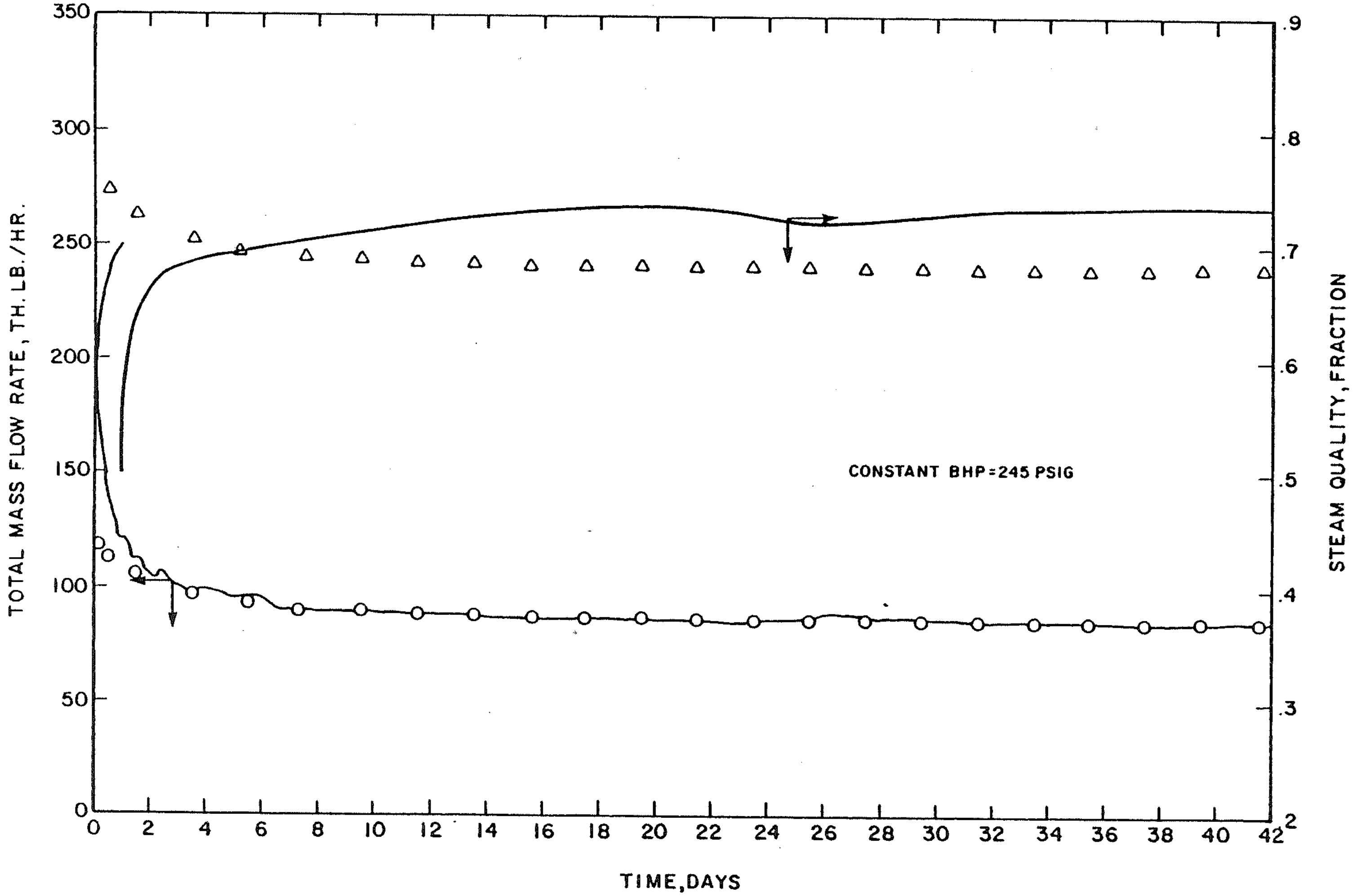

FIGURE 32

MATCH OF WELLHEAD PRESSURES DURING MARCH–MAY FLOW TESTS, HGP-A

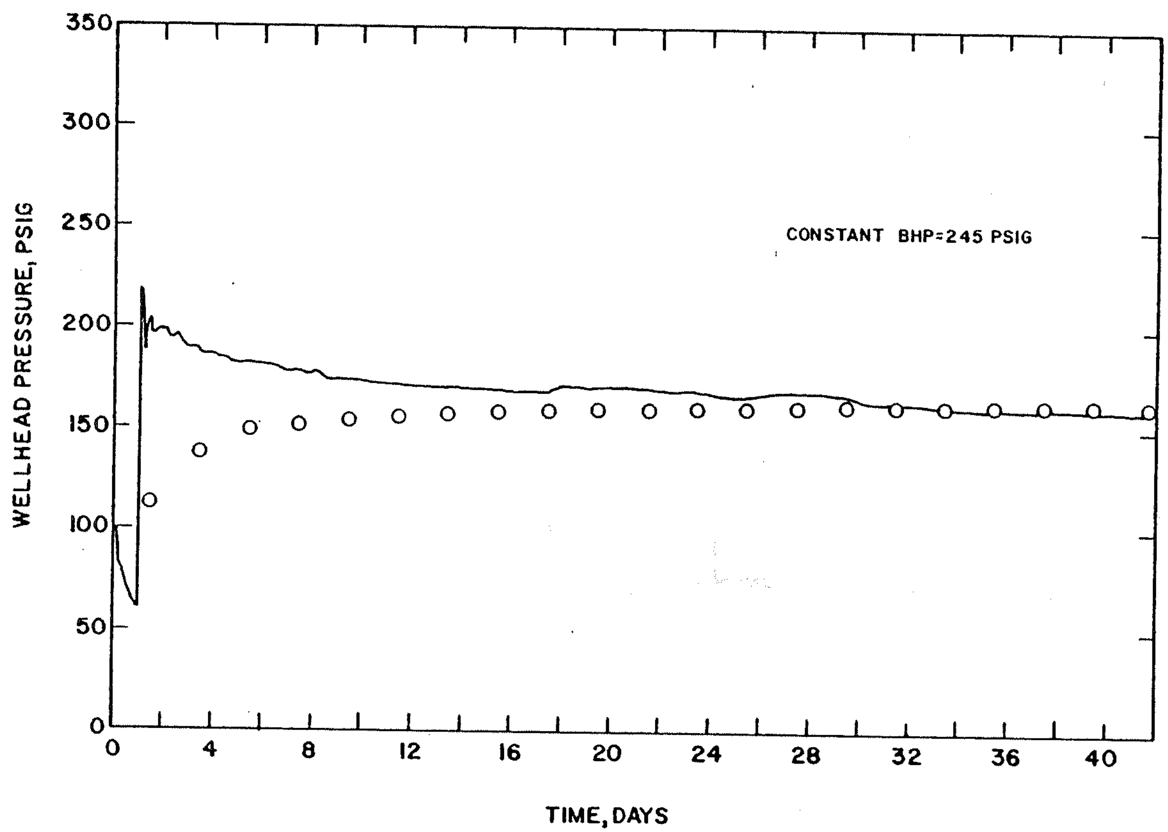

FIGURE 33

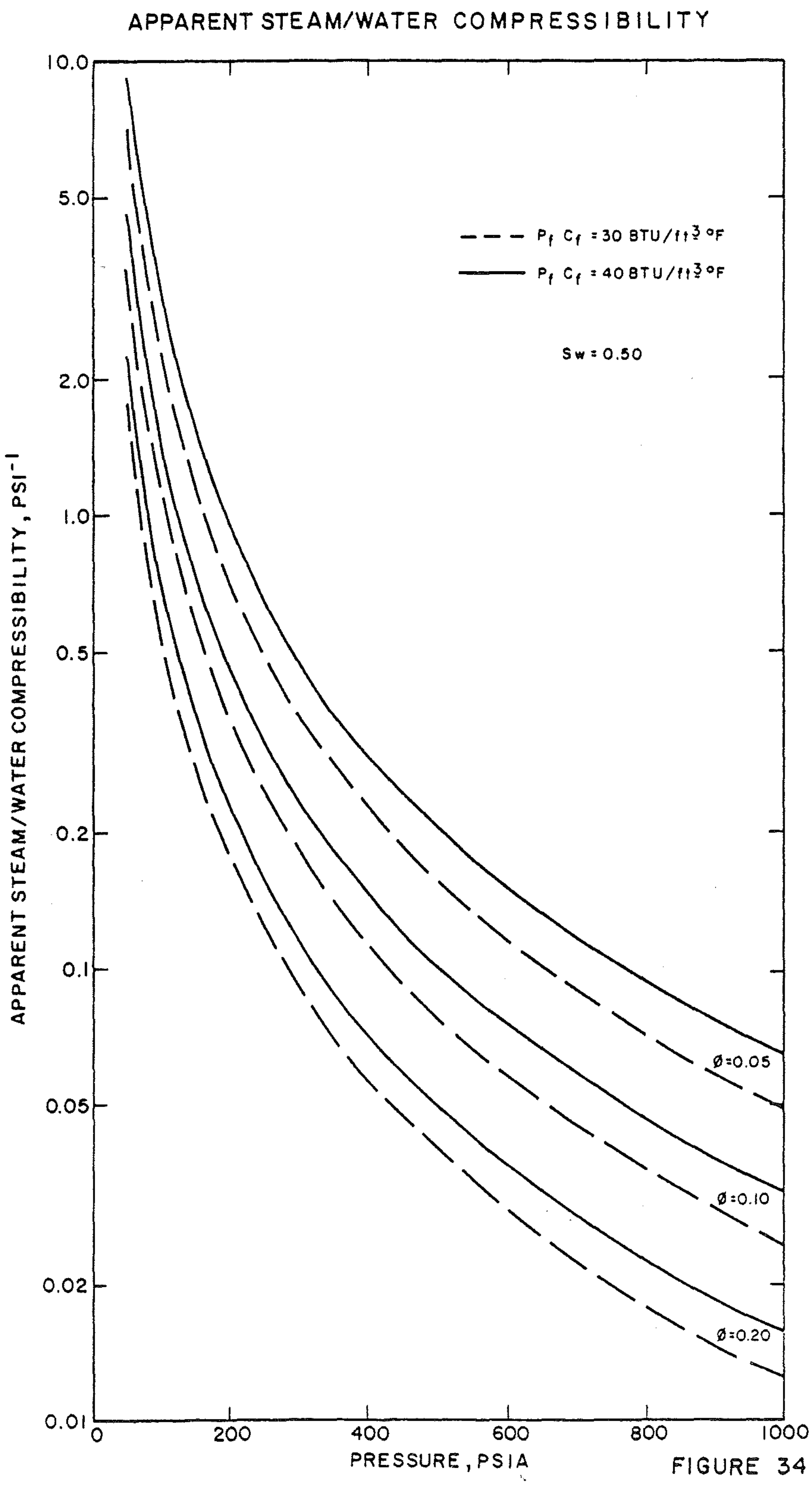
APPARENT STEAM/WATER COMPRESSIBILITY
10.0
5.0
2.0
1.0
0.5
0.2
0.1
0.05
0.02
0.01
APPARENT STEAM/WATER COMPRESSIBILITY, PSI^{-1}
0
200
400
600
800
1000
PRESSURE, PSIA
$P_f C_f$ = 30 BTU/ft^3 °F
$P_f C_f$ = 40 BTU/ft^3 °F
Sw = 0.50
Ø=0.05
Ø=0.10
Ø=0.20

FIGURE 34

ANALYTICAL RELATIVE PERMIABILITY RATIO
FOR CERO PRITO WELL TEST ANALYSES

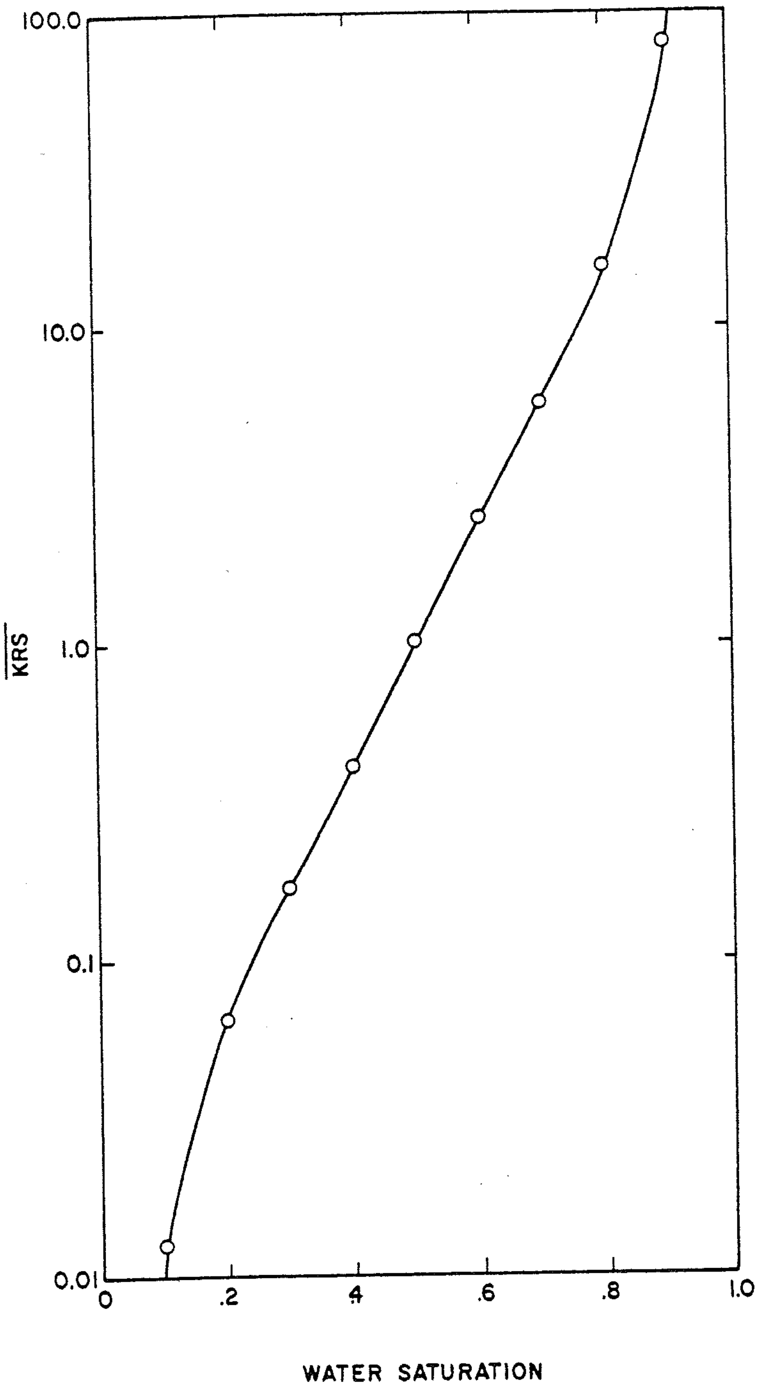

FIGURE 35

CALCULATED PERMEABILITY
FROM SINGLE RATE DRAWDOWN TESTS

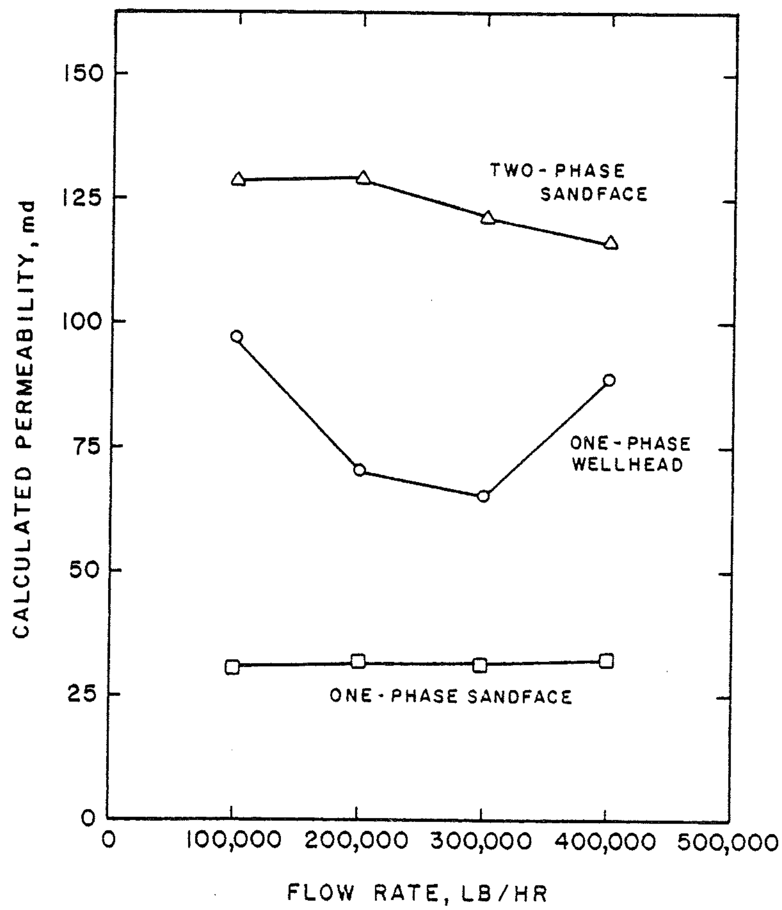

FIGURE 36

EFFECT OF RESERVOIR PERMEABILITY ON PRESSURE RESPONSE

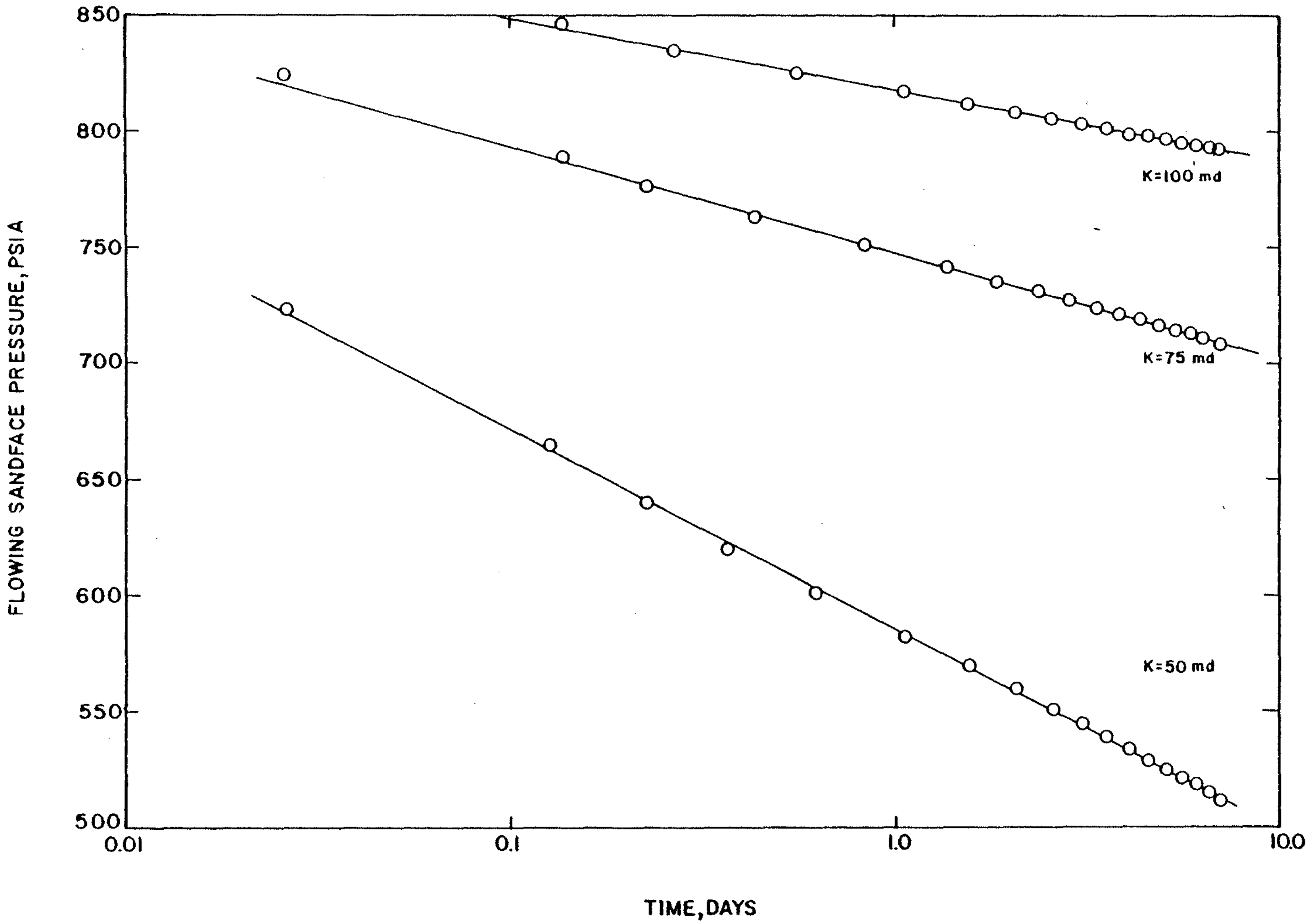

FIGURE 37

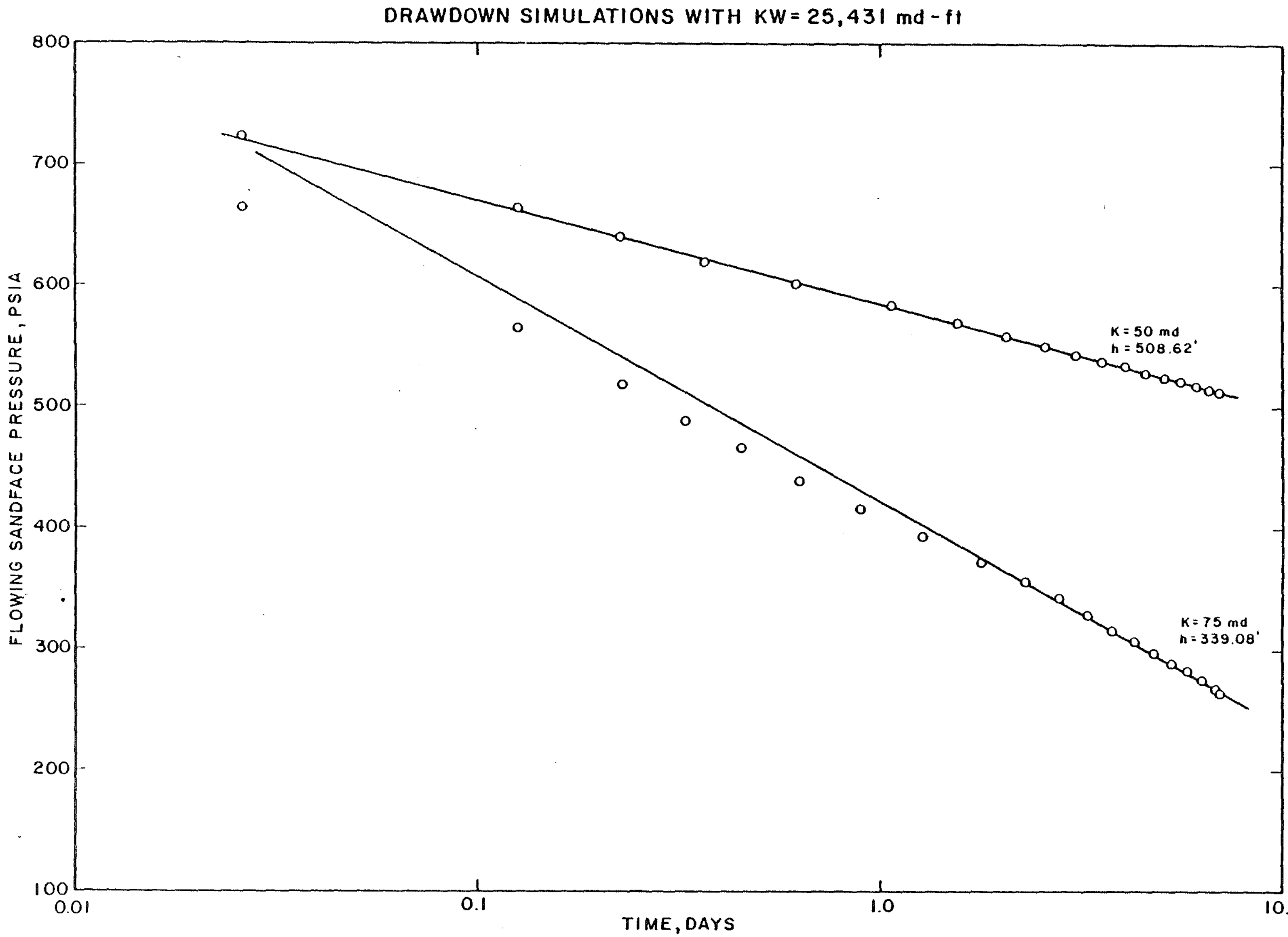
DRAWDOWN SIMULATIONS WITH KW= 25,431 md-ft
FLOWING SANDFACE PRESSURE, PSIA
TIME, DAYS
800
700
600
500
400
300
200
100
0.01
0.1
1.0
10.0
K = 50 md
h = 508.62'
K = 75 md
h = 339.08'

FIGURE 38

DRAWDOWN TESTS WITH KH=50,862 md ft

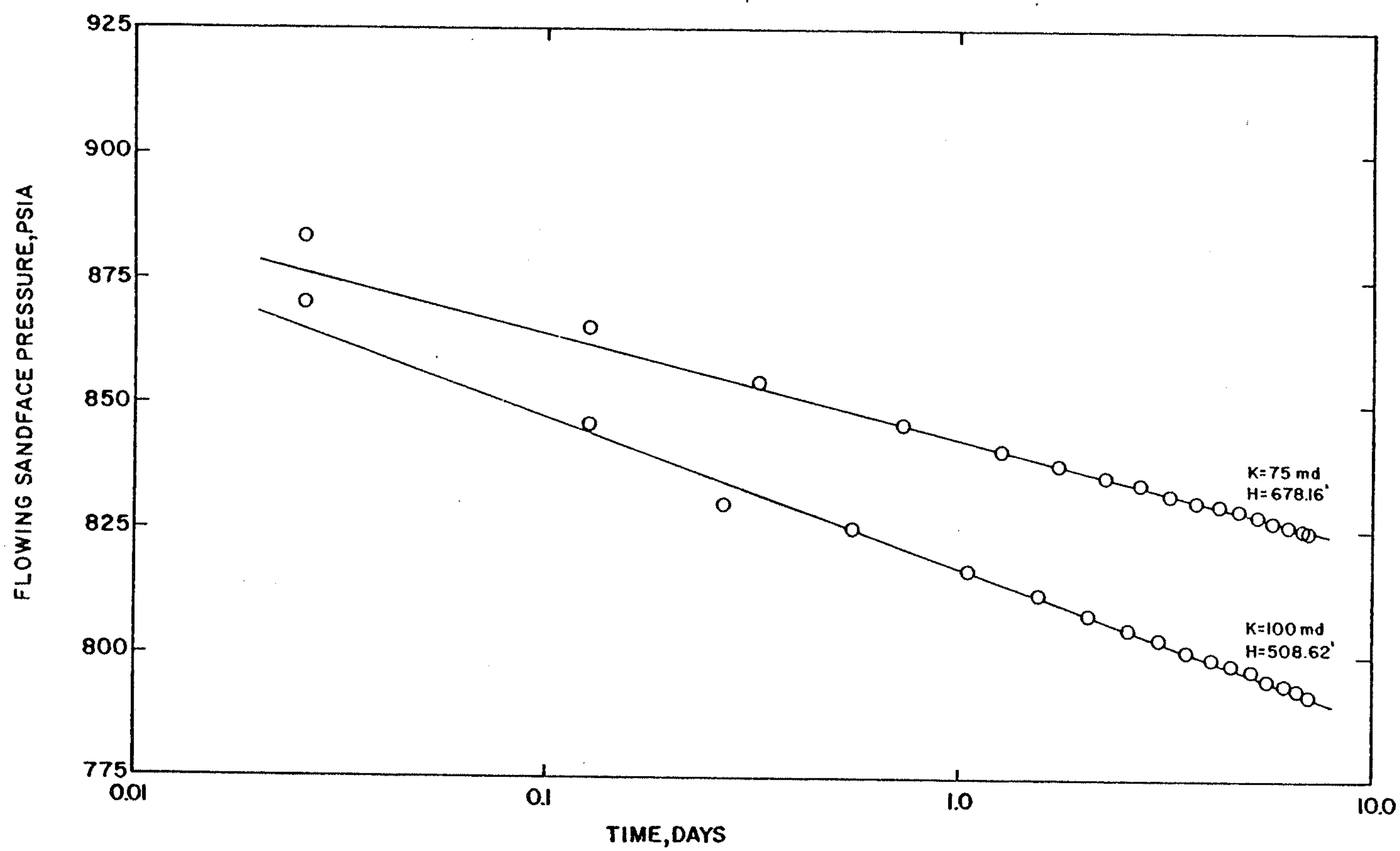

FIGURE 39

EFFECT OF CHANGING POROSITY

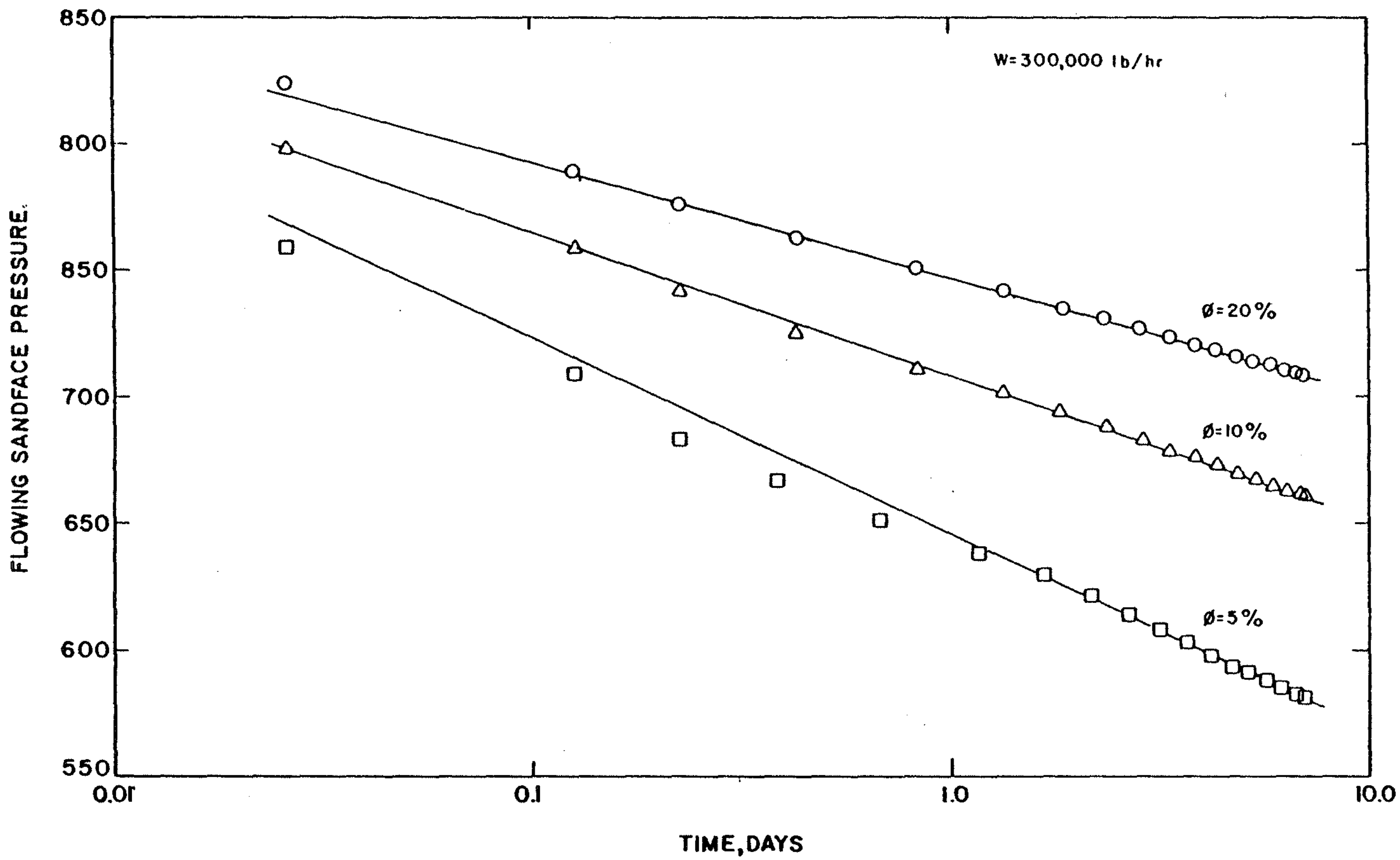

FIGURE 40

EFFECT OF ROCK HEAT TRANSFER ON PRESSURE BEHAVIOR

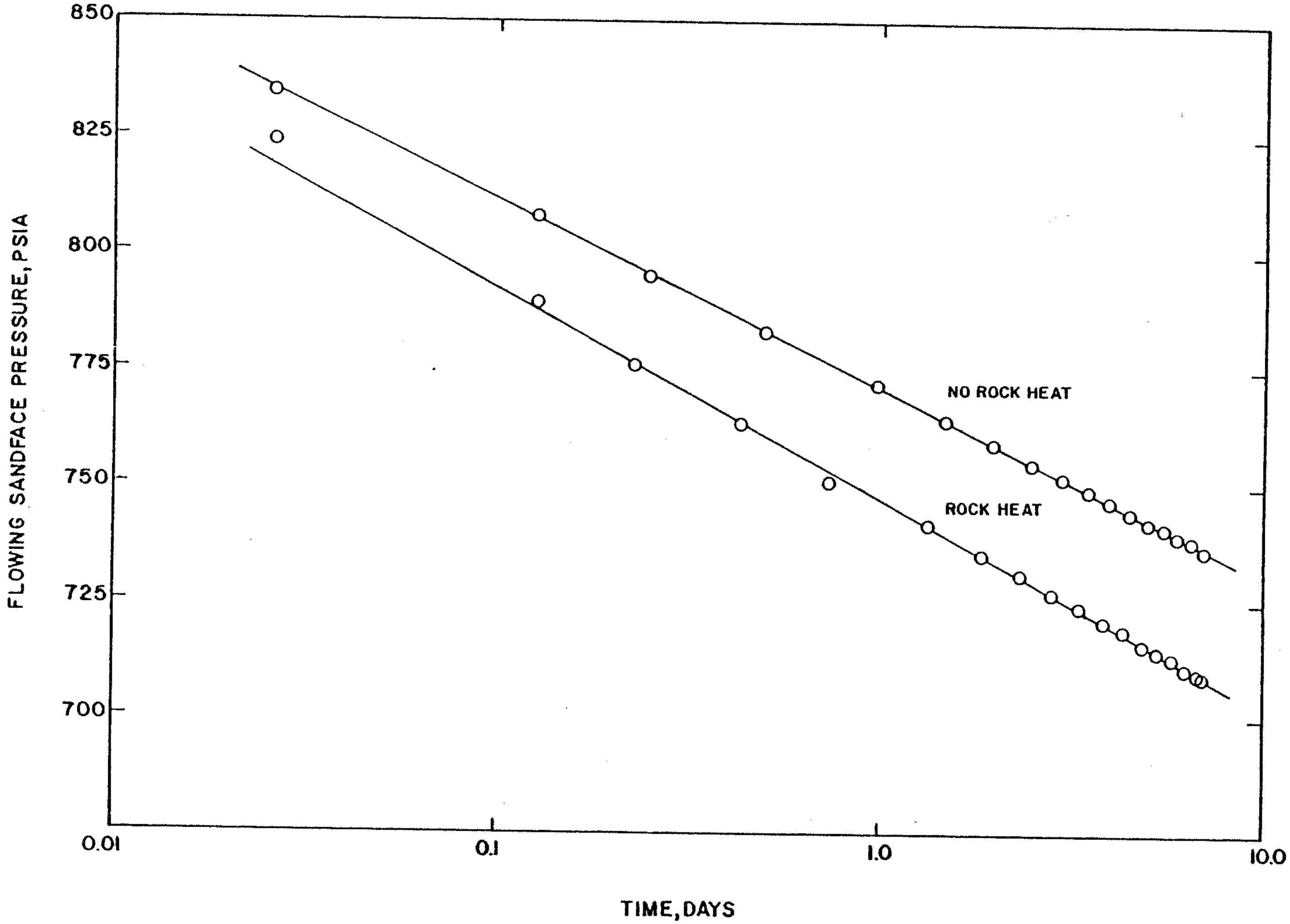

FIGURE 41

EFFECT OF ROCK HEAT TRANSFER ON CALCULATED STEAM SATURATION

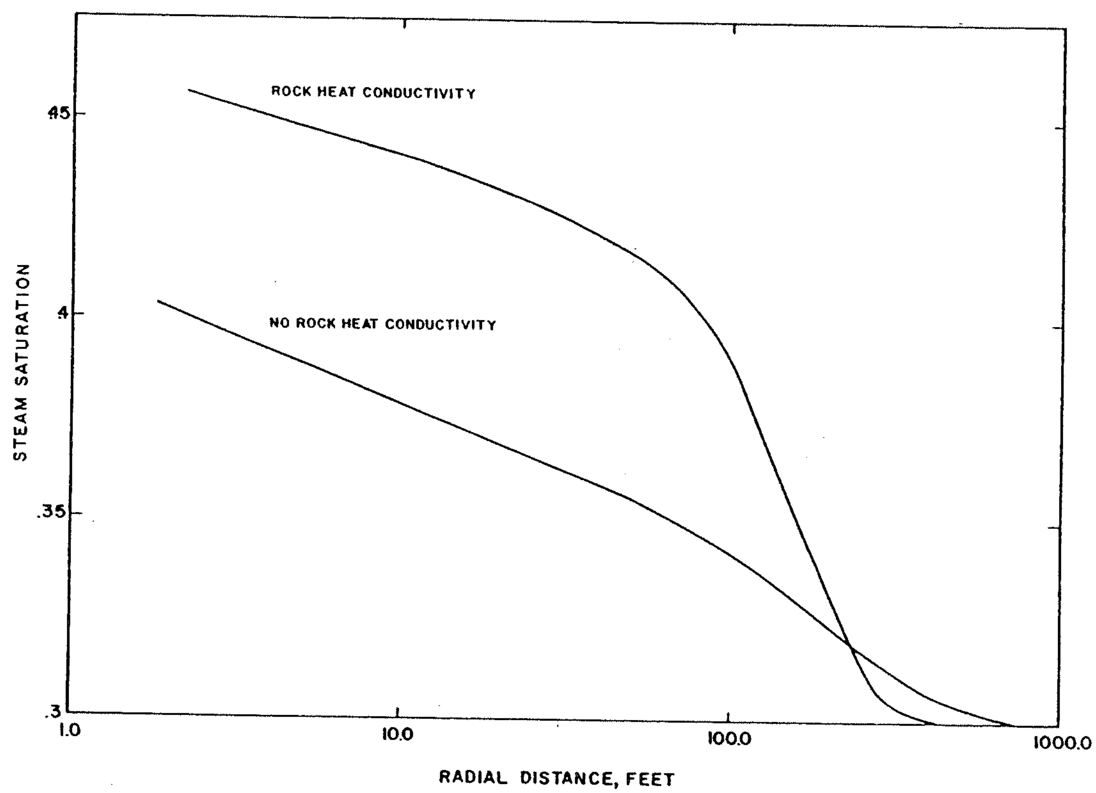

FIGURE 42

APPENDIX D

GEOTHERMAL WELL TESTS FOR CERRO PRIETO M21 AND HGP-A

CERRO PRIETO WELL TEST I

MULTI-RATE DRAWDOWN

Time days	P_{wh} psia	X_{wh} frac.	P_{sf} psia	X_{sf} frac.
W = 400,000 lb/hr				
.0010	381.5	.1975	836.	.0924
.0260	314.1	.2435	749.	.1479
.1260	265.7	.2705	701.	.1690
.2260	225.7	.2877	679.	.1771
.3886	188.2	.2979	663.	.1827
.6949	183.4	.3064	644.	.1871
1.1949	169.7	.3117	630.	.1896
1.6949	166.9	.3127	620.	.1918
2.1949	152.6	.3186	612.	.1937
2.6949	141.5	.3242	605.	.1952
3.1949	131.9	.3291	600.	.1966
3.6949	123.9	.3330	595.	.1979
4.1949	116.9	.3364	591.	.1990
4.6949	111.2	.3391	587.	.2000
5.1949	106.3	.3414	584.	.2009
5.6949	102.0	.3433	581.	.2016
6.1949	98.5	.3451	578.	.2023
6.6949	75.5	.3591	576.	.2030
7.0000	73.0	.3523	574.	.2033
W = 100,00 lb/hr				
7.025	469.1	.1188	828.	.0393
7.125	468.7	.1104	868.	.0200
7.225	475.3	.1093	883.	.0175
7.4152	482.3	.1087	895.	.0161
7.7956	489.8	.1082	908.	.0152
8.2956	500.0	.1088	915.	.0175
8.7956	509.5	.1102	918.	.0212
9.2956	518.5	.1117	920.	.0250
9.7956	524.0	.1129	921.	.0277
10.2956	528.5	.1140	922.	.0301
10.7956	532.4	.1149	923.	.0321
11.2956	535.8	.1158	923.	.0340
11.7956	538.8	.1166	923.	.0357
12.2956	541.5	.1174	923.	.0373
12.7956	543.9	.1181	923.	.0388
13.2956	546.2	.1188	923.	.0402
13.7956	548.3	.1194	923.	.0415
14.0000	549.0	.1197	923.	.0420

SINGLE RATE DRAWDOWN, W = 400,000 lb/hr

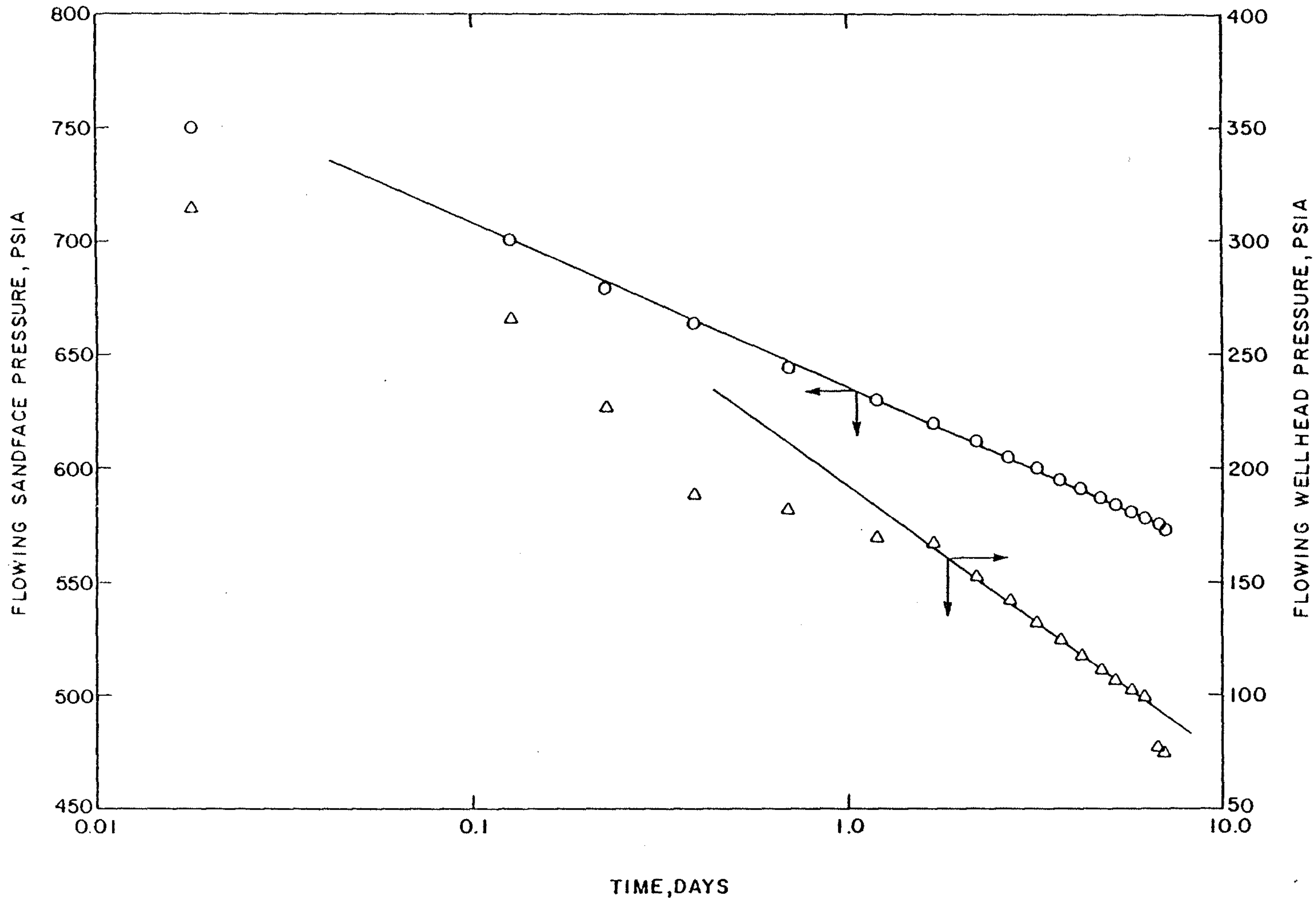

FIGURE 1–A

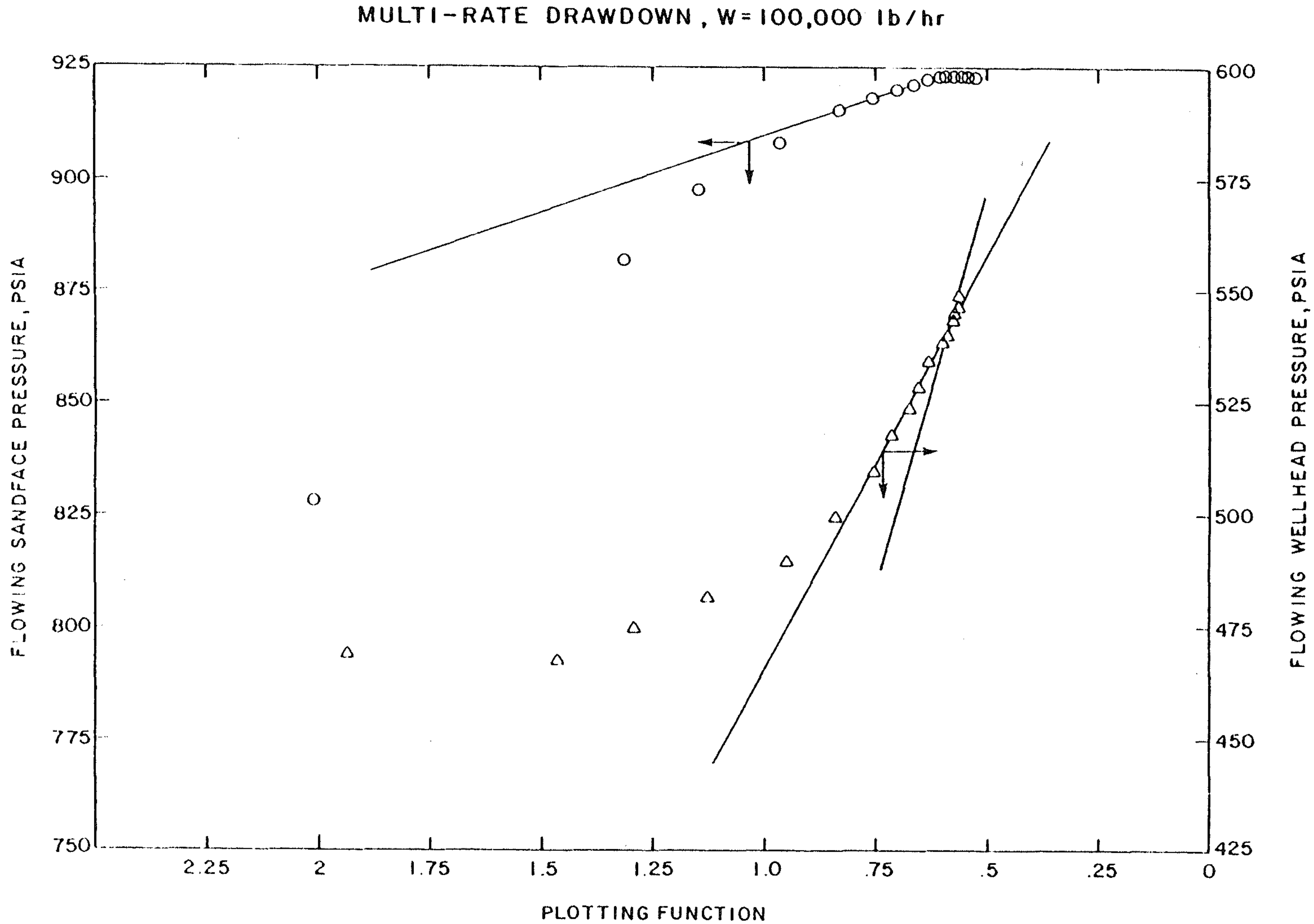
MULTI-RATE DRAWDOWN, W=100,000 lb/hr
925
900
875
850
825
800
775
750
600
575
550
525
500
475
450
425
2.25
2
1.75
1.5
1.25
1.0
.75
.5
.25
0
PLOTTING FUNCTION
FLOWING SANDFACE PRESSURE, PSIA
FLOWING WELLHEAD PRESSURE, PSIA

FIGURE 1-B

CERRO PRIETO WELL TEST 2

MULTI-RATE DRAWDOWN

Time days	P_{wh} psia	X_{wh} frac.	P_{sf} psia	X_{sf} frac.
W = 100,000 lb/hr				
.001	594.4	.1284	960.	.0518
.026	598.3	.1083	948.	.0683
.126	601.5	.1226	940.	.0740
.326	600.5	.1302	935.	.0759
.726	599.5	.1344	931.	.07738
1.226	598.4	.1364	928.	.0782
1.726	597.7	.1375	927.	.0787
2.226	597.1	.1383	925.	.0790
2.726	596.7	.1388	924.	.0793
3.226	596.3	.1392	924.	.0795
3.726	595.9	.1395	923.	.0796
4.226	595.6	.1398	922.	.0797
4.726	595.3	.14	922.	.0798
5.226	595.1	.1402	921.	.0799
5.726	594.9	.1404	921.	.08
6.226	594.7	.1405	921.	.0801
6.726	594.5	.1407	920.	.0802
7.000	594.4	.1408	920.	.0802
W = 350,000 lb/hr				
7.025	348.8	.2526	742.	.1659
7.125	315.9	.2691	706.	.1815
7.225	303.6	.2735	694.	.1852
7.425	291.1	.2771	681.	.1877
7.825	280.1	.2790	670.	.1881
8.325	272.1	.2794	662.	.1874
8.825	267.0	.2796	657.	.1868
9.325	253.2	.2827	654.	.1863
9.825	249.8	.2829	651.	.1859
10.325	246.8	.2833	648.	.1856
10.825	244.3	.2836	646.	.1854
11.325	242.1	.2840	644.	.1853
11.825	240.1	.2842	642.	.1852
12.325	238.2	.2845	640.	.1851
12.825	236.5	.2849	639.	.1851
13.325	234.9	.2852	637.	.1850
13.825	233.4	.2855	636.	.1850
14.000	232.8	.2856	636.	.1851

SINGLE RATE DRAWDOWN, W= 100,000 lb/hr

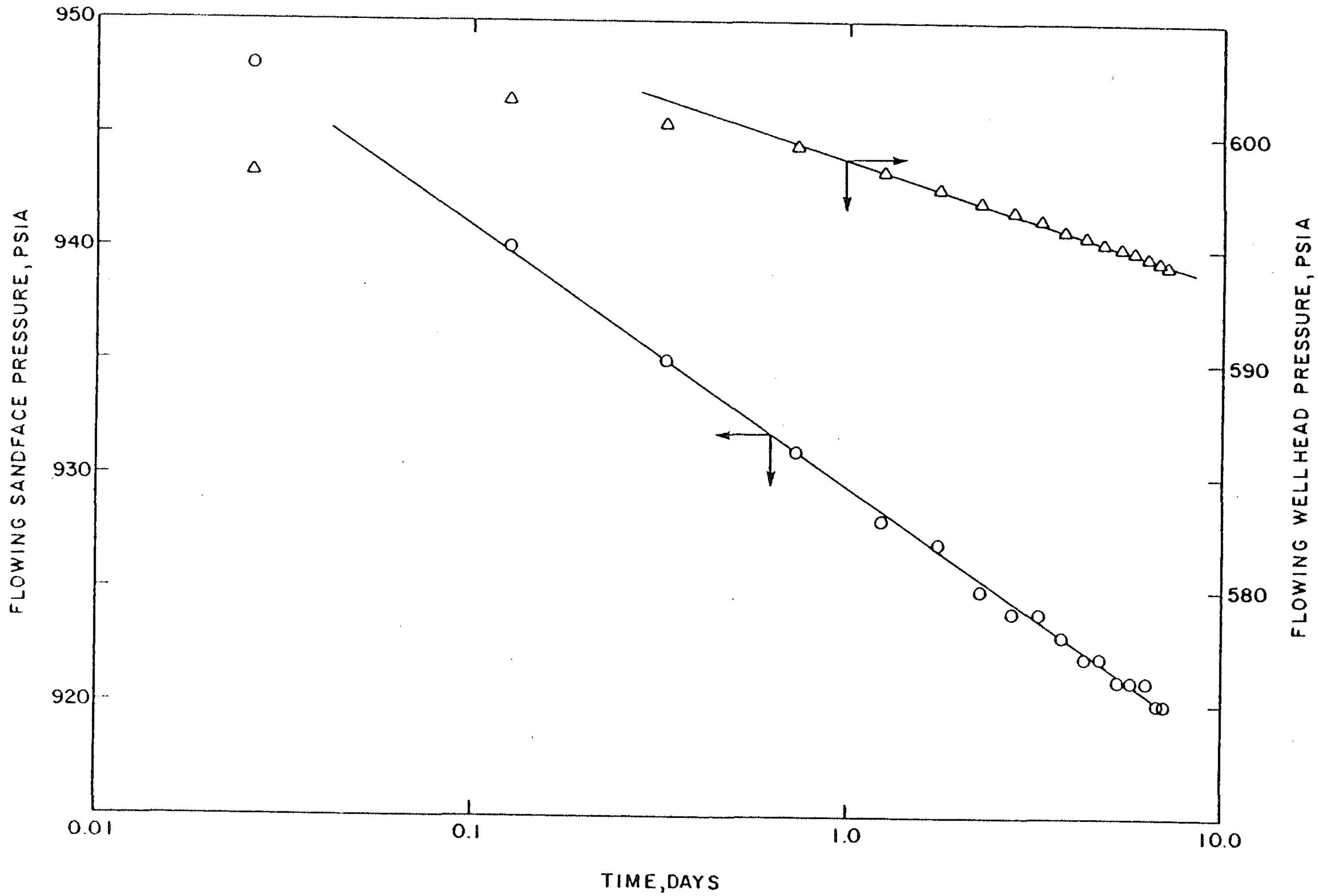

FIGURE 2-A

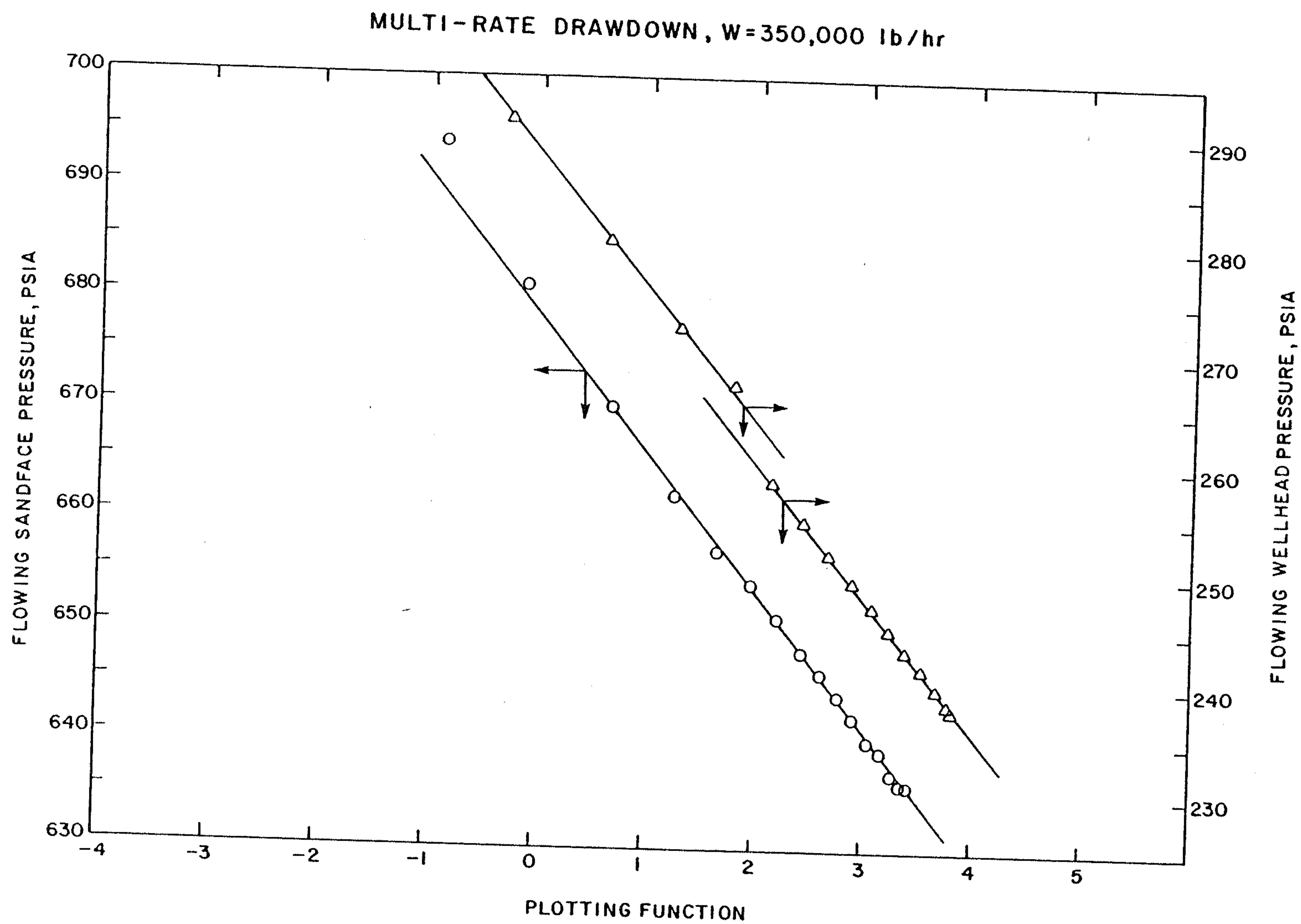

MULTI-RATE DRAWDOWN, W=350,000 lb/hr
FLOWING SANDFACE PRESSURE, PSIA
FLOWING WELLHEAD PRESSURE, PSIA
PLOTTING FUNCTION
700
690
680
670
660
650
640
630
290
280
270
260
250
240
230
−4
−3
−2
−1
0
1
2
3
4
5

FIGURE 2-B

CERRO PRIETO WELL TEST 3

MULTI-RATE DRAWDOWN

Time days	P_{wh} psia	X_{wh} frac.	P_{sf} psia	X_{sf} frac.
W = 300,000 lb/hr				
.001	475.3	.1677	880.	.0783
.026	443.2	.1943	824.	.1208
.126	416.8	.2115	789.	.1359
.2274	405.9	.2179	776.	.1415
.4303	395.1	.2231	763.	.1458
.8361	384.1	.2277	751.	.1491
1.3361	376.1	.2303	742.	.1509
1.8361	370.7	.2320	735.	.1521
2.3361	366.6	.2334	731.	.1531
2.8361	363.2	.2346	727.	.1540
3.3361	360.4	.2356	724.	.1548
3.8361	357.9	.2365	721.	.1556
4.3361	355.7	.2373	719.	.1562
4.8361	353.7	.2380	716.	.1567
5.3361	351.6	.2387	714.	.1573
5.8361	350.0	.2393	713.	.1577
6.3361	348.5	.2398	711.	.1581
6.8361	347.2	.2403	710.	.1585
7.0	346.7	.2405	709.	.1586
W = 200,000 lb/hr				
7.025	457.7	.1803	791.	.1095
7.125	467.1	.1741	805.	.1023
7.325	472.3	.1728	811.	.1011
7.725	476.3	.1739	815.	.1026
8.225	478.5	.1751	817.	.1043
8.725	479.7	.1761	817.	.1056
9.225	480.4	.1769	818.	.1066
10.225	481.1	.1786	817.	.1086
11.225	481.3	.1801	817.	.1104
12.225	481.2	.1813	816.	.1119
13.225	481.0	.1823	815.	.1131
14.00	480.8	.1830	815.	.1139

SINGLE RATE DRAWDOWN, W = 300,000 lb/hr

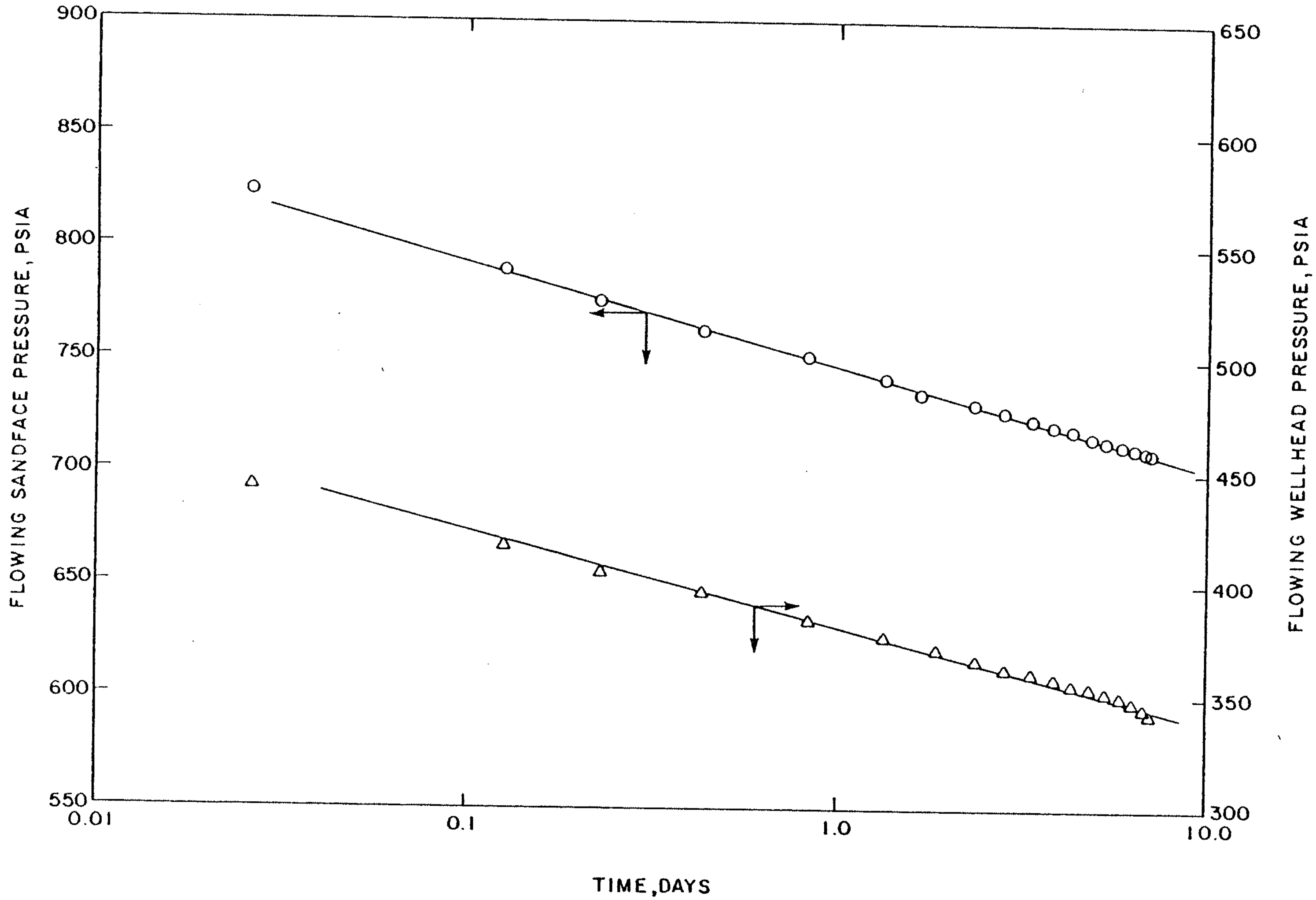

FIGURE 3-A

MULTI-RATE DRAWDOWN, W=200,000 lb/hr

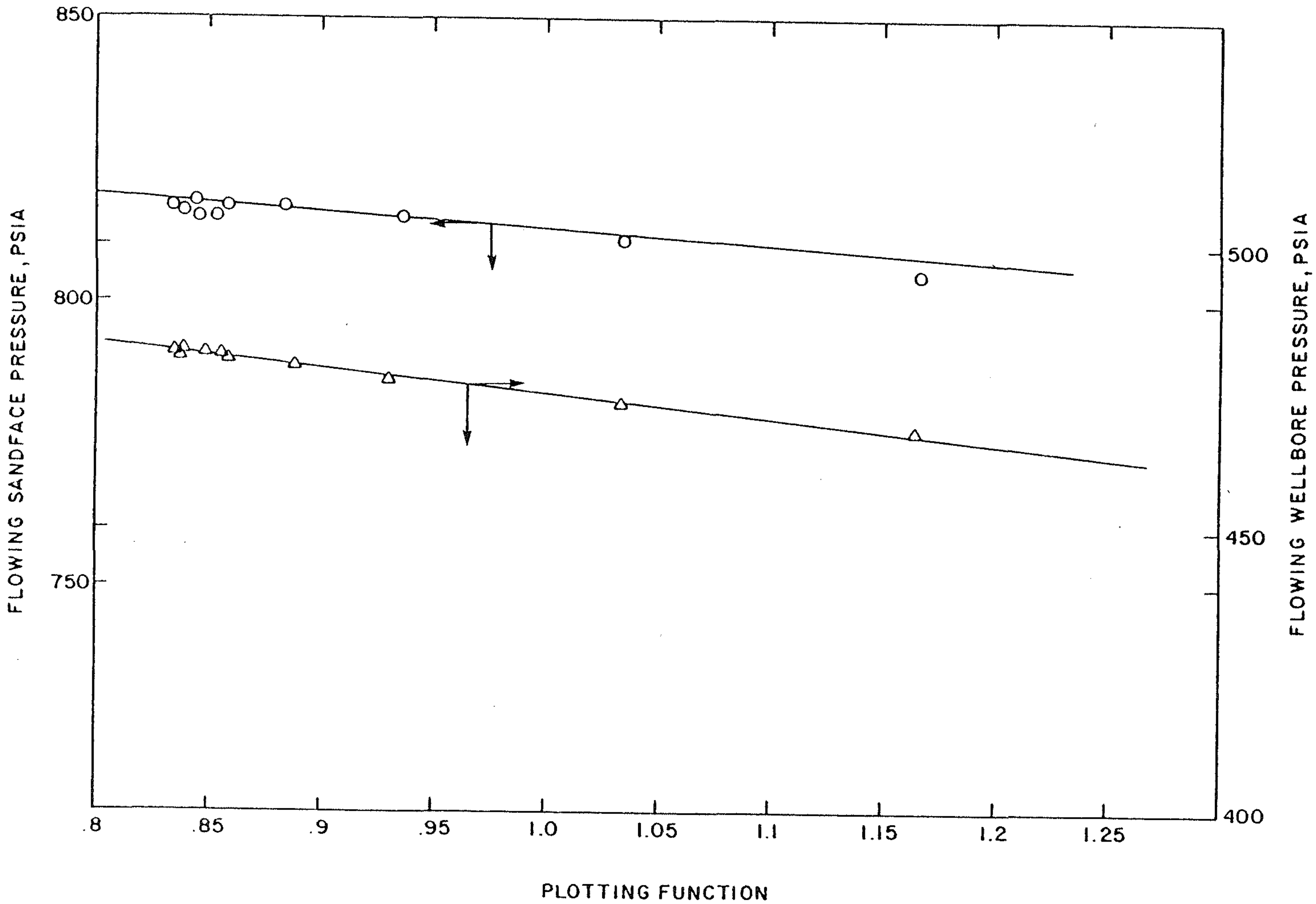

FIGURE 3-B

CERRO PRIETO WELL TEST 4

EXTENDED MULTI-RATE TEST

Time days	P_{wh} psia	X_{wh}	P_{sf} psia	X_{sf}
W = 300,000 lb/hr				
(For First 7 Days is Identical to Test 3)				
7.3361	345.9	.2408	708.	.1588
8.3361	343.6	.2415	706.	.1594
9.3361	341.5	.2422	703.	.1600
10.3361	339.7	.2428	701.	.1604
11.3361	338.1	.2433	700.	.1608
12.3361	336.6	.2438	698.	.1613
13.3361	335.2	.2442	696.	.1616
14.3361	333.9	.2446	695.	.1619
15.3361	332.7	.2450	694.	.1622
16.3361	331.5	.2453	693.	.1625
17.3361	330.4	.2457	691.	.1628
18.3361	329.4	.2460	690.	.1631
19.3361	328.5	.2462	689.	.1633
20.3361	327.6	.2465	688.	.1635
21.0	327.0	.2467	688.	.1637
W = 200,000 lb/hr				
21.025	441.7	.1846	771.	.1133
21.125	451.6	.1783	785.	.1061
21.325	457.0	.1762	792.	.1039
21.725	461.7	.1753	798.	.1029
22.225	464.6	.1758	801.	.1037
22.725	466.4	.1768	802.	.1050
23.225	467.7	.1777	803.	.1062
23.725	468.5	.1783	804.	.1071
24.225	469.2	.1788	804.	.1076
24.725	469.7	.1791	805.	.1081
25.225	470.2	.1793	805.	.1084
25.725	470.6	.1795	805.	.1086
26.225	470.9	.1797	806.	.1089
26.725	471.2	.1799	806.	.1091
27.225	471.4	.1801	806.	.1094
27.725	471.6	.1804	806.	.1097
28.0	471.7	.1805	806.	.1099

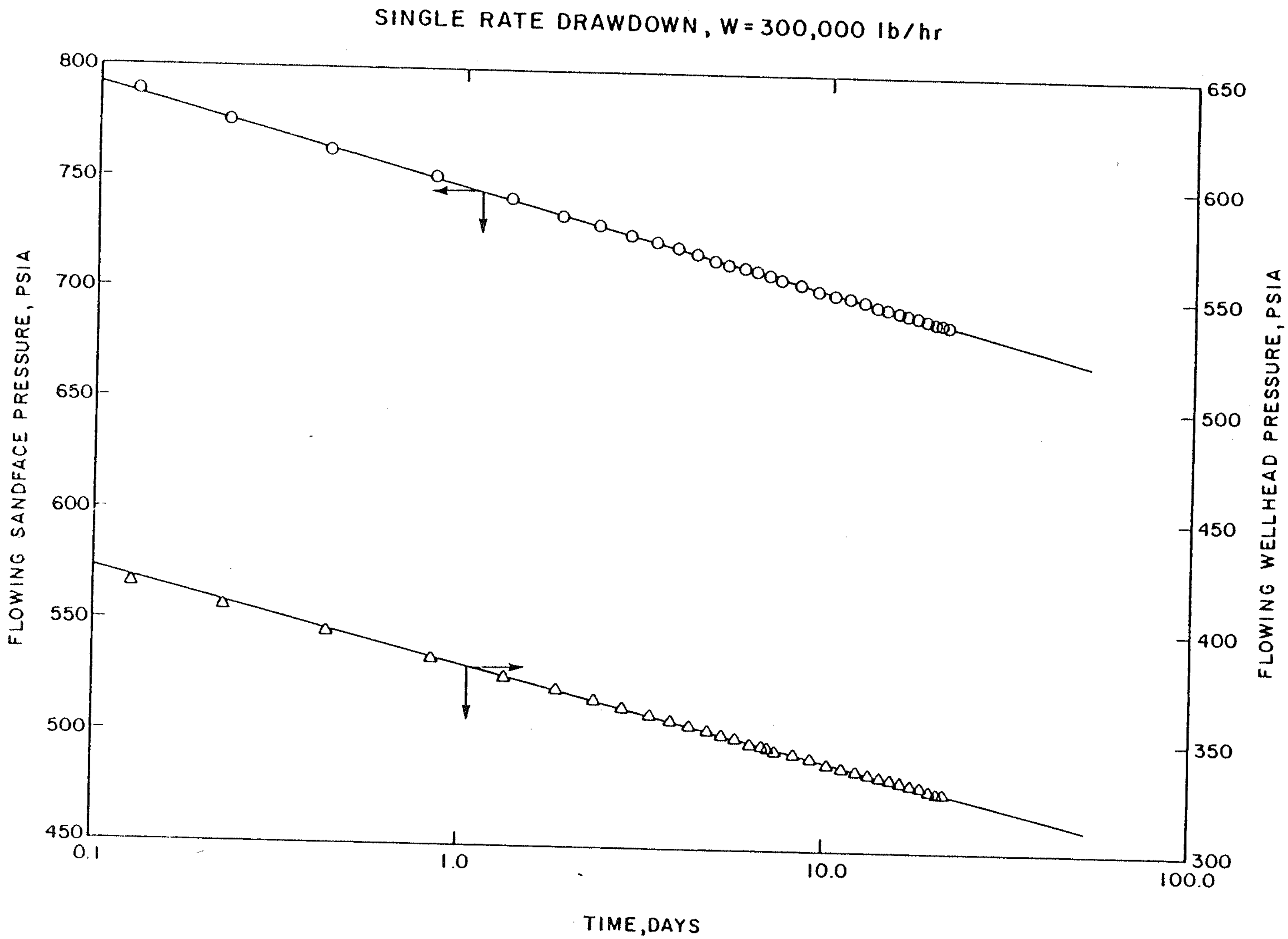
SINGLE RATE DRAWDOWN, W=300,000 lb/hr
FLOWING SANDFACE PRESSURE, PSIA
800
750
700
650
600
550
500
450
FLOWING WELLHEAD PRESSURE, PSIA
650
600
550
500
450
400
350
300
0.1
1.0
10.0
100.0
TIME, DAYS

FIGURE 4-A

MULTI-RATE DRAWDOWN, W=200,000 lb/hr

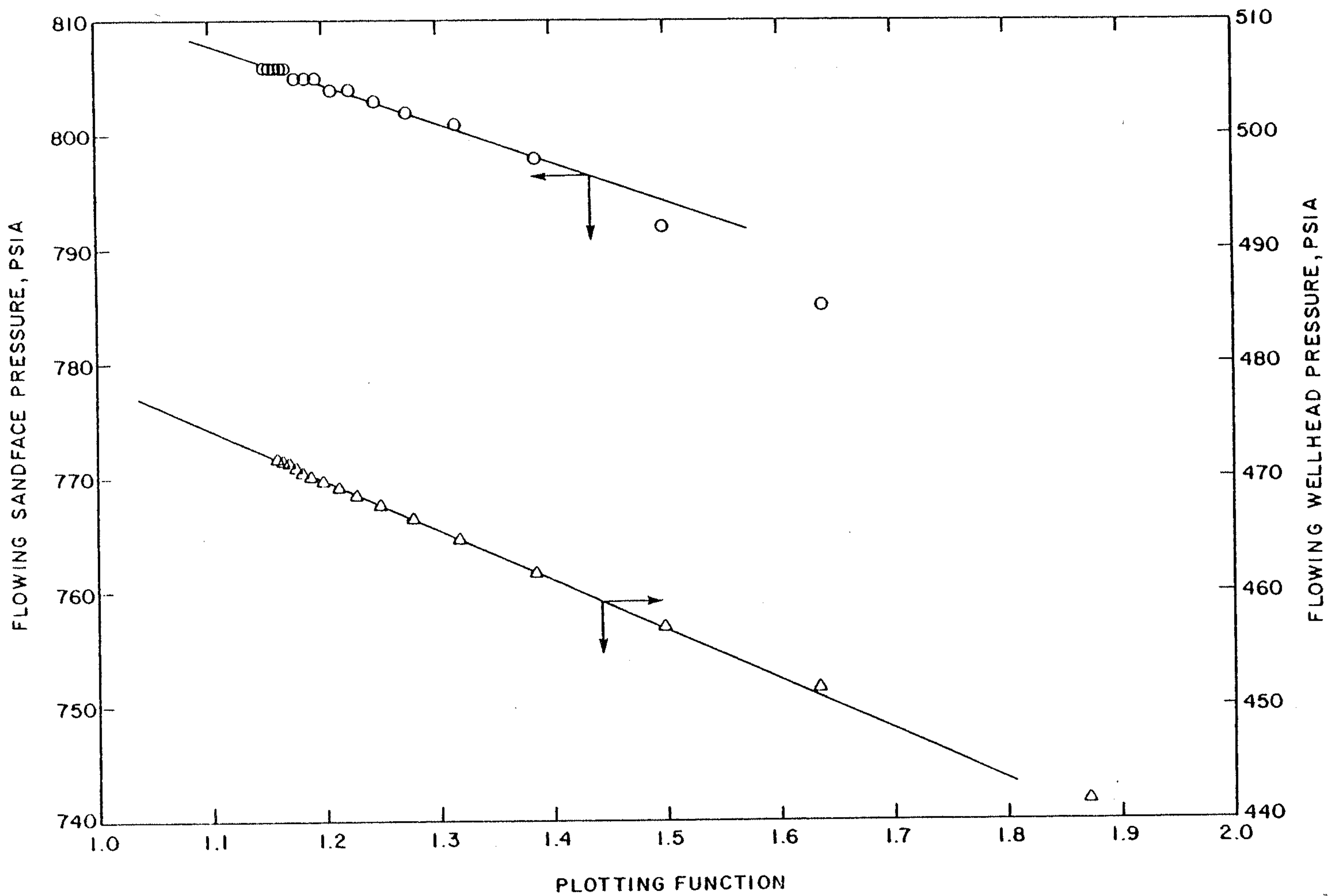

FIGURE 4-B

CERRO PRIETO WELL TEST 5

MULTI-RATE TEST

Time days	P_{wh} psia	X_{wh}	P_{sf} psia	X_{sf}
W = 200,000 lb/hr				
.001	544.4	.1456	921.	.0646
.026	537.2	.1535	890.	.0947
.126	524.0	.1673	868.	.1051
.2939	517.1	.1738	858.	.1095
.6296	510.6	.1777	849.	.1122
1.1296	505.5	.18	842.	.1139
1.6296	502.2	.1812	838.	.1148
2.1296	499.8	.182	835.	.1154
2.6296	497.9	.1827	833.	.1159
3.1296	496.3	.1832	831.	.1163
3.6296	495.0	.1837	830.	.1166
4.1296	493.9	.1841	828.	.1170
4.6296	492.9	.1845	827.	.1173
5.1296	492.0	.1849	826.	.1176
5.6296	491.9	.1852	825.	.1178
6.1296	490.4	.1854	824.	.1180
6.6296	489.7	.1857	823.	.1182
7.00	489.2	.1859	822.	.1184
W = 300,000 lb/hr				
7.025	381.9	.2383	746.	.1602
7.125	368.9	.2449	730.	.1664
7.325	360.6	.2471	722.	.1680
7.725	354.7	.2478	715.	.1681
8.225	350.7	.2477	711.	.1675
8.725	348.2	.2475	709.	.1669
9.225	346.3	.2471	707.	.1663
9.725	344.7	.2469	705.	.1659
10.225	343.3	.2468	704.	.1656
10.725	342.1	.2467	703.	.1653
11.225	341.0	.2466	702.	.1650
11.725	340.0	.2466	701.	.1649
12.225	339.1	.2465	700.	.1647
12.725	338.2	.2465	699.	.1646
13.225	337.4	.2465	698.	.1645
13.725	336.7	.2465	697.	.1644
14.0	336.2	.2465	697.	.1644

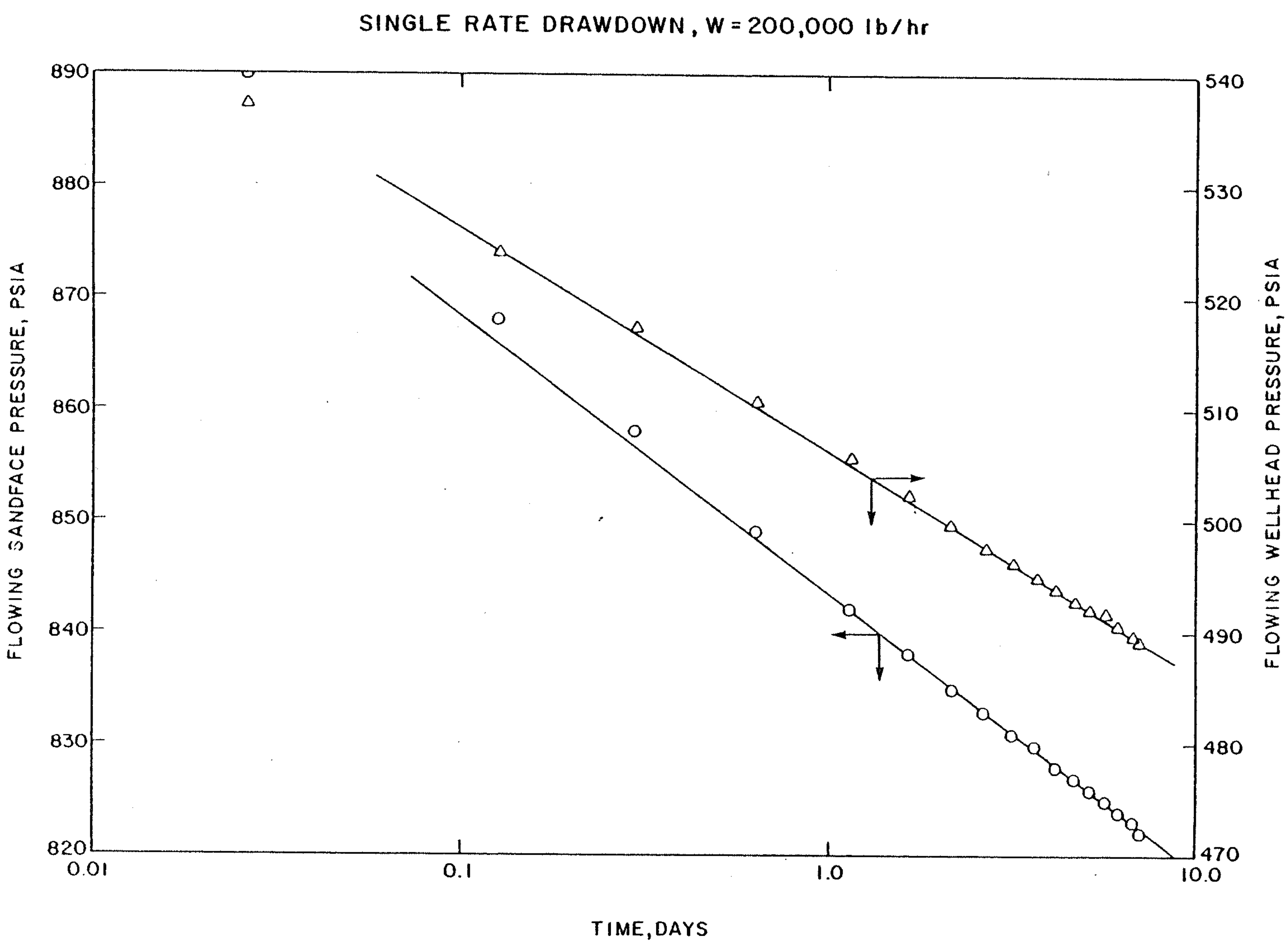
SINGLE RATE DRAWDOWN, W = 200,000 lb/hr
890
880
870
860
850
840
830
820
540
530
520
510
500
490
480
470
0.01
0.1
1.0
10.0
FLOWING SANDFACE PRESSURE, PSIA
FLOWING WELLHEAD PRESSURE, PSIA
TIME, DAYS

FIGURE 5-A

MULTI-RATE DRAWDOWN, W 300,000 lb/hr

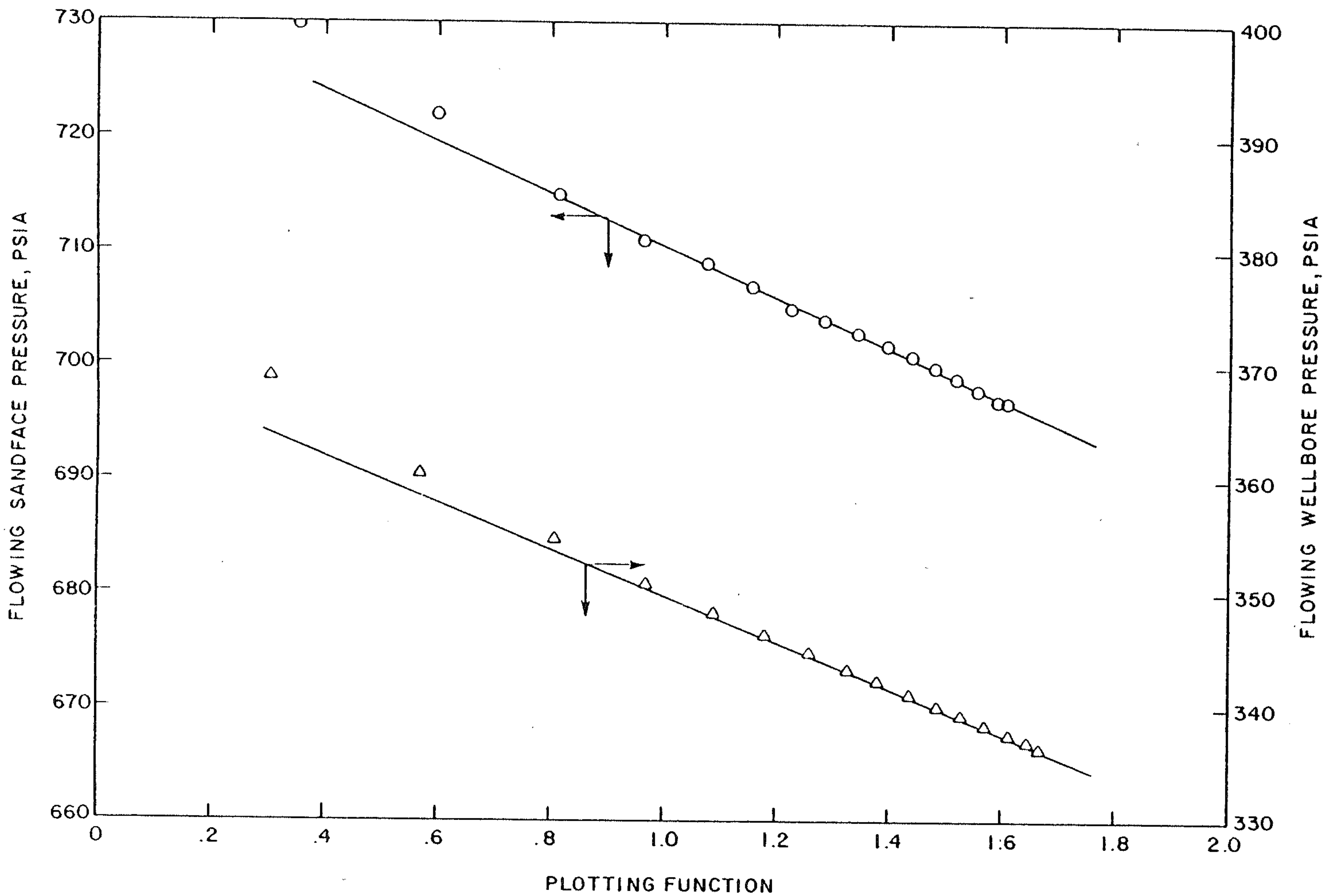

FIGURE 5-B

CERRO PRIETO WELL TEST 6

INJECTION OF COLD WATER INTO TWO PHASE RESERVOIR

Time	P_{sf} psia
Wi = 350,000 lb/hr at 100°F	
.001	1242.
.002	1254.
.003	1261.
.004	1271.
.005	1279.
.006	1289.
.007	1295.
.008	1300.
.009	1304.
.01	1308.
.0112	1312.
.0141	1319.
.0156	1322.
.0172	1326.
.0190	1330.
.0209	1333.
.0230	1337.
.0254	1340.
.0278	1344.
.0304	1346.
.0331	1350.
.0361	1353.
.0393	1356.
.0429	1359.
.0466	1363.
.0504	1365.
.0546	1368.
.0590	1371.
.0640	1374.
.0690	1376.
.0743	1379.
.08	1382.
.0833	1383.
Wi = 700,000 lb/hr at 100°F	
.0898	1771.
.0919	1775.
.0954	1780.
.0993	1786.
.103	1791.
.108	1796.
.112	1801.
.117	1806.
.122	1811.
.127	1815.
.132	1820.
.138	1824.
.145	1829.
.151	1833.
.158	1838.
.165	1842.
.167	1843.

SINGLE RATE INJECTION TEST, W = 350,000 lb/hr

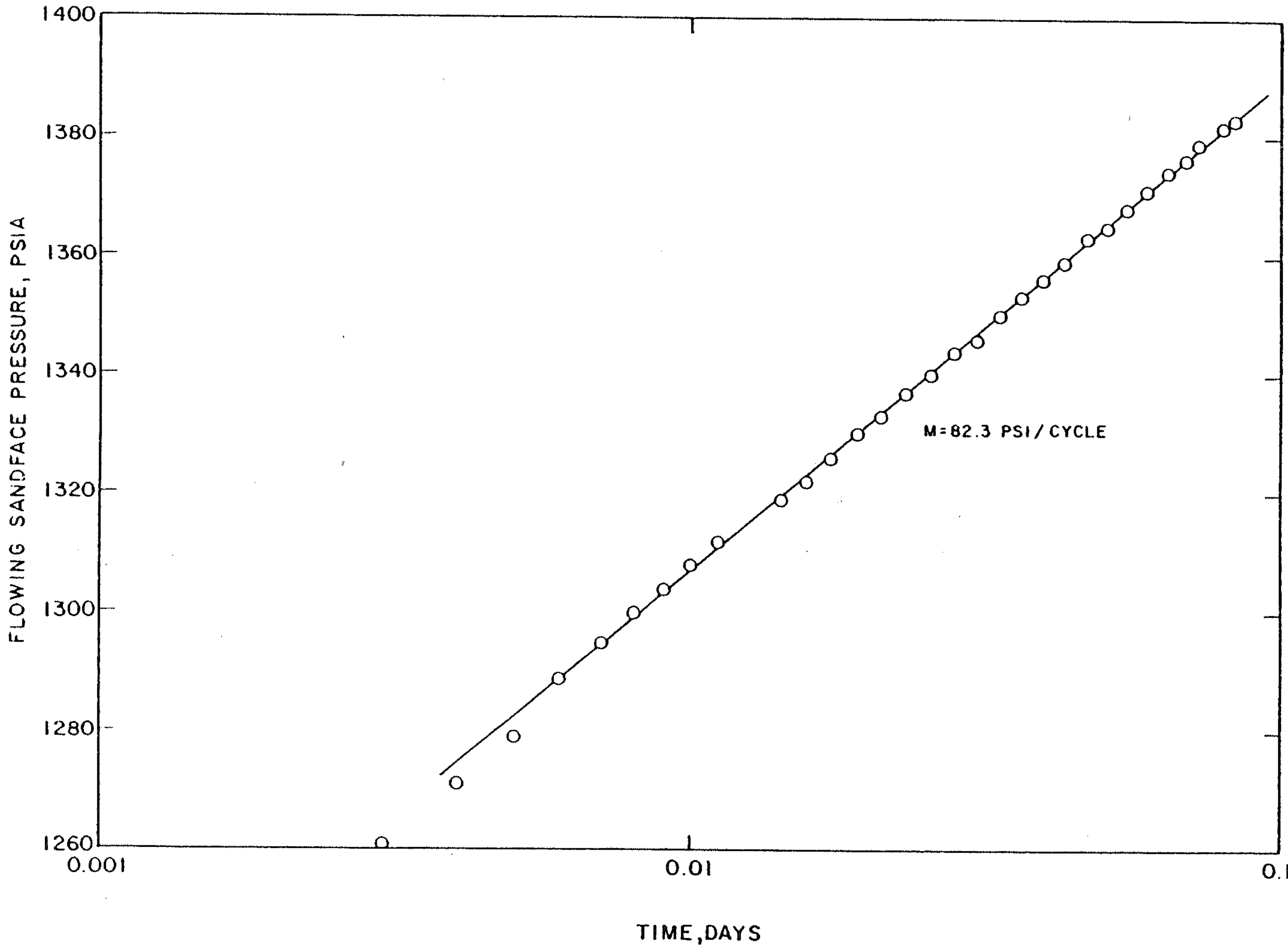

FIGURE 6-A

MULTI-RATE INJECTION TEST, W = 700,000 lb/hr

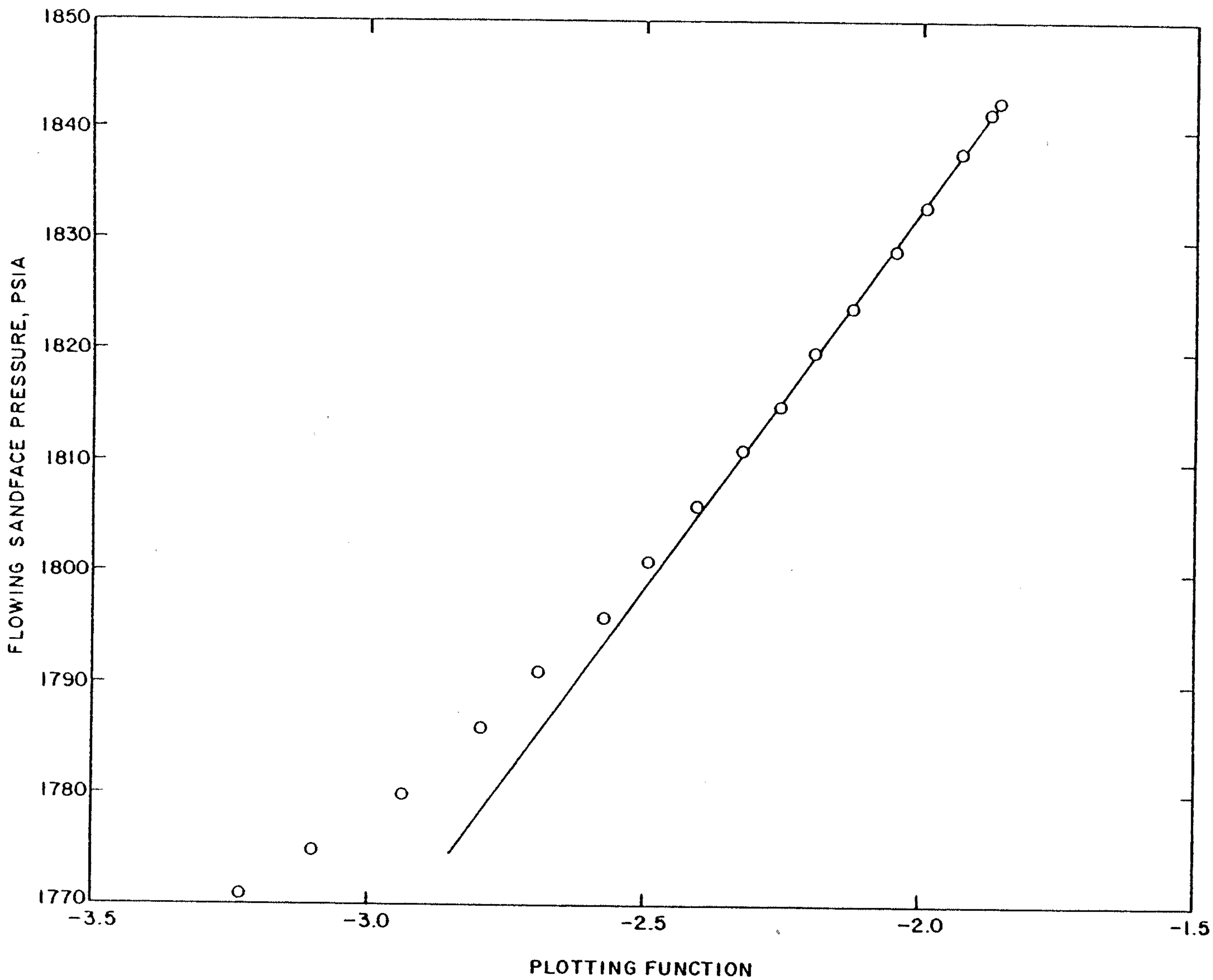

FIGURE 6–B

CERRO PRIETO WELL TEST 7

MULTI-RATE TEST WITH SKIN = -2.31

Time days	P_{wh} psia	X_{wh}	P_{sf} psia	X_{sf}
W = 400,000 lb/hr				
.001	452.5	.1776	919.	.0736
.026	412.9	.2144	856.	.1254
.126	378.1	.2361	815.	.1447
.226	361.8	.2449	797.	.1519
.3886	348.1	.2511	782.	.1570
.6949	332.9	.2563	766.	.1608
1.1949	319.7	.2601	753.	.1633
1.6949	310.2	.2627	744.	.1651
2.1949	303.1	.2648	737.	.1666
2.6949	297.3	.2668	731.	.1679
3.1949	292.3	.2686	726.	.1691
3.6949	288.1	.2702	722.	.1702
4.1949	284.4	.2717	719.	.1711
4.6949	281.2	.2729	716.	.1719
5.1949	278.2	.2740	713.	.1727
5.6949	275.5	.2750	710.	.1733
6.1949	273.0	.2759	708.	.1739
6.6949	270.7	.2768	706.	.1745
7.0	269.3	.2773	704.	.1748
W = 100,000 lb/hr				
7.025	477.2	.1164	846.	.0351
7.125	472.9	.1091	881.	.0168
7.225	478.8	.1082	895.	.0144
7.4152	485.6	.1076	908.	.0131
7.7956	492.8	.1071	920.	.0122
8.2956	503.3	.1077	928.	.0144
8.7956	513.2	.1090	932.	.0178
9.2956	522.5	.1104	935.	.0215
9.7956	528.7	.1114	936.	.024
10.2956	534.0	.1123	938.	.0263
10.7956	538.4	.1131	939.	.0283
11.2956	542.2	.1139	939.	.0301
11.7956	545.4	.1146	940.	.0317
12.2956	548.2	.1154	940.	.0332
12.7956	550.8	.1161	941.	.0347
13.2956	553.2	.1167	941.	.0360
13.7956	555.4	.1173	941.	.0373
14.0	556.2	.1176	941.	.0378

SINGLE RATE DRAWDOWN, W=400,000 lb/hr, SKIN=-2.31

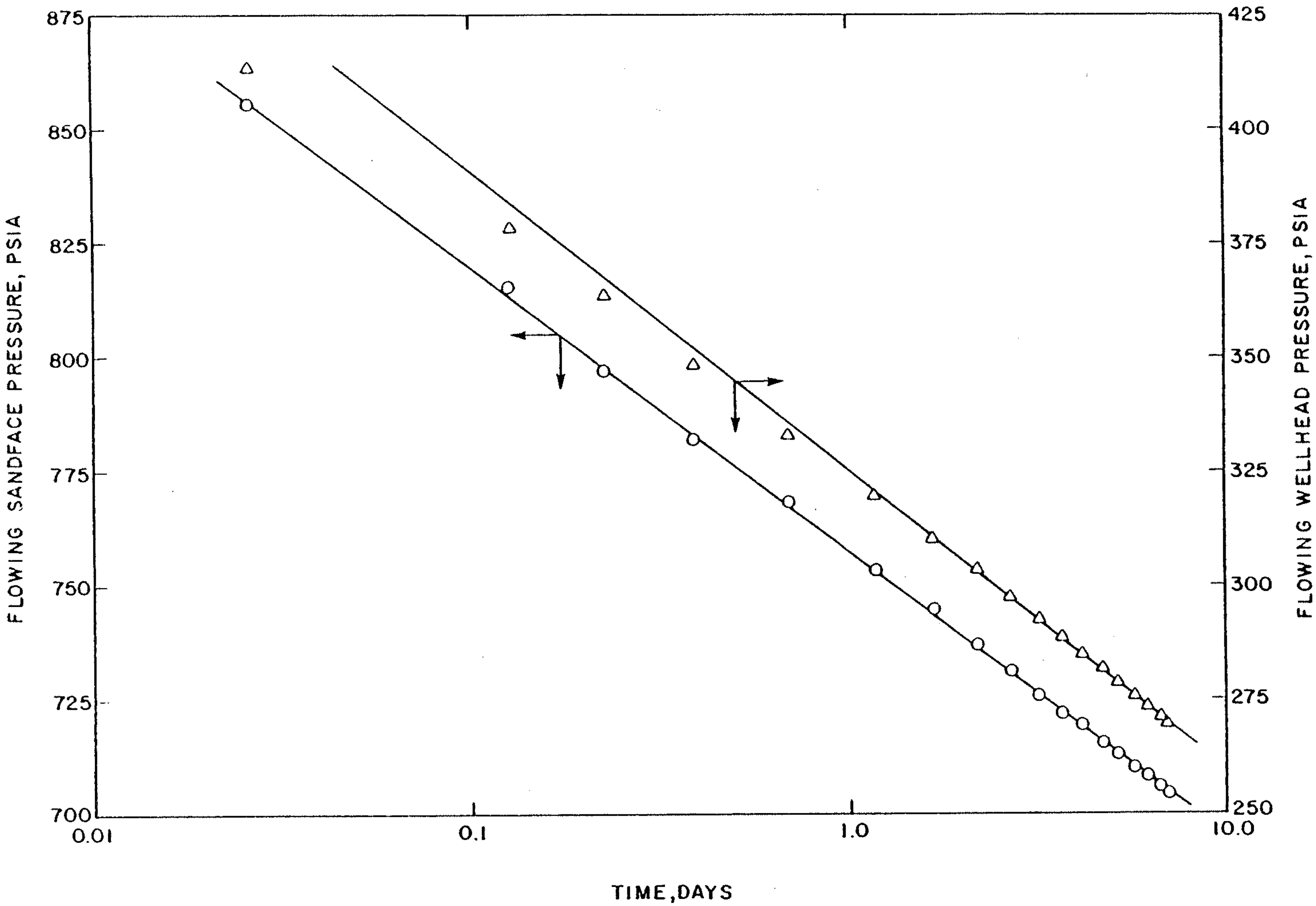

FIGURE 7-A

CERRO PRIETO WELL TEST 8

MULTI-RATE TEST WITH SKIN = -2.33

Time days	P_{wh} psia	X_{wh}	P_{sf} psia	X_{sf}
W = 400,000 lb/hr				
.001	478.9	.1703	953.	.0662
.026	448.1	.2051	899.	.1163
.126	419.9	.2245	860.	.1353
.226	405.4	.2323	844.	.1424
.3886	392.8	.2383	829.	.1475
.6949	379.3	.2432	815.	.1510
1.1949	367.5	.2467	802.	.1531
1.6949	359.1	.2489	793.	.1546
2.1949	352.9	.2506	787.	.1558
2.6949	347.9	.2521	782.	.1569
3.1949	343.7	.2534	777.	.1580
3.6949	340.0	.2546	773.	.1589
4.1949	336.6	.2558	770.	.1598
4.6949	333.7	.2568	767.	.1606
5.1949	331.0	.2577	764.	.1613
5.6949	328.6	.2585	762.	.1620
6.1949	326.4	.2592	760.	.1625
6.6949	324.3	.2599	758.	.1631
7.0	323.1	.2603	756.	.1634
W = 100,000 lb/hr				
7.025	480.3	.1155	855.	.0334
7.125	474.4	.1086	887.	.0155
7.225	480.2	.1077	900.	.0132
7.4152	486.8	.1071	912.	.0119
7.7956	494.0	.1067	925.	.0110
8.2956	504.8	.1072	933.	.0131
8.7956	514.8	.1085	937.	.0164
9.2956	524.3	.1099	940.	.0201
9.7956	530.7	.1109	942.	.0227
10.2956	536.7	.1118	944.	.0249
10.7956	540.7	.1125	945.	.0269
11.2956	544.7	.1133	946.	.0286
11.7956	548.3	.1139	947.	.0303
12.2956	551.2	.1146	947.	.0318
12.7956	553.9	.1153	947.	.0332
13.2956	556.3	.1160	948.	.0345
13.7956	558.6	.1166	948.	.0358
14.0	559.4	.1168	948.	.0362

SINGLE RATE DRAWDOWN, W=400,000 lb/hr, SKIN=-2.33

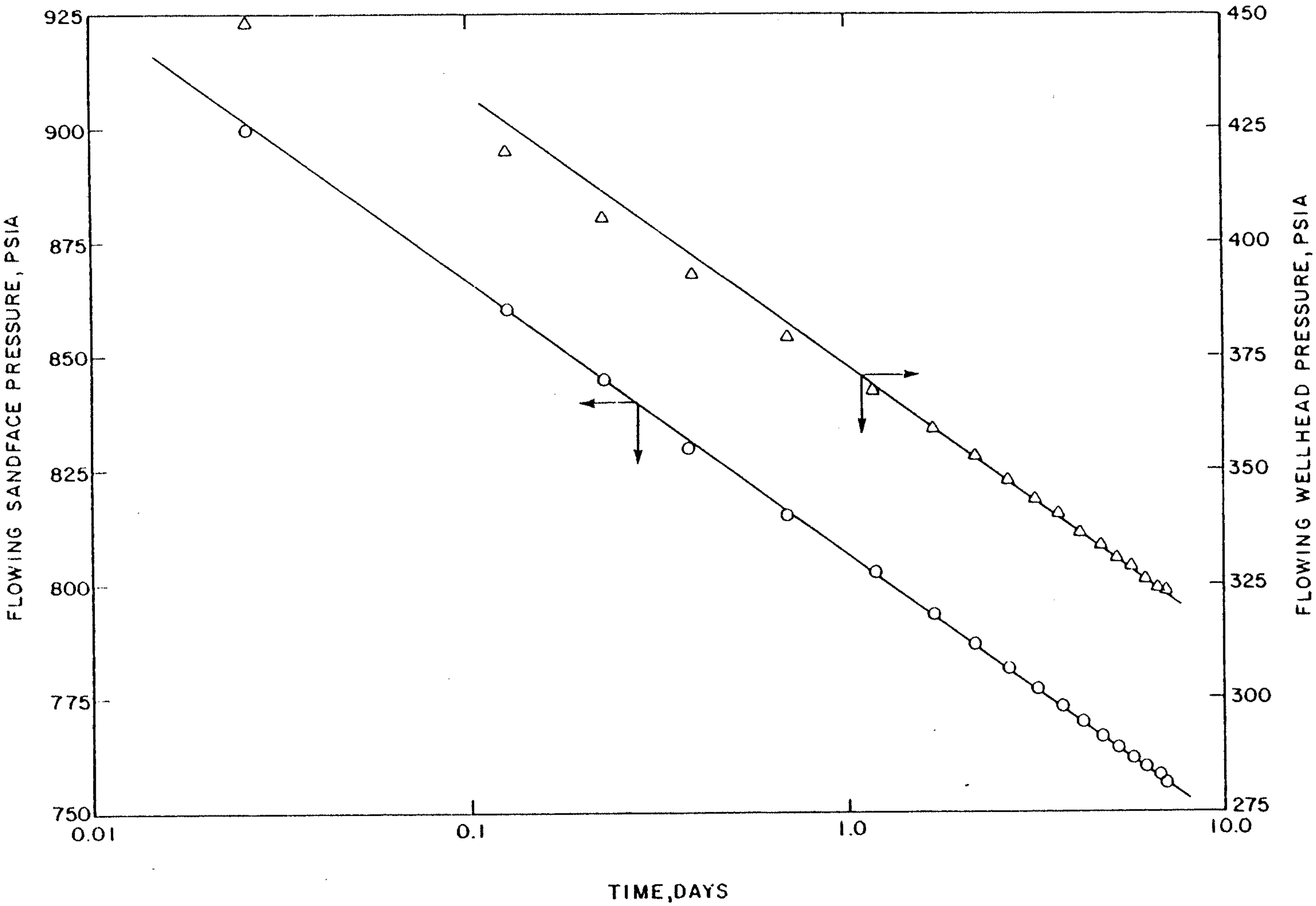

FIGURE 8-A

CERRO PRIETO WELL TEST 9

MULTI-RATE TEST OF ONE PHASE RESERVOIR
AT THE BOILING POINT

Time days	P_{wh} psia	X_{wh}	P_{sf} psia	X_{sf}
W = 400,000 lb/hr				
.001	401.2	.1448	924.	.0181
.026	388.2	.1493	880.	.0362
.126	369.9	.1602	847.	.0469
.2336	360.2	.1652	833.	.0513
.4488	350.8	.1694	820.	.0549
.8791	341.5	.1730	807.	.0580
1.3791	334.7	.1754	799.	.0600
1.8791	329.6	.1771	793.	.0614
2.3791	325.8	.1784	789.	.0625
2.8791	322.8	.1794	785.	.0633
3.3791	320.3	.1802	782.	.0640
3.8791	318.0	.1808	780.	.0646
4.3791	316.1	.1815	777.	.0651
4.8791	314.2	.1820	775.	.0655
5.3791	312.4	.1826	773.	.0659
5.8791	310.9	.1831	772.	.0663
6.3791	309.5	.1835	770.	.0668
6.8791	308.2	.1839	769.	.0671
7.0	307.8	.1841	768.	.0672
W = 100,000 lb/hr				
7.025	469.2	.1050	911.	.0038
7.125	476.3	.1042	930.	.0008
7.225	479.6	.1040	937.	.0001
7.3472	482.7	.1039	941.	.0000
7.5750	486.6	.1039	946.	.0002
7.9839	490.6	.1039	950.	.0005
8.4839	494.1	.1038	953.	.0009
8.9839	496.2	.1039	955.	.0011
9.4839	497.8	.1039	957.	.0014
9.9839	499.1	.1040	958.	.0015
10.4839	500.1	.1040	958.	.0017
10.9839	501.0	.1041	959.	.0019
11.4839	501.7	.1042	960.	.0020
11.9839	502.3	.1043	960.	.0022
12.4839	502.9	.1044	960.	.0023
12.9839	503.4	.1044	961.	.0024
13.4839	503.9	.1045	961.	.0025
14.0	504.3	.1045	961.	.0026

SINGLE RATE DRAWDOWN, W = 400,000 lb/hr

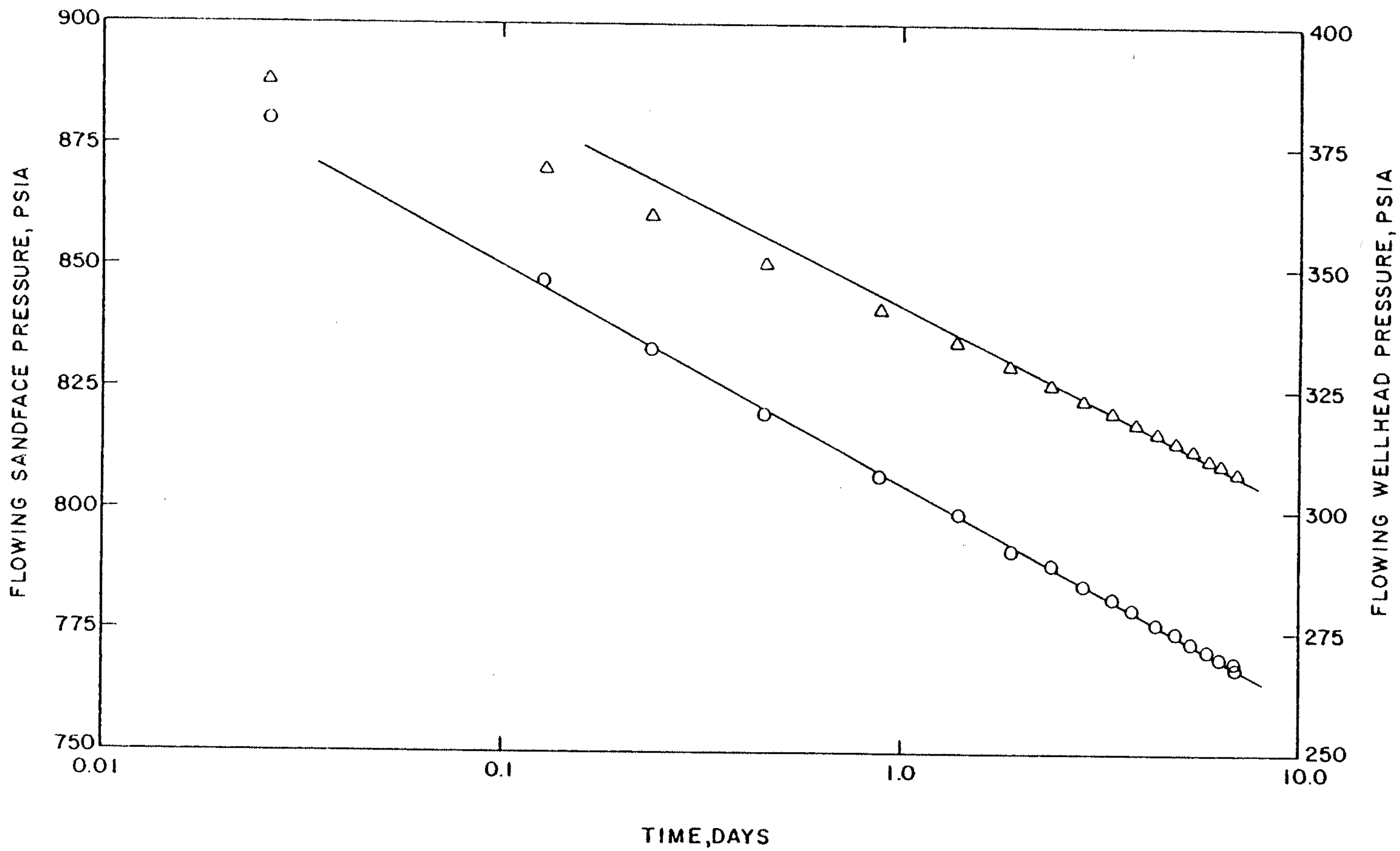

FIGURE 9–A

CERRO PRIETO WELL TEST 10

MULTI-RATE TEST OF ONE PHASE RESERVOIR
$10^{\circ}F$ BELOW THE BOILING POINT

Time days	P_{wh} psia	X_{wh}	P_{sf} psia	X_{sf}
W = 400,000 lb/hr				
.001	356.1	.1432	895.	.0054
.026	345.8	.1403	874.	.0105
.126	341.2	.1440	863.	.0132
.326	338.1	.1463	856.	.0148
.726	335.4	.1478	851.	.0161
1.226	333.2	.1489	847.	.0172
1.726	331.1	.1497	843.	.0181
2.226	329.1	.1505	839.	.0191
2.726	327.2	.1511	836.	.0198
3.226	385.5	.1517	833.	.0205
3.726	323.8	.1523	830.	.0213
4.226	322.1	.1529	827.	.0220
4.726	320.6	.1534	824.	.0226
5.226	319.2	.1538	822.	.0232
5.726	318.0	.1542	819.	.0237
6.226	317.1	.1545	818.	.0241
6.726	320.4	.1535	817.	.0244
7.0	319.9	.1537	816.	.0245
W = 100,000 lb/hr				
7.025	458.2	.1036	919.	0
7.125	462.6	.1027	935.	0
7.2805	465.1	.1025	940.	0
7.5914	467.3	.1024	943.	0
8.0914	469.0	.1023	946.	0
8.5914	469.9	.1023	947.	0
9.0914	470.4	.1023	948.	0
9.5914	470.8	.1023	949.	0
10.0914	471.0	.1023	950.	0
10.5914	471.2	.1023	950.	0
11.0914	471.4	.1023	951.	0
11.5914	471.5	.1023	951.	0
12.0914	471.6	.1023	951.	0
12.5914	471.6	.1023	951.	0
13.0914	471.7	.1024	951.	0
13.5914	471.7	.1024	952.	0
14.0	471.8	.1024	952.	0

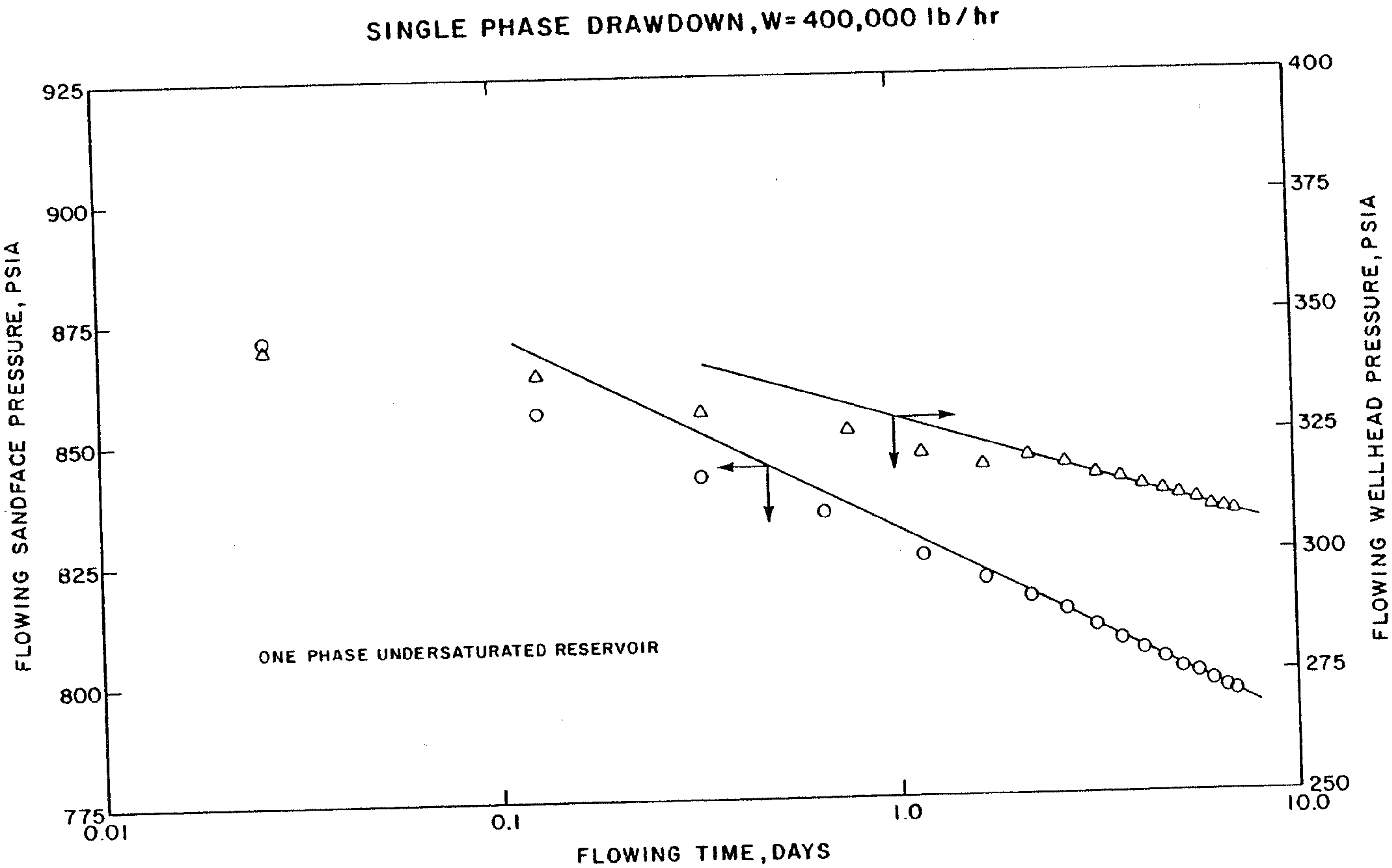
SINGLE PHASE DRAWDOWN, W=400,000 lb/hr
925
900
875
850
825
800
775
0.01
0.1
1.0
10.0
400
375
350
325
300
275
250
FLOWING SANDFACE PRESSURE, PSIA
FLOWING WELLHEAD PRESSURE, PSIA
ONE PHASE UNDERSATURATED RESERVOIR
FLOWING TIME, DAYS

FIGURE 10-A

CERRO PRIETO WELL TEST II

MULTI-RATE TEST WITH PERMEABILITY = 35 md

Time days	P_{wh} psia	X_{wh}	P_{sf} psia	X_{sf}
W = 300,000 lb/hr				
.001	284.2	.2254	649.	.1325
.026	97.1	.3468	451.	.2353
.126	-	-	330.	.2850
.226	-	-	275.	.3086
.326	-	-	240.	.3232
.4627	-	-	209.	.3364
.6652	-	-	180.	.3495
.9658	-	-	152.	.3626
1.4182	-	-	124.	.3745
1.9182	-	-	104.	.3834
Minimum Pressure Reached P_{sf} = 100 psia				
			W, lb/hr	X_{sf}
2.4182	-	-	296,590	.3842
2.9182	-	-	293,540	.3892
3.4182	-	-	290,960	.3821
3.9182	-	-	288,730	.3814
4.4182	-	-	286,800	.3809
4.9182	-	-	285,050	.3805
5.4182	-	-	283,510	.3802
5.9182	-	-	282,100	.3799
6.4182	-	-	280,800	.3797
7.0	-	-	279,470	.3794
W = 100,000 lb/hr			P_{sf}	X_{sf}
7.025	354.7	.1553	638.	.0870
7.125	400.9	.1290	718.	.0549
7.225	417.3	.1262	743.	.0510
7.3453	429.1	.1251	760.	.0494
7.5607	438.2	.1245	773.	.0485
7.9466	450.4	.1245	787.	.0490
8.4466	461.5	.1249	799.	.0500
8.9466	466.9	.1255	804.	.0513
9.4466	471.4	.1265	807.	.0532
9.9466	475.3	.1279	808.	.0558
10.4466	478.7	.1299	807.	.0592
10.9466	481.9	.1323	805.	.0633
11.4466	484.3	.1353	803.	.0678
11.9466	486.2	.1381	800.	.0721
12.4466	487.6	.1407	798.	.0758
12.9466	488.6	.1429	796.	.0791
13.4466	489.0	.1449	794.	.0817
14.0	489.2	.1468	793.	.0842

CERRO PRIETO WELL TEST 12

MULTI-RATE TEST WITH PERMEABILITY = 50 md

Time days	P_{wh} psia	X_{wh}	P_{sf} psia	X_{sf}
W = 300,000 lb/hr				
.001	431.2	.1808	822.	.0924
.026	360.3	.2309	723.	.1565
.126	308.4	.2602	665.	.1819
.226	284.8	.2724	640.	.1917
.3679	265.4	.2817	620.	.1985
.6195	245.7	.2901	601.	.2043
1.0603	226.1	.2974	582.	.2084
1.5603	212.5	.3020	570.	.2108
2.0603	201.2	.3060	560.	.2130
2.5603	192.8	.3094	551.	.2148
3.0603	186.2	.3123	545.	.2164
3.5603	182.0	.3142	539.	.2178
4.0603	176.7	.3165	534.	.2191
4.5603	172.5	.3184	529.	.2203
5.0603	169.0	.3201	525.	.2213
5.5603	166.2	.3212	521.	.2222
6.0603	164.0	.3221	518.	.2231
6.5603	162.4	.3228	515.	.2238
7.0	164.3	.3221	512.	.2244
W = 100,000 lb/hr				
7.025	461.2	.1342	778.	.0655
7.125	471.5	.1204	825.	.0426
7.225	478.9	.1185	840.	.0393
7.4023	487.4	.1175	853.	.0380
7.7569	496.0	.1167	866.	.0369
8.2569	505.5	.1170	877.	.0376
8.7569	512.3	.1183	880.	.0400
9.2569	519.3	.1206	881.	.0443
9.7569	525.1	.1228	881.	.0484
10.2569	529.5	.1246	881.	.0519
10.7569	533.2	.1261	881.	.0545
11.2569	536.3	.1273	881.	.0567
11.7569	538.7	.1285	881.	.0586
12.2569	540.6	.1295	881.	.0603
12.7569	542.3	.1305	881.	.0618
13.2569	543.7	.1314	881.	.0633
13.7569	545.1	.1323	880.	.0646
14.0	545.7	.1327	880.	.0653

DRAWDOWN TEST OF RESERVOIR, K=50 md

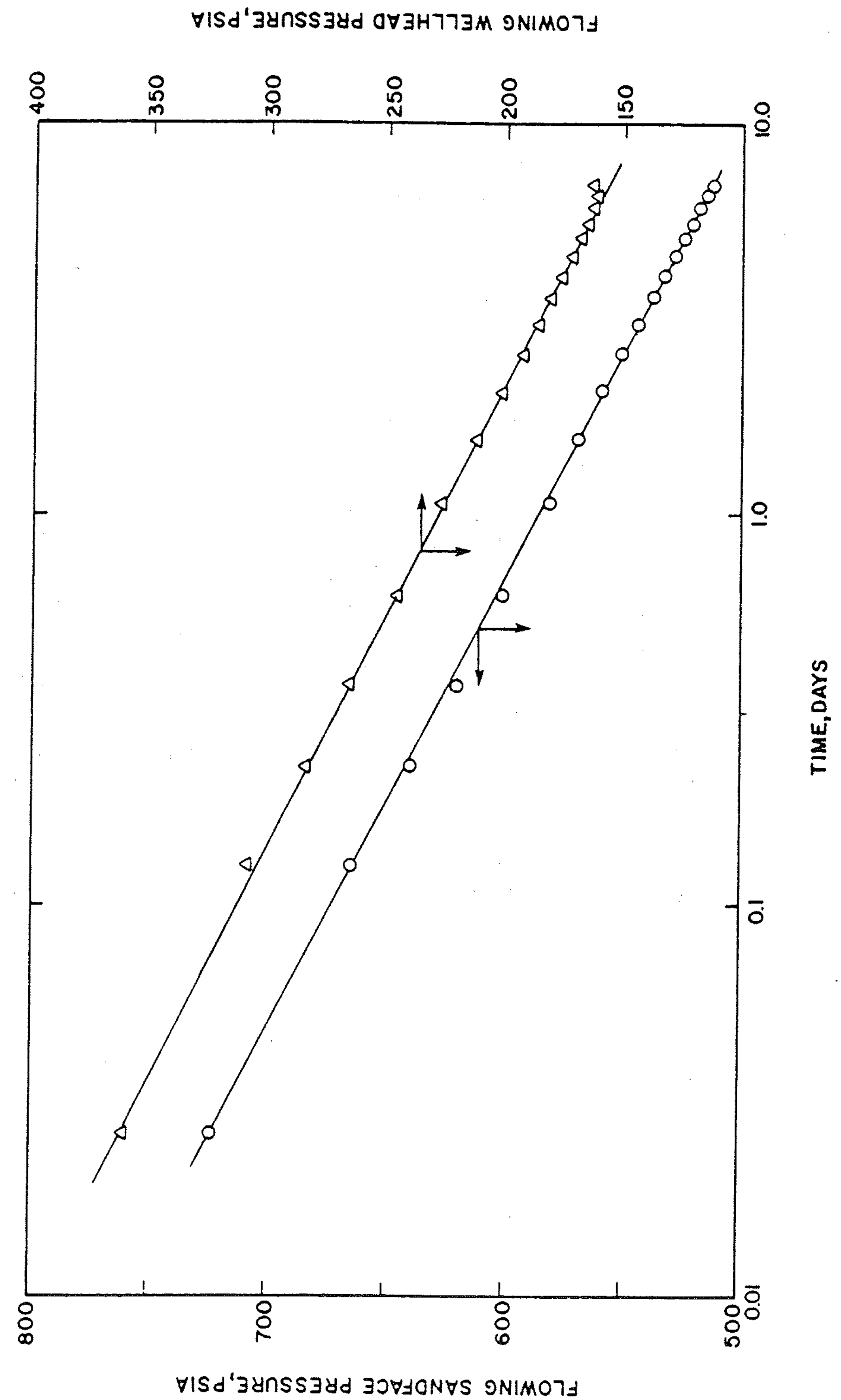

FIGURE 12-A

CERRO PRIETO WELL TEST 13

MULTI-RATE TEST WITH PERMEABILITY = 75 md

Time days	P_{wh} psia	X_{wh}	P_{sf} psia	X_{sf}
W = 300,000 lb/hr				
(First 7 Days Identical to Test 3)				
W = 100,000 lb/hr				
7.025	520.2	.1271	861.	.0569
7.125	520.7	.1195	886.	.0427
7.2499	524.7	.1179	897.	.0396
7.4997	533.3	.1186	905.	.0410
7.9992	543.3	.1204	911.	.0446
8.4992	549.0	.1216	914.	.0468
8.9992	552.3	.1223	916.	.0481
9.4992	555.2	.1231	917.	.0495
9.9992	557.9	.1239	918.	.0509
10.4992	560.2	.1247	918.	.0523
10.9992	562.3	.1254	919.	.0536
11.4992	564.2	.1261	919.	.0548
11.9992	565.8	.1268	919.	.0560
12.4992	567.3	.1274	919.	.0571
12.9992	568.7	.1280	919.	.0581
13.4992	570.0	.1286	919.	.0591
14.0	571.2	.1291	919.	.0600

CERRO PRIETO WELL TEST 14

MULTI-RATE TEST WITH PERMEABILITY = 100 md

Time days	P_{wh} psia	X_{wh}	P_{sf} psia	X_{sf}
W = 300,000 lb/hr				
.001	496.4	.1609	909.	.0708
.026	478.2	.1777	870.	.1032
.126	460.9	.1909	846.	.1141
.2676	452.7	.1965	835.	.1184
.5508	445.1	.2003	825.	.1214
1.0508	438.4	.2028	817.	.1232
1.5508	434.1	.2041	812.	.1241
2.0508	431.0	.2050	808.	.1248
2.5508	428.7	.2057	805.	.1254
3.0508	426.7	.2063	803.	.1259
3.5508	425.0	.2069	801.	.1264
4.0508	423.6	.2074	799.	.1268
4.5508	422.3	.2078	798.	.1272
5.0508	421.1	.2081	797.	.1275
5.5508	420.1	.2085	795.	.1278
6.0508	419.1	.2087	794.	.1281
6.5508	418.3	.2090	793.	.1283
7.0	417.5	.2092	792.	.1285
W = 100,000 lb/hr				
7.025	545.7	.1249	899.	.0531
7.125	547.7	.1204	916.	.0449
7.2977	553.4	.1205	923.	.0451
7.6431	560.1	.1210	929.	.0462
8.1431	563.5	.1213	933.	.0466
8.6431	566.4	.1217	935.	.0474
9.1431	569.1	.1223	936.	.0486
9.6431	571.4	.1230	937.	.0497
10.1431	573.3	.1236	937.	.0508
10.6431	575.0	.1242	938.	.0518
11.1431	576.5	.1247	938.	.0527
11.6431	577.8	.1252	938.	.0536
12.1431	578.9	.1256	938.	.0543
12.6431	580.0	.1261	938.	.0550
13.1431	581.0	.1264	938.	.0557
13.6431	581.8	.1268	938.	.0563
14.0	582.4	.1270	938.	.0567

DRAWDOWN TEST OF RESERVOIR, K=100 md

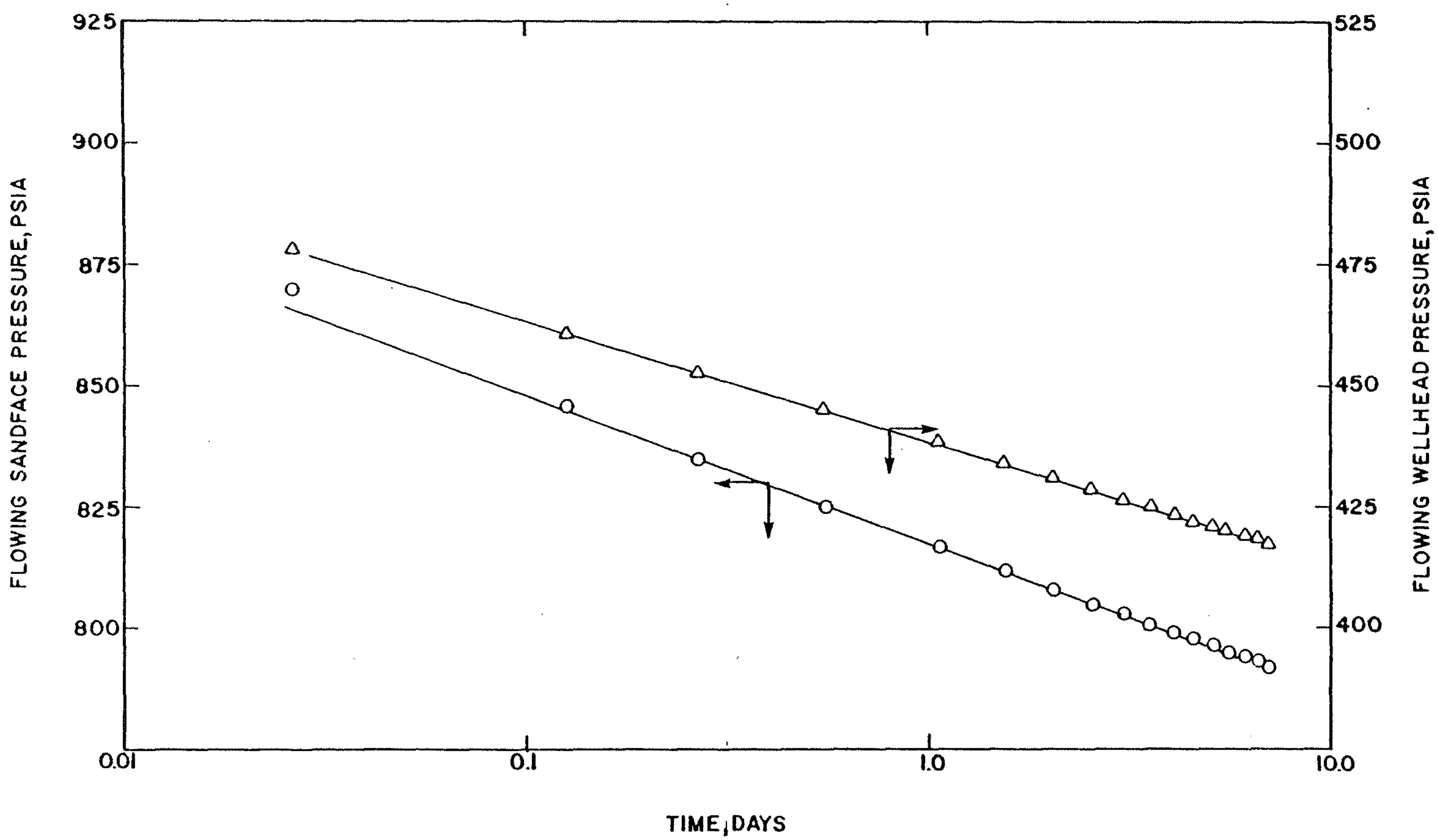

FIGURE 14-A

CERRO PRIETO WELL TEST 15

MULTI-RATE TEST WITH THICKNESS = 169.54'

Time days	P_{wh} psia	X_{wh}	P_{sf} psia	X_{sf}
W = 300,000 lb/hr				
.001	213.4	.2720	573.	.1744
.026	-	-	281.	.3144
Minimum Pressure Reached P_{sf} = 100 psia				
			W, lb/hr	X_{sf}
.126	-	-	294,060	.4035
.226	-	-	275,110	.4017
.326	-	-	264,960	.4011
.4798	-	-	256,570	.3996
.7316	-	-	249,250	.3970
1.1444	-	-	242,580	.3940
1.6444	-	-	237,420	.3916
2.1444	-	-	233,580	.3901
2.6444	-	-	230,490	.3892
3.1444	-	-	227,930	.3886
3.6444	-	-	225,750	.3881
4.1444	-	-	223,880	.2878
4.6446	-	-	222,270	.3874
5.1444	-	-	220,800	.3872
5.6444	-	-	219,500	.3870
6.1444	-	-	218,370	.3867
6.6444	-	-	217,320	.3865
7.0	-	-	216,600	.3864
W = 100,000 lb/hr			P_{sf}	X_{sf}
7.025	304.2	.1698	574.	.1011
7.125	365.0	.1500	652.	.0814
7.225	382.9	.1510	671.	.0842
7.3403	395.8	.1509	685.	.0853
7.5551	408.4	.1512	698.	.0864
7.9480	420.2	.1526	711.	.0886
8.4480	427.1	.1548	717.	.0917
8.9480	430.8	.1571	720.	.0946
9.4480	433.3	.1593	722.	.0973
9.9480	434.9	.1614	722.	.1000
10.4480	435.6	.1638	722.	.1028
10.9480	435.5	.1666	721.	.1060
11.4480	434.8	.1696	718.	.1095
11.9480	434.3	.1725	717.	.1130
12.4480	433.8	.1754	715.	.1163
12.9480	433.2	.1781	713.	.1194
13.4480	432.6	.1805	711.	.1222
14.0	431.9	.1828	710.	.1249

CERRO PRIETO WELL TEST 16

MULTI-RATE DRAWDOWN WITH THICKNESS = 339.08'

Time days	P_{wh} psia	X_{wh}	P_{sf} psia	X_{sf}
W = 300,000 lb/hr				
.001	427.2	.1892	813.	.1027
.026	308.5	.2675	864.	.1934
.126	209.0	.3188	565.	.2321
.226	172.9	.3397	519.	.2488
.326	137.7	.3583	489.	.2595
.4501	113.4	.3117	466.	.2676
.6287	-	-	440.	.2747
.8913	-	-	417.	.2796
1.2800	-	-	394.	.2843
1.7800	-	-	373.	.2893
2.2800	-	-	357.	.2934
2.7800	-	-	342.	.2974
3.2800	-	-	329.	.3010
3.7800	-	-	317.	.3046
4.2800	-	-	307.	.3080
4.7800	-	-	298.	.3113
5.2800	-	-	289.	.3141
5.7800	-	-	282.	.3168
6.2800	-	-	274.	.3194
6.7800	-	-	267.	.3215
7.0	-	-	265.	.3223
W = 100,000 lb/hr				
7.0250	354.0	.1301	665.	.0520
7.1250	381.9	.1134	751.	.0223
7.2250	404.1	.1126	778.	.0229
7.3250	418.5	.1131	792.	.0246
7.4885	432.0	.1134	806.	.0259
7.7642	445.1	.1138	821.	.0273
8.2324	459.2	.1145	834.	.0296
8.7324	470.7	.1155	843.	.0324
9.2324	477.8	.1163	848.	.0345
9.7324	483.9	.1173	851.	.0369
10.2324	489.3	.1185	853.	.0394
10.7324	494.1	.1197	854.	.0421
11.2324	499.0	.1213	854.	.0454
11.7324	503.8	.1234	853.	.0494
12.2324	508.6	.1257	852.	.0537
12.7324	512.4	.1283	850.	.0578
13.2324	515.6	.1306	849.	.0616
13.7324	518.3	.1326	847.	.0649
14.0	519.5	.1336	847.	.0665

CERRO PRIETO WELL TEST 17

MULTI-RATE DRAWDOWN WITH THICKNESS = 678.16'

Time days	P_{wh} psia	X_{wh}	P_{sf} psia	X_{sf}
W = 300,000 lb/hr				
.001	496.4	.1583	912.	.0672
.026	485.3	.1693	883.	.0932
.126	472.8	.1802	865.	.1017
.326	465.6	.1857	854.	.1057
.726	459.2	.1889	846.	.1080
1.226	455.0	.1905	841.	.1091
1.726	452.5	.1914	838.	.1098
2.226	450.6	.1920	836.	.1103
2.726	449.1	.1925	834.	.1106
3.226	447.8	.1930	832.	.1110
3.726	446.7	.1933	831.	.1113
4.226	445.8	.1937	830.	.1116
4.726	445.0	.1940	829.	.1118
5.226	444.2	.1942	828.	.1120
5.726	443.5	.1944	827.	.1122
6.226	442.9	.1947	826.	.1124
6.726	442.3	.1948	825.	.1126
7.0	442.0	.1949	825.	.1126
W = 100,000 lb/hr				
7.025	566.6	.1267	919.	.0568
7.125	566.4	.1230	930.	.0501
7.325	570.1	.1224	936.	.0491
7.725	572.6	.1220	940.	.0485
8.225	574.5	.1221	943.	.0485
8.725	576.3	.1224	944.	.0490
9.225	578.0	.1228	945.	.0497
9.725	579.5	.1232	945.	.0504
10.225	580.7	.1236	946.	.0511
10.725	581.8	.1240	946.	.0517
11.225	582.8	.1243	946.	.0523
11.725	583.7	.1247	947.	.0529
12.225	584.5	.1250	947.	.0534
12.725	585.2	.1253	947.	.0539
13.225	585.8	.1256	947.	.0543
13.725	586.4	.1258	947.	.0547
14.0	586.7	.1260	947.	.0549

DRAWDOWN TEST OF RESERVOIR, h=678.16 ft

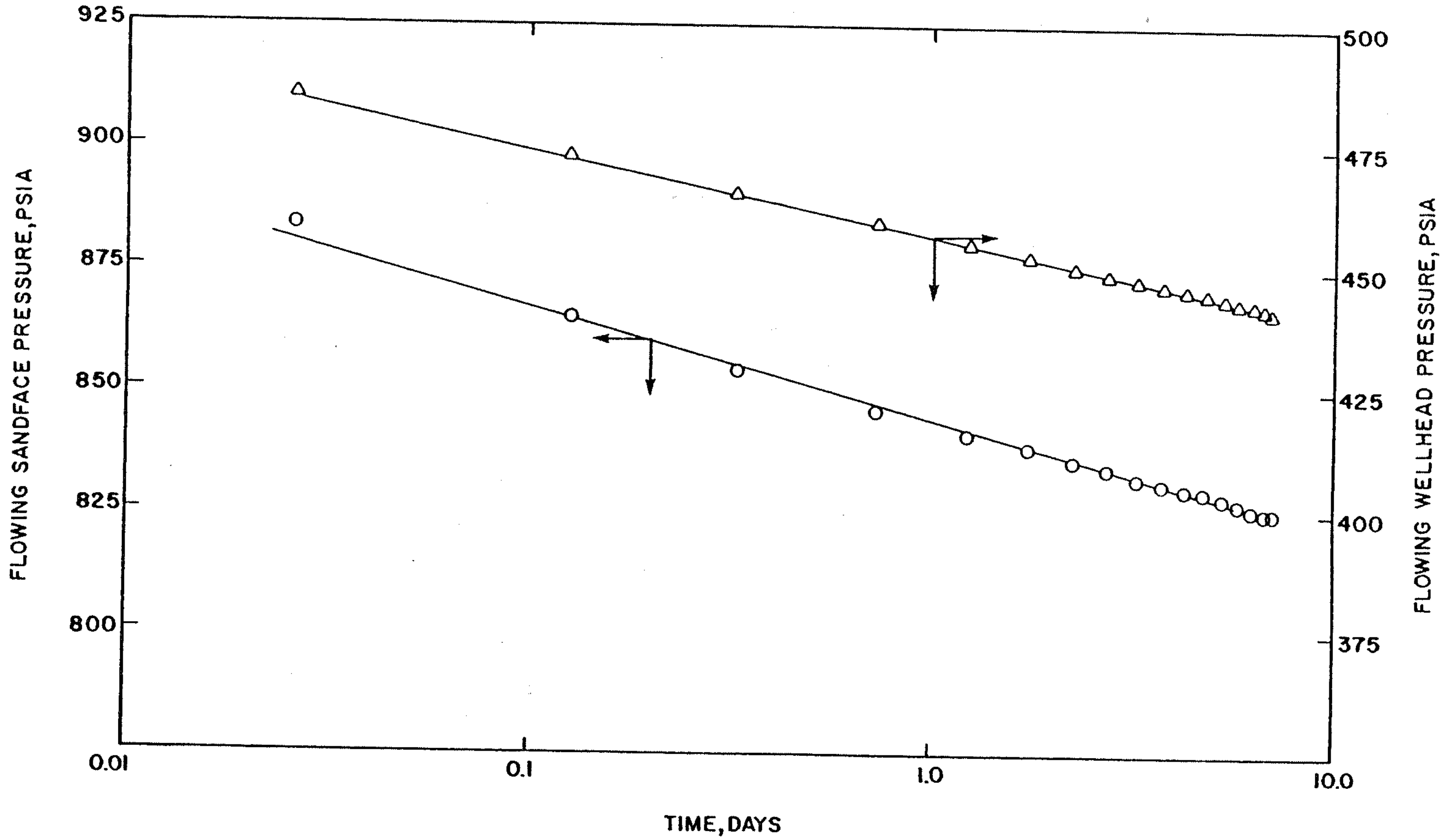

FIGURE 17-A

CERRO PRIETO WELL TEST 18

MULTI-RATE TEST WITH POROSITY = 0.10

Time days	P_{wh} psia	X_{wh}	P_{sf} psia	X_{sf}
W = 300,000 lb/hr				
.001	473.7	.1806	868.	.0950
.026	431.4	.2292	798.	.1618
.126	398.4	.2532	758.	.1841
.226	383.5	.2635	741.	.1928
.4259	369.2	.2714	725.	.1994
.8256	356.2	.2756	711.	.2018
1.3256	347.9	.2776	702.	.2030
1.8256	339.9	.2800	694.	.2046
2.3256	334.2	.2819	688.	.2061
2.8256	329.6	.2836	683.	.2076
3.3256	325.6	.2851	679.	.2088
3.8256	322.3	.2863	676.	.2099
4.3256	319.5	.2873	673.	.2107
4.8256	316.9	.2882	670.	.2115
5.3256	314.7	.2890	668.	.2122
5.8256	312.7	.2897	665.	.2127
6.3256	310.7	.2903	663.	.2133
6.8256	309.0	.2909	662.	.2137
7.0	308.4	.2911	661.	.2139
W = 200,000 lb/hr				
7.025	443.7	.1962	768.	.1281
7.125	456.1	.1876	765.	.1183
7.304	463.9	.1860	795.	.1168
7.6619	469.0	.1887	799.	.1203
8.1619	471.8	.1929	800.	.1255
8.6619	473.1	.1957	800.	.1289
9.1619	473.9	.1976	800.	.1312
9.6619	474.3	.1991	800.	.1330
10.1619	474.5	.2004	800.	.1345
10.6619	474.6	.2016	799.	.1359
11.1619	474.6	.2026	799.	.1372
11.6619	474.5	.2036	798.	.1383
12.1619	474.4	.2045	798.	.1393
12.6619	474.2	.2053	797.	.1403
13.1619	474.0	.2060	797.	.1411
13.6619	473.8	.2068	796.	.1420
14.0	473.7	.2072	796.	.1425

DRAWDOWN TEST OF RESERVOIR, Ø=0.10

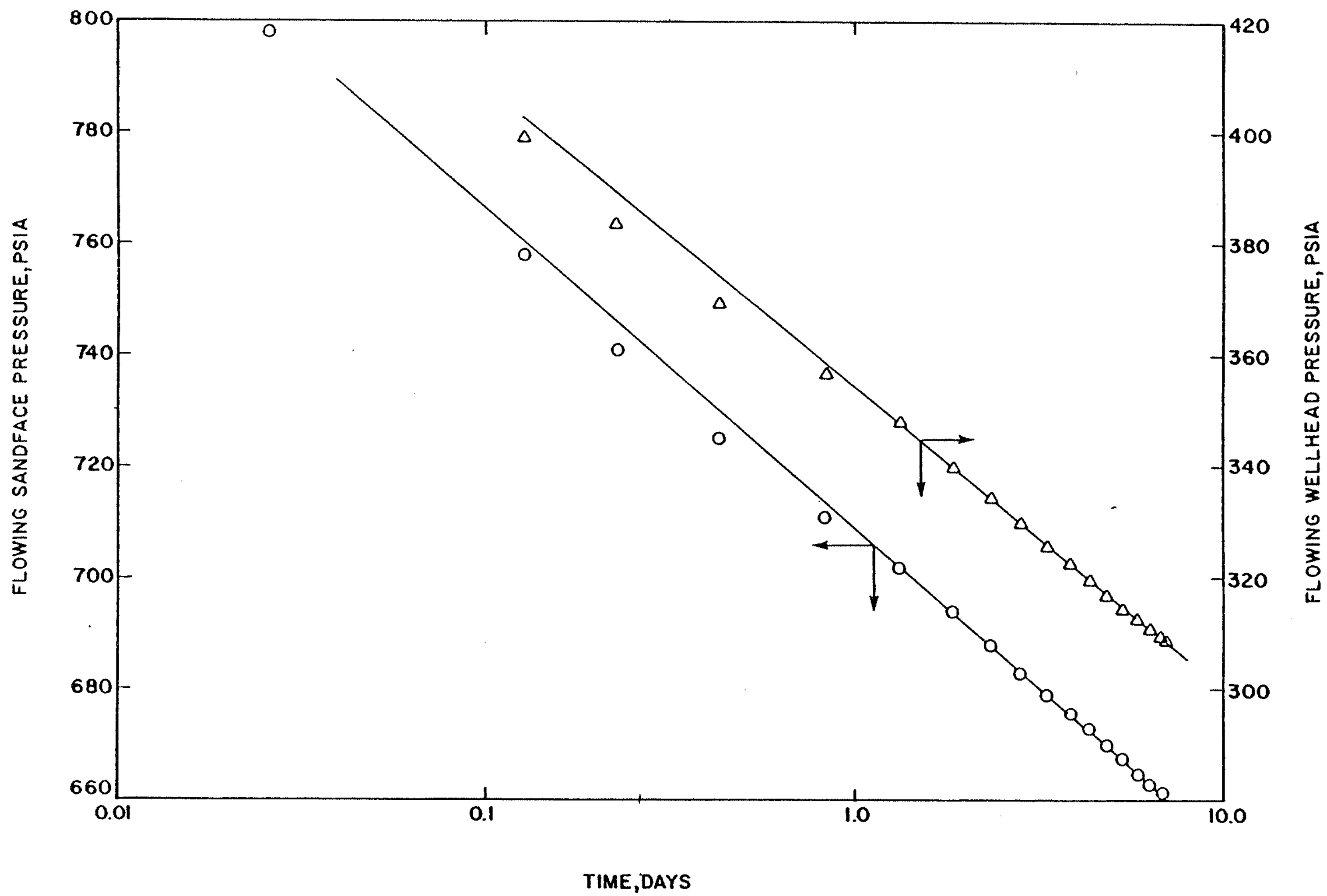

FIGURE 18-A

CERRO PRIETO WELL TEST 19

MULTI-RATE TEST WITH POROSITY = 0.05

Time days	P_{wh} psia	X_{wh}	P_{sf} psia	X_{sf}
W = 300,000 lb/hr				
.001	468.3	.2117	846.	.1331
.026	406.9	.2916	759.	.2325
.126	366.2	.3287	709.	.2676
.226	344.4	.3451	684.	.2830
.3844	327.2	.3553	666.	.2921
.6805	312.1	.3586	651.	.2939
1.1805	299.1	.3598	638.	.2936
1.6805	288.9	.3626	629.	.2949
2.1805	281.1	.3662	621.	.2975
2.6805	272.7	.3699	614.	.3002
3.1805	266.1	.3731	608.	.3027
3.6805	260.7	.3757	603.	.3048
4.1805	256.1	.3779	598.	.3066
4.6805	251.9	.3797	594.	.3079
5.1805	248.3	.3811	591.	.3091
5.6805	245.2	.3824	588.	.3100
6.1805	242.3	.3837	585.	.3109
6.6805	239.7	.3845	583.	.3116
7.0	238.3	.3850	581.	.3119
W = 200,000 lb/hr				
7.025	419.8	.2147	735.	.1487
7.125	438.8	.2023	760.	.1351
7.2509	448.8	.2013	771.	.1343
7.5027	455.1	.2044	777.	.1384
8.0027	459.7	.2135	779.	.1495
8.5027	460.5	.2214	777.	.1588
9.0027	461.0	.2270	775.	.1653
9.5027	461.2	.2310	774.	.1700
10.0027	461.1	.2344	773.	.1739
10.5027	460.9	.2374	772.	.1773
11.0027	460.6	.2401	771.	.1804
11.5027	460.2	.2425	770.	.1832
12.0027	459.7	.2448	769.	.1858
12.5027	459.1	.2470	767.	.1883
13.0027	458.6	.2489	766.	.1905
13.5027	458.0	.2508	765.	.1926
14.0	457.4	.2525	764.	.1945

DRAWDOWN TEST OF RESERVOIR, Ø=0.05

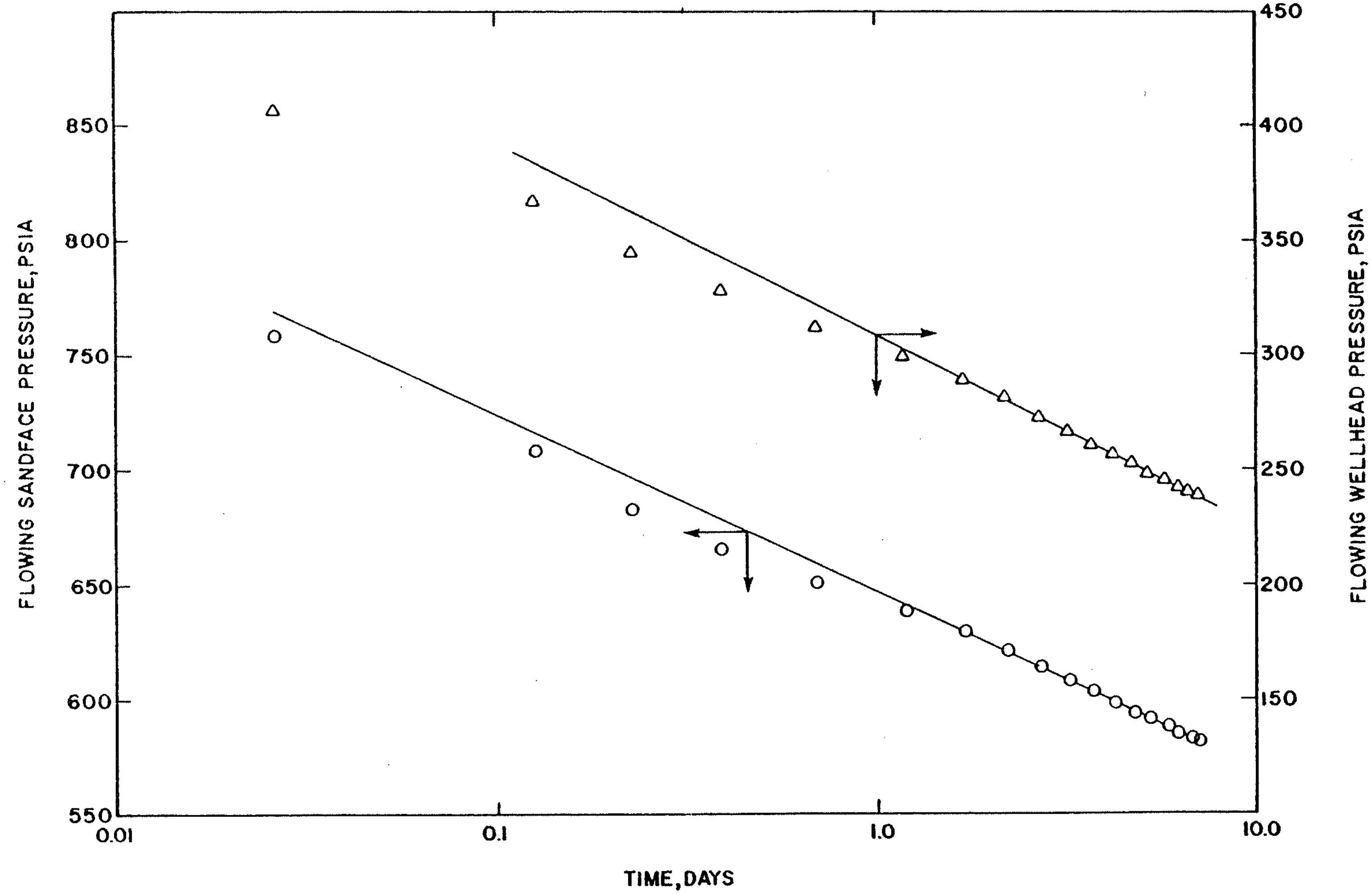

FIGURE 19-A

<u>CERRO PRIETO WELL TEST 20</u>

MULTI-RATE TEST WITHOUT ROCK HEAT LOSS

Time days	P_{wh} psia	X_{wh}	P_{sf} psia	X_{sf}
W = 300,000 lb/hr				
.001	468.7	.1632	876.	.0719
.026	439.0	.1671	834.	.0865
.126	418.6	.1767	808.	.0933
.2486	408.4	.1811	795.	.0964
.4937	398.9	.1846	783.	.0990
.9840	389.5	.1880	772.	.1015
1.4840	383.3	.1903	764.	.1032
1.9840	379.1	.1918	759.	.1045
2.4840	375.8	.1930	755.	.1054
2.9840	373.1	.1940	752.	.1062
3.4840	370.8	.1948	749.	.1069
3.9840	368.8	.1955	747.	.1075
4.4840	367.0	.1961	744.	.1080
4.9840	365.4	.1966	742.	.1084
5.4840	364.0	.1971	741.	.1088
5.9840	362.7	.1976	739.	.1092
6.4840	361.5	.1980	738.	.1096
7.0	360.3	.1984	736.	.1099
W = 100,000 lb/hr				
7.025	539.9	.1335	870.	.0676
7.125	549.2	.1304	888.	.0627
7.2843	553.9	.1292	896.	.0609
7.6028	558.3	.1287	902.	.0601
8.1028	561.3	.1285	907.	.0597
8.6028	563.0	.1284	910.	.0595
9.1028	564.2	.1284	911.	.0594
9.6028	565.1	.1285	912.	.0593
10.1028	565.8	.1285	913.	.0594
10.6028	566.4	.1286	914.	.0594
11.1028	566.8	.1286	914.	.0594
11.6028	567.2	.1287	915.	.0595
12.1028	567.6	.1288	915.	.0596
12.6028	567.9	.1289	915.	.0596
13.1028	568.2	.1289	916.	.0597
13.6028	568.4	.1290	916.	.0598
14.0	568.6	.1290	916.	.0598

HGP-A WELL TEST I

SINGLE RATE DRAWDOWN TEST

Time days	P_{wh} psia	X_{wh}	P_{sf} psia	X_{sf}
W = 86,000 lb/hr				
.001	837.6	.0716	1392.	.0488
.0019	988.4	.1723	1309.	.2113
.0039	750.3	.4386	979.	.4856
.0164	709.9	.4346	936.	.4765
.1164	545.8	.5624	714.	.5943
.2164	460.1	.6102	603.	.6336
.3922	416.4	.6210	551.	.6381
1.0732	366.7	.6307	492.	.6391
3.0732	312.7	.6428	427.	.6435
5.0732	286.7	.6500	392.	.6472
7.0732	270.2	.6539	367.	.6492
9.0732	257.6	.6570	348.	.6510
11.0732	250.8	.6602	336.	.6537
13.0732	245.9	.6614	324.	.6545
15.0732	236.5	.6641	313.	.6556
17.0732	227.1	.6672	303.	.6569
19.0732	217.4	.6702	294.	.6581
21.0732	208.6	.6727	287.	.6592
23.0732	200.7	.6750	280.	.6602
25.0732	193.3	.6771	274.	.6610
27.0732	186.3	.6797	268.	.6618
29.0732	179.7	.6822	263.	.6625
31.0732	173.3	.6846	258.	.6632
33.0732	167.2	.6869	253.	.6639
35.0732	161.6	.6896	249.	.6653
37.0732	158.5	.6916	247.	.6666
39.0732	154.4	.6930	244.	.6670
41.0732	150.4	.6940	241.	.6671
41.6700	148.5	.6945	239.	.6672

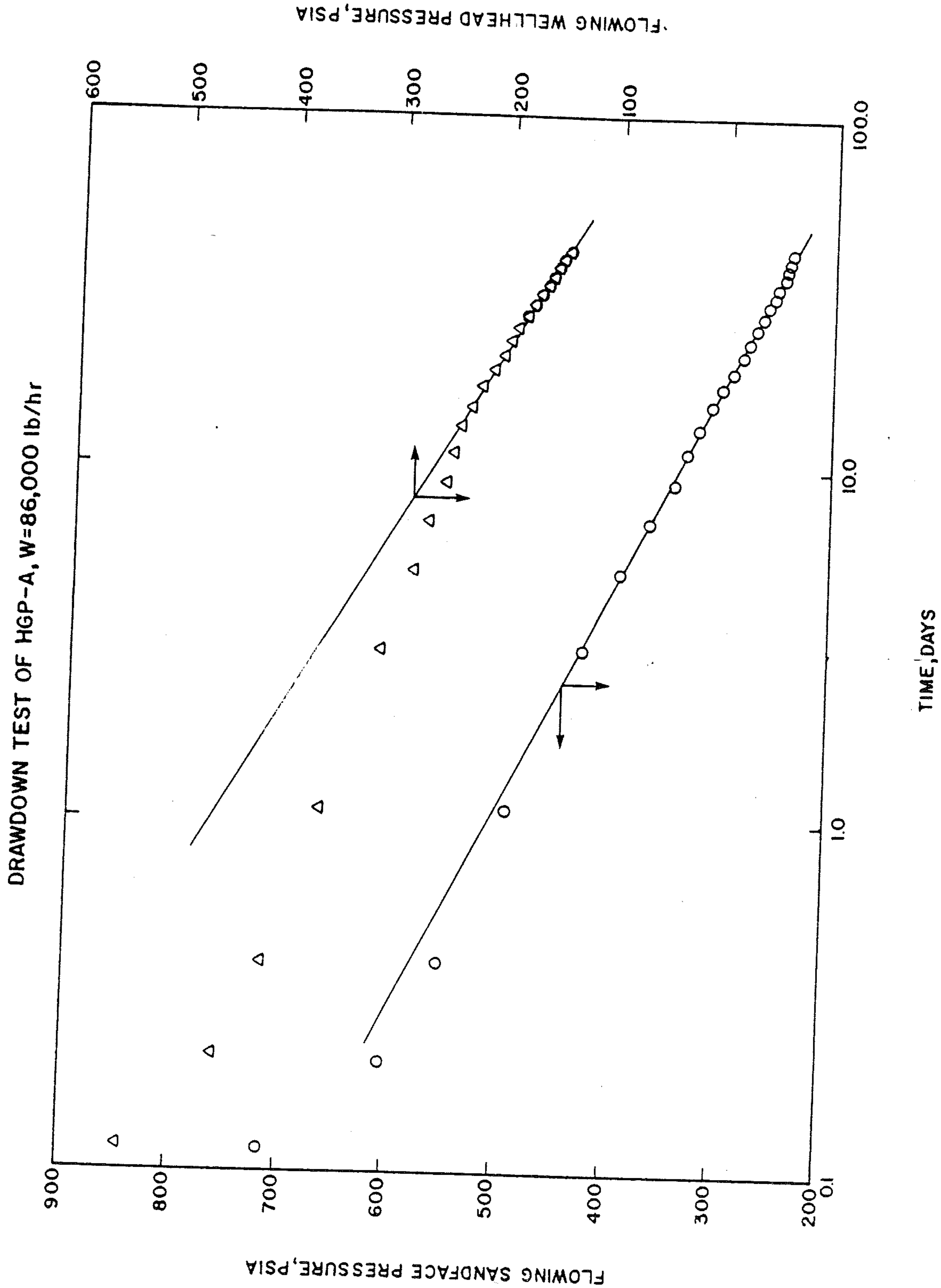
DRAWDOWN TEST OF HGP-A, W=86,000 lb/hr
FLOWING WELLHEAD PRESSURE, PSIA
600
500
400
300
200
100
FLOWING SANDFACE PRESSURE, PSIA
900
800
700
600
500
400
300
200
0.1
1.0
10.0
100.0
TIME, DAYS

FIGURE 21-A

HGP-A WELL TEST 2

SINGLE RATE DRAWDOWN TEST

W = 75,000 lb/hr

Time days	P_{wh} psia	X_{wh}	P_{sf} psia	X_{sf}
.001	1060.1	.1954	1369.	.2586
.0072	784.4	.5567	973.	.6270
.1072	755.6	.5157	955.	.5739
.2072	705.7	.5570	887.	.6090
.3819	671.2	.5731	844.	.6186
1.1196	628.3	.5838	794.	.6196
3.1196	564.5	.6006	719.	.6260
5.1196	497.9	.6033	643.	.6204
7.1196	463.5	.6060	602.	.6188
9.1196	447.0	.6079	583.	.6188
11.1196	435.6	.6095	569.	.6192
13.1196	426.3	.6117	558.	.6201
15.1196	420.1	.6127	551.	.6201
17.1196	413.7	.6138	543.	.6203
19.1196	408.2	.6149	537.	.6206
21.1196	403.4	.6158	531.	.6208
23.1196	399.1	.6166	526.	.6210
25.1196	395.2	.6173	522.	.6212
27.1196	391.7	.6179	517.	.6213
29.1196	388.5	.6185	513.	.6215
31.1196	385.4	.6191	510.	.6217
33.1196	382.6	.6197	506.	.6219
35.1196	380.0	.6202	503.	.6221
37.1196	377.5	.6208	500.	.6223
39.1196	375.2	.6212	497.	.6225
41.1196	373.0	.6216	495.	.6227
41.6700	372.4	.6217	494.	.6227

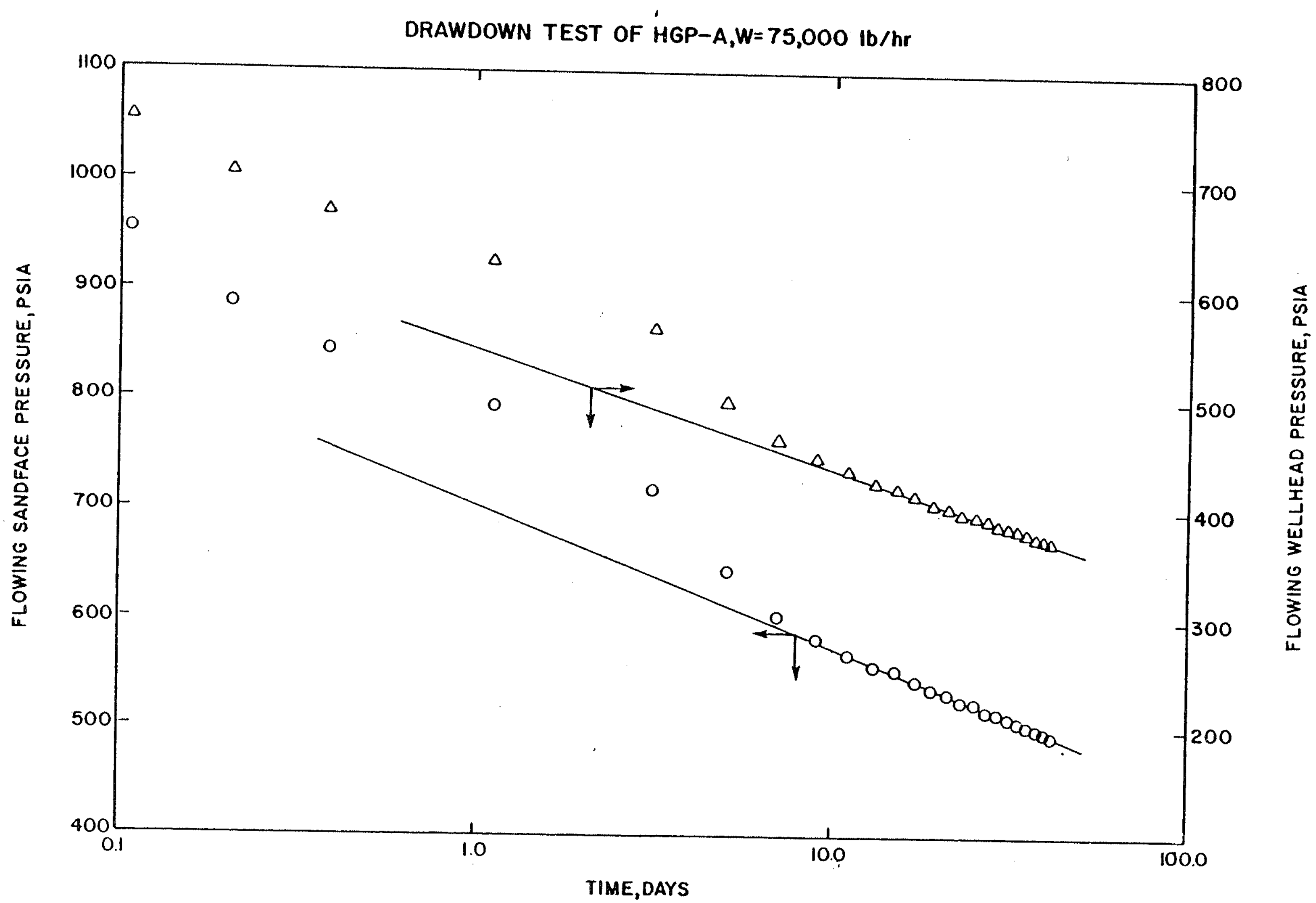
DRAWDOWN TEST OF HGP-A, W=75,000 lb/hr
FLOWING SANDFACE PRESSURE, PSIA
1100
1000
900
800
700
600
500
400
FLOWING WELLHEAD PRESSURE, PSIA
800
700
600
500
400
300
200
0.1
1.0
10.0
100.0
TIME, DAYS

FIGURE 22-A

HGP-A WELL TEST 3

SINGLE RATE DRAWDOWN TEST

Time days	P_{wh} psia	X_{wh}	P_{sf} psia	X_{sf}
W = 65,000 lb/hr				
.001	1090.3	.1556	1411.	.2346
.0022	970.1	.4058	1212.	.4989
.0522	807.0	.5457	993.	.6264
.1522	815.9	.5080	1015.	.5809
.2810	789.3	.5322	979.	.5986
.6164	760.9	.5480	944.	.6058
2.1173	718.8	.5608	895.	.6059
4.1173	674.7	.5756	842.	.6127
6.1173	628.9	.5747	791.	.6052
8.1173	605.7	.5754	765.	.6023
10.1173	594.1	.5772	752.	.6021
12.1173	586.0	.5787	743.	.6022
14.1173	579.5	.5800	735.	.6023
16.1173	574.1	.5810	729.	.6024
18.1173	569.4	.5820	723.	.6026
20.1173	565.8	.5827	719.	.6026
22.1173	562.3	.5834	715.	.6027
24.1173	559.2	.5840	711.	.6027
26.1173	556.4	.5845	708.	.6028
28.1173	553.8	.5850	705.	.6029
30.1173	551.4	.5854	702.	.6029
32.1173	549.2	.5858	699.	.6030
34.1173	547.1	.5862	697.	.6030
36.1173	545.2	.5865	695.	.6031
38.1173	543.3	.5868	693.	.6031
40.1173	541.6	.5871	690.	.6032
41.6700	540.3	.5873	689.	.6032

DRAWDOWN TEST OF HGP-A, W=65,000 lb/hr

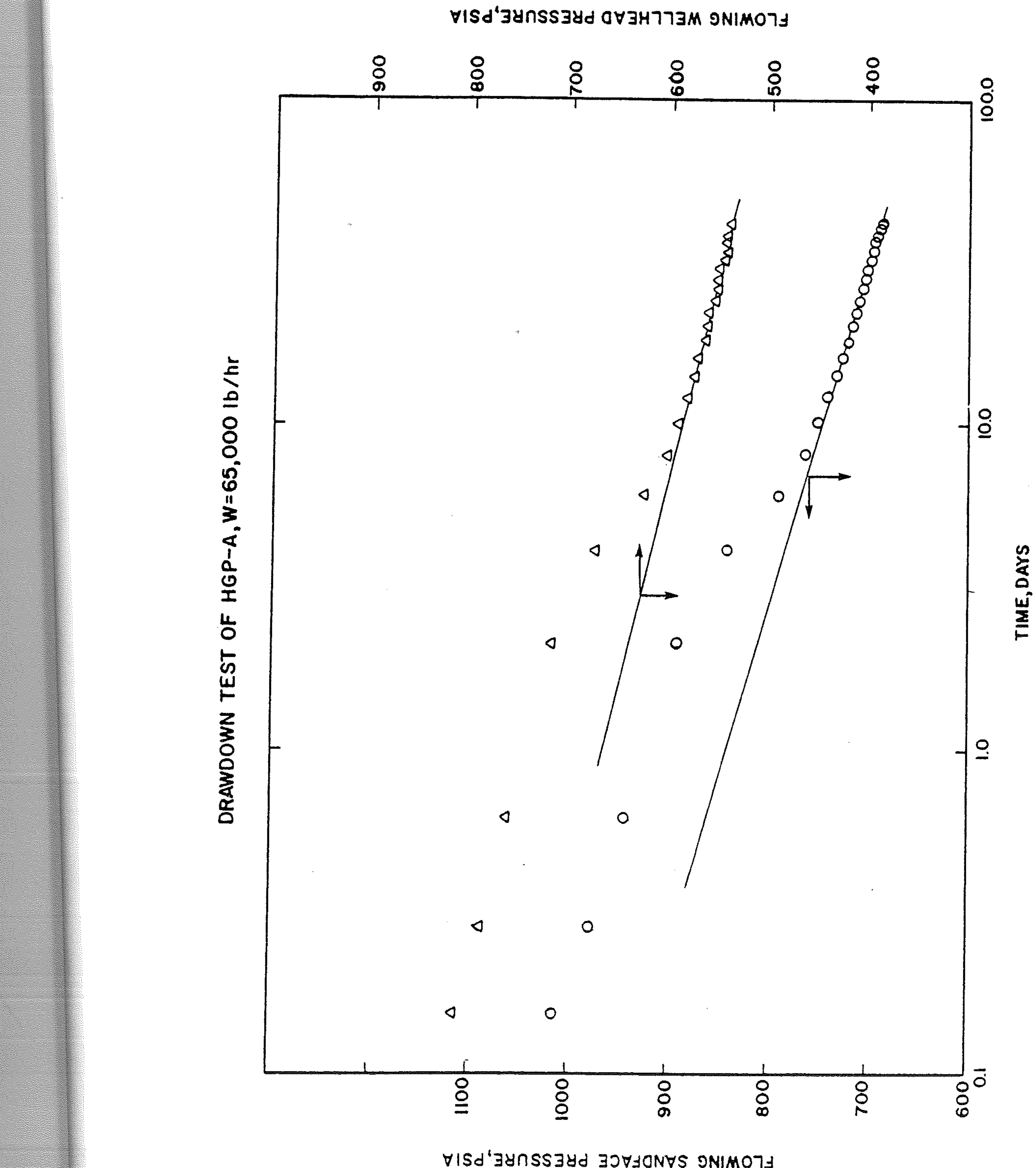

FIGURE 23-A

<u>HGP-A WELL TEST 4</u>

SINGLE RATE DRAWDOWN TEST - FRACTURED RESERVOIR

Time days	P_{wh} psia	X_{wh}	P_{sf} psia	X_{sf}
W = 86,000 lb/hr				
.0003	914.9	.3809	1176.	.4381
.0010	747.9	.2728	1022.	.3029
.0135	752.3	.2115	1043.	.2338
.0260	806.8	.2196	1099.	.2473
.0336	804.7	.2660	1085.	.2983
.0369	787.1	.2986	1058.	.3325
.0653	677.3	.3905	912.	.4217
.1653	590.0	.4052	811.	.4255
.2678	565.1	.3964	786.	.4109
.5223	570.3	.3652	801.	.3734
.8645	587.7	.3367	830.	.3407
1.7645	587.4	.3055	840.	.3018
3.5124	584.7	.2965	840.	.2878
5.5124	559.9	.2955	812.	.2821
7.5124	534.4	.2960	785.	.2794
9.5124	522.3	.3037	769.	.2863
11.5124	516.6	.3145	759.	.2972
13.5124	517.5	.3238	757.	.3072
15.5124	512.2	.3291	749.	.3122
17.5124	504.8	.3306	741.	.3127
19.5124	493.8	.3294	729.	.3099
21.5124	477.7	.3256	712.	.3256
23.5124	458.1	.3190	691.	.2944
25.5124	448.5	.3128	682.	.2865
27.5124	439.6	.3079	674.	.2802
29.5124	440.8	.3051	676.	.2771
31.5124	441.2	.3036	677.	.2752
33.5124	442.6	.3019	679.	.2734
35.5124	452.0	.3044	689.	.2768
37.5124	457.6	.3068	695.	.2797
39.5124	463.1	.3087	701.	.2823
41.6700	470.0	.3110	708.	.2853

DRAWDOWN TEST OF FRACTURED RESERVOIR W=86,000 lb/hr

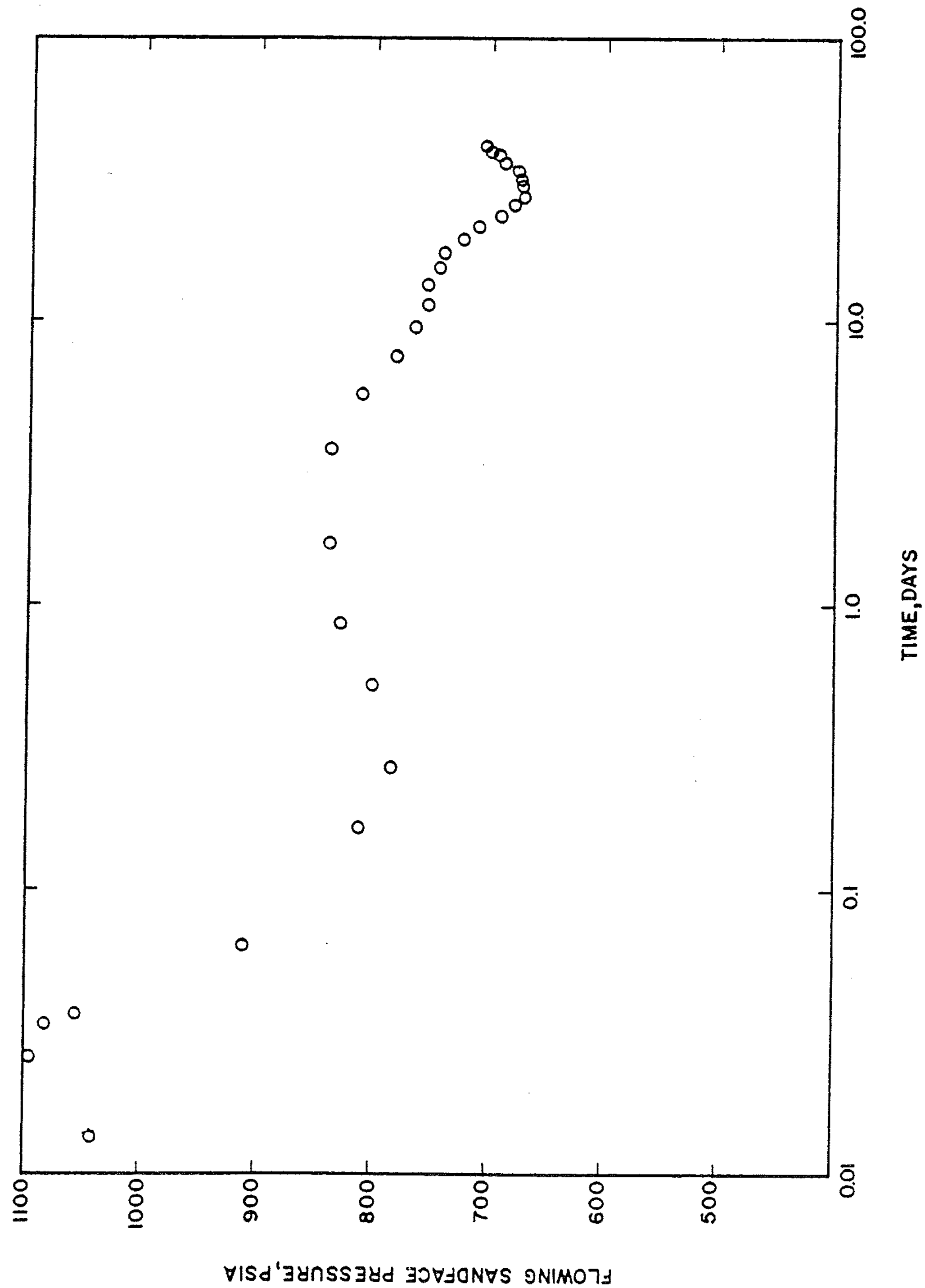

FIGURE 24-A

HGP-A WELL TEST 5

SINGLE RATE DRAWDOWN TEST - FRACTURED RESERVOIR

W = 100,000 lb/hr

Time days	P_{wh} psia	X_{wh}	P_{sf} psia	X_{sf}
.001	712.4	.2602	995.	.2746
.0135	743.6	.2102	1042.	.2203
.0186	762.3	.2259	1058.	.2393
.0206	764.4	.2416	1056.	.2510
.0222	764.0	.2582	1052.	.2754
.0232	762.5	.2710	1047.	.2896
.0243	758.8	.2878	1039.	.3079
.0253	753.3	.3048	1029.	.3261
.0264	744.1	.3245	1013.	.3472
.0274	732.0	.3444	995.	.3682
.0287	713.8	.3680	969.	.3680
.0412	571.8	.4641	783.	.4641
.0662	453.9	.4949	639.	.5053
.1662	373.5	.4949	546.	.4937
.2662	345.8	.4836	517.	.4767
.4780	367.3	.4476	553.	.4379
.7197	381.7	.4192	579.	.4067
1.3362	404.6	.3852	617.	.3695
2.2564	409.5	.3721	627.	.3535
3.9056	388.0	.3745	602.	.3515
5.9056	361.2	.3795	569.	.3533
7.9056	338.0	.3908	538.	.3631
9.9056	308.6	.4072	497.	.3771
11.9056	279.3	.4195	458.	.3874
13.9056	259.3	.4263	432.	.3917
15.9056	246.0	.4285	416.	.3920
17.9056	233.3	.4279	400.	.3891
19.9056	209.6	.4282	368.	.3852
21.9056	193.8	.4254	347.	.3793
23.9056	193.1	.4221	347.	.3757
25.9056	198.4	.4207	356.	.3750
27.9056	210.9	.4184	374.	.3747
29.9056	225.3	.4167	393.	.3755
31.9056	232.5	.4175	402.	.3777
33.9056	231.0	.4207	399.	.3807
35.9056	224.1	.4252	389.	.3843
37.9056	214.1	.4303	374.	.3883
39.9056	205.8	.4344	361.	.3915
41.6700	198.8	.4378	349.	.3943

DRAWDOWN TEST OF FRACTURED RESERVOIR W=100,000 lb/hr

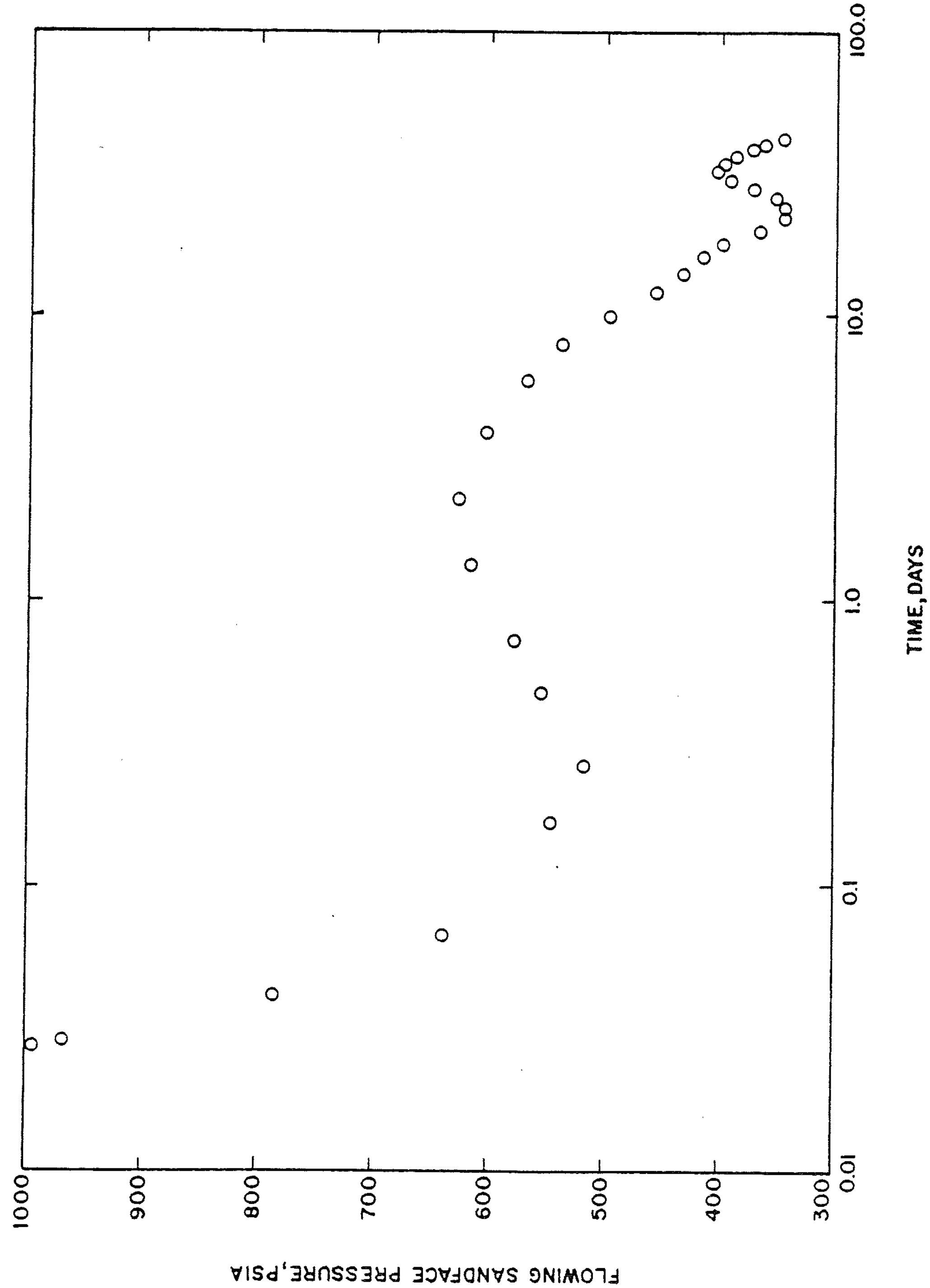

FIGURE 25-A

U.S.GPO;1980-695-287/230

TECHNICAL INFORMATION DEPARTMENT
LAWRENCE BERKELEY LABORATORY
UNIVERSITY OF CALIFORNIA
BERKELEY, CALIFORNIA 94720